The Modulation of Multi-walled Carbon Nanotube-induced Acute Lung Pathology by Mouse Strain, Glutathione Status, and Nanotube Characteristics

Megan Cartwright

A dissertation

submitted in partial fulfillment of the

requirements for the degree of

Doctor of Philosophy

University of Washington

2015

Reading Committee:

Terrance Kavanagh, Chair

William Altemeier

Edward Kelly

Program Authorized to Offer Degree:

School of Public Health

Environmental and Occupational Health Sciences

University of Washington

Abstract

The Modulation of Multi-walled Carbon Nanotube-induced Acute Lung Pathology by Mouse Strain, Glutathione Status, and Nanotube Characteristics

Megan Cartwright

Chair of the Supervisory Committee:

Professor Terrance Kavanagh

Department of Environmental and Occupational Health Sciences

Multi-walled carbon nanotubes (MWCNTs) are concentric cylinders of graphene with useful industrial properties and possible human toxicities due to their high aspect ratio, reactive surface chemistry, and respirable size. Worldwide manufacturing capacity of carbon nanotubes (CNTs) increased ten-fold from 2006 to 2011, reflecting manufacturing improvements and increased demand. However, this dramatic expansion has outpaced animal testing for toxicity—thereby presenting a potential occupational health hazard to workers at risk for inhaling MWCNTs during manufacturing and handling.

While several human studies into the effects of occupational exposure have been published, current understanding of MWCNT-induced lung pathology largely derives from *in vitro* cell culture studies and *in vivo* animal studies. However, the literature frequently contradicts itself on the consequences of MWCNT introduction into the rodent lung: CNTs have been reported as highly inflammogenic, pro-fibrotic, damaging to cellular and lung barrier integrity, and capable of engendering severe oxidative stress. CNTs have also been reported as non-inflammogenic, non-fibrotic, non-cytotoxic, and capable of scavenging reactive oxygen species. These contradictions may derive from significant interlaboratory

differences in MWCNT preparation and rodent exposures, as well as from the incredible diversity in physicochemical properties of various manufactured MWCNTs.

These contradictory data impede effective risk assessments and regulations to reduce the risk of lung exposure in workers. Furthermore, the majority of studies only examined MWCNT-induced pathology in a narrow selection of rodent strains, predominantly the C57BL/6 mouse. This narrow approach likely fails to capture important variations in genetic susceptibility to lung pathology within a workforce growing 14% annually in the United States.

To improve understanding of the associations between MWCNT-induced lung inflammation and specific physicochemical characteristics, along with genetic differences in susceptibility, I have developed the following aims:

Aim 1: To elucidate which physicochemical characteristics of nine well-characterized MWCNTs are associated with acute lung inflammation in A/J mice.

Aim 2: To determine if there is a differential response to MWCNT-induced acute lung inflammation across ten isogenic mouse strains.

Aim 3: To investigate how a genetically-induced deficiency in the cellular antioxidant glutathione modulates susceptibility to MWCNT-induced acute lung inflammation in a gender-dependent manner in C57BL/6 mice.

Table of Contents

List of Figures vi

List of Tables vii

Chapter 1 : Introduction 1

1.1. Multi-walled carbon nanotube synthesis and industrial uses. 1

1.2. Occupational and environmental exposures to multi-walled carbon nanotubes. 2

1.3. Potential effects of respiratory exposure to multi-walled carbon nanotubes. 3

1.4. Knowledge gaps in understanding MWCNT-induced lung toxicity. 11

Chapter 2 : Aim 1 20

2.1. Introduction 20

2.2. Materials and Methods 21

2.3. Results 27

2.4. Discussion 35

2.5. Figures 40

2.6. Tables 48

Chapter 3 : Aim 2 54

3.1. Introduction 54

3.2. Materials and Methods 55

3.3. Results 61

3.4. Discussion 67

3.5. Figures 71

3.6. Tables 76

Chapter 4 : Aim 3 79

4.1. Introduction 79

4.2. Materials and Methods 81

4.3. Results 86

4.4. Discussion 91

4.5. Figures 95

4.6. Tables 103

Chapter 5 : Conclusions 106

References 110

Appendix: Acronyms and Abbreviations 118

List of Figures

Figure 2.1. Representative Helium Ion Microscope images of MWCNTs. 40

Figure 2.2. Lung neutrophilia. 41

Figure 2.3. Representative images of lung neutrophilia. 43

Figure 2.4. Correlation between bulk nickel content and neutrophilia. 44

Figure 2.5. MWNCT internalization by alveolar macrophages. 45

Figure 2.6. Representative images of MWCNT internalization by alveolar macrophages. 46

Figure 2.7. Heatmap of MWCNT panel with pathological endpoints. 47

Figure 3.1. Neutrophilia varies by mouse strain. 71

Figure 3.2. Heatmap of each strain's log(fold-change) values for all pathological endpoints. 72

Figure 3.3. BALF cytokine levels in AJ vs. C57 mouse strains. 73

Figure 3.4. Semi-quantitative Western blotting for redox-sensitive protein expression and nitrated residues. 74

Figure 4.1. Lung neutrophilia. 95

Figure 4.2. Lung eosinophilia. 96

Figure 4.3. Pro-inflammatory cytokines in lungs. 97

Figure 4.4. Glutathione levels in lungs. 99

Figure 4.5. Glutathione levels in epithelial lining fluid. 100

Figure 4.6. Expression of redox-sensitive proteins. 101

Figure 4.7. Representative Western blots for redox-sensitive proteins and nitrated residues. 102

List of Tables

Table 2.1. Manufacturer's Specifications of MWCNT Physical Dimensions. 48

Table 2.2. Measured Physicochemical Characteristics of MWCNT Panel. 49

Table 2.3. Aggregative Characteristics of MWCNT Panel. 50

Table 2.4. Effects of MWCNT Exposure on mRNA Expression of Chemoattractant and Pro-Inflammatory Genes. 51

Table 2.5. Effects of MWCNT Exposure on Lung Injury and Oxidative Stress. 52

Table 2.6. Effects of MWCNT Exposure on mRNA Expression of Oxidative Stress- and Fibrosis-Associated Genes. 53

Table 3.1. Effects of MWCNT Exposure on Lung Injury and Oxidative Stress in Multiple Strains. 76

Table 3.2. Effects of MWCNT Exposure on mRNA Expression of Chemoattractant and Pro-Inflammatory Genes in Multiple Strains. 77

Table 3.3. Effects of MWCNT Exposure on mRNA Expression of Oxidative Stress- and Fibrosis-Associated Genes in Multiple Strains. 78

Table 4.1. Lung mRNA Expression Levels of Inflammation-, Oxidative Stress-, and Fibrosis-Associated Genes 24 h After Aspiration of MWCNTs by Male *Gclm* Mice. 103

Table 4.2. Lung mRNA Expression Levels of Inflammation-, Oxidative Stress-, and Fibrosis-Associated Genes 24 h After Aspiration of MWCNTs by Female *Gclm* Mice. 104

Table 4.3. Parameters for Lung Toxicity and Alveolar/Capillary Barrier Integrity 24 h After Aspiration of MWCNTS by *Gclm* Mice. 105

Acknowledgements

This dissertation would not have been possible without the hard work, support, and collaborative efforts of many people at the University of Washington, Pacific Northwest National Laboratory, and New York University. I would like to thank and acknowledge the following organizations and individuals for their valuable contributions:

University of Washington

Kavanagh Laboratory

Terrance Kavanagh, Ph.D.
Dianne Botta
Collin White
Stefanie Schmuck
Lisa McConnachie, Ph.D.
Christopher Carosino, Ph.D.
Claire Chisholm
David Scoville
Christopher Schaupp
Eunmi Hwang
Isaac Mohar, Ph.D.
Chad Weldy, Ph.D

Center for Ecogenetics and Environmental Health Functional Genomics and Proteomics Core

Hui-Wen (Jasmine) Wilkerson
Zahra Afsharinejad
Theo Bammler, Ph.D.

Posner Laboratory

Charlie Corredor, Ph.D.
Jonathan Posner, Ph.D.

Office of Animal Welfare

Department of Comparative Medicine

Department of Pharmaceutics

Edward Kelly, Ph.D.

Division of Pulmonary & Critical Care Medicine

William Altemeier, M.D.

Department of Environmental & Occupational Health Sciences

Evan Gallagher, Ph.D.
David Eaton, Ph.D.

New York University School of Medicine

Gordon Laboratory

Terry Gordon, Ph.D.

Karen Galdanes

Pacific Northwest National Laboratory

Environmental Molecular Sciences Laboratory

Donald Baer, Ph.D.

Vaithiyalingam Shutthanandan, Ph.D.

Vamsi Kodali, Ph.D.

Bingbing Wang, Ph.D.

Mark Engelhard, Ph.D.

Andreas Vasdekis, Ph.D.

Brian Thrall, Ph.D.

I would also like to thank and acknowledge the following organizations and individuals for providing research and salary support for this work, and travel funds for sharing this work at professional meetings:

Bruce Kelman, Ph.D.

Department of Environmental and Occupational Health Sciences

National Institute of Environmental Health Sciences

University of Washington Graduate School

Chapter 1 : Introduction

1.1. Multi-walled carbon nanotube synthesis and industrial uses.

Multi-walled carbon nanotubes (MWCNTs) are concentric cylinders of graphene sheets which are typically under 100 nm in diameter, but which can reach hundreds of microns in length (De Volder *et al.*, 2013). With their fiber-like aspect ratios and reactive surface chemistry, they are frequently compared to much-larger asbestos fibers (Poland *et al.*, 2008; Ma-Hock *et al.*, 2009; Nagai *et al.*, 2011; Nymark *et al.*, 2014). Unlike asbestos, MWCNTs were only first discovered and characterized in 1991 (Iijima, 1991). However, they were quickly embraced by the burgeoning nanotechnology sector: Since 2006, worldwide carbon nanotube (CNT) production capacity has grown approximately ten-fold, reaching an estimated four million kilograms per year in 2011 (Dahm *et al.*, 2012; De Volder *et al.*, 2013).

The increasing popularity of MWCNTs is unsurprising, given that these nanomaterials possess characteristics useful to the materials, electronic, and biomedical industries. CNTs are predominantly manufactured for making composite materials, such as those used in sporting goods, car parts, and aeronautics, which take advantage of their light weight and high tensile strength (Liu *et al.*, 2010; De Volder *et al.*, 2013). Due to CNTs' electrical and semiconducting properties, they are also used in rechargeable batteries and transistors (De Volder *et al.*, 2013; Shulaker *et al.*, 2013). Furthermore, MWCNTs are under development for use in biology and medicine as biological sensors, carriers for drug molecules, probes for atomic force microscopy, and ultrasound contrast agents (Delogu *et al.*, 2012; Jain, 2012). Presently, a clinical trial is underway comparing the efficacy of a standard tissue imaging technique to a CNT X-ray-based imaging device for evaluating breast lesions (NIH, 2015).

This rapid expansion in CNT production has been enabled by continued developments in manufacturing processes, notably chemical vapor deposition. In chemical vapor deposition, MWCNTs are grown from metal catalysts (e.g., iron and nickel) in contained reactors enabling the uniform diffusion of heat and carbon-based gases. With improvements to the chemical vapor deposition process, purified MWCNTs are sold for approximately $100/kg—making them approximately ten times more expensive than carbon fiber (De Volder *et al.*, 2013).

Unlike single-walled CNTs (SWCNTs), MWCNTs can be produced without these metal catalysts, although this method requires more energy and often produces poorly-aligned CNTs (Lam *et al.*, 2006).

In contrast, chemical vapor deposition efficiently produces MWCNTs, although this process can significantly contaminate MWCNTs with metal catalysts and non-graphene carbonaceous materials. Consequently, MWCNTs require post-synthesis treatments involving heat and/or acid to remove these contaminants, and subsequently to anneal defects introduced into the graphene structure (De Volder *et al.*, 2013; Kim *et al.*, 2014). Unfortunately, this post-synthesis handling—as well as related activities, such as grinding and sonication—increases the opportunities for workers to be exposed to MWCNTs (Lee *et al.*, 2015a).

1.2. Occupational and environmental exposures to multi-walled carbon nanotubes.

During manufacture and handling, MWCNTs can be released into ambient air, where they aggregate into complex bundles of nanotubes and contaminants up to 4 μm in diameter (Han *et al.*, 2008; Lee *et al.*, 2010; Dahm *et al.*, 2012) and constitute a significant fraction of ambient elemental carbon (Dahm *et al.*, 2012). While dermal exposure is possible (Maynard *et al.*, 2004), the principal exposure route of concern is via inhalation of airborne MWCNTs (NIOSH, 2013). Among American CNT manufacturers, inhalable elemental carbon has been measured at 7.86 $\mu g/m^3$, corresponding to approximately 1 CNT/cc (Dahm *et al.*, 2012); among American research laboratories, this level reached as high as 53 $\mu g/m^3$ (Maynard *et al.*, 2004). Studies of Korean manufacturers have reported air concentrations of 1.6 – 2.3 $\mu g/m^3$ (Lee *et al.*, 2015b), 0.3 – 2.5 $\mu g/m^3$ (Lee *et al.*, 2015a), and even an astonishing 430 $\mu g/m^3$, which corresponded to 193.6 MWCNT/cc (Han *et al.*, 2008). This concentration was significantly higher than current threshold limit values for other fibers, such as asbestos (0.1/cc), refractory ceramic fiber (0.1/cc), and rock wool (1/cc) (Han *et al.*, 2008).

While workers involved in manufacturing and handling are the most likely to be exposed, MWCNTs have also been detected in the environment and even in the general population. MWCNTs can be unintentionally produced during combustion; consequently, they have been recovered from propane and natural gas kitchen stoves, and from outdoor particulate matter collected in Texas (Lam *et al.*, 2006). The combustion of jet fuel during the 2001 World Trade Center terrorist attacks was the likely source for the CNT-like structures recovered from the lung biopsies acquired in 2006 – 2007 from four first responders with respiratory disorders; indeed, the CNT tissue burdens among these first responders

reached as high as 230,000 CNT/g of lung tissue (Wu *et al.*, 2010). Similarly, traffic pollution is the likely source for the MWCNT-like structures recently observed in alveolar macrophages and bronchoalveolar lavage fluid (BALF) extracts of 66 Parisian children with asthma (Kolosnjaj-Tabi *et al.*, 2015)

Although it is difficult to conclusively prove that these CNT-like structures recovered from first responders and Parisian children are CNTs, these reports do confirm that carbonaceous nanomaterials comparable in size to MWCNTs are capable of entering and being retained by the human lung.

1.3. Potential effects of respiratory exposure to multi-walled carbon nanotubes.

Once in the lung, the same characteristics which make MWCNTs so useful—their fiber-like aspect ratio, reactive surface chemistry, and structural stability—may also render them harmful (Ma-Hock *et al.*, 2009).

At the present time, there are few published studies investigating the effects of CNT exposure on humans. The largest and best-controlled epidemiological study to date compared 124 Taiwanese workers and 77 controls at baseline and then six months later to identify potential exposure biomarkers (Liao *et al.*, 2014). When adjusted for confounders (e.g., age, gender, smoking status), exposure to nanomaterials was associated with lung dysfunction, elevated serum levels of the lung damage marker CC16, and significant decreases in the activity of the antioxidant enzymes superoxide dismutase and glutathione peroxidase in serum. Exposure to CNTs specifically was associated with lung dysfunction and a decrease in serum glutathione peroxidase activity. Similarly, a case series comparing 9 workers and 4 controls in the largest Korean MWCNT manufacturing firm found that workers had significantly higher levels of the oxidative stress markers malondialdehyde, n-hexanal, and 4-HHE (an oxidized polyunsaturated fatty acid) in breath condensate. However, this case series found no pulmonary dysfunction, nor any abnormalities in hematology and blood biochemistry, in workers (Lee *et al.*, 2015b).

In the absence of human data conclusively linking CNT exposure to human disease (Bonner *et al.*, 2013), researchers and risk assessors rely on data from *in vivo* animal and *in vitro* cell culture models to investigate pathologies associated with CNT exposure. Data from these models suggest that the introduction of CNTs into the lung may be associated with lung inflammation, oxidative stress, fibrosis, gross cellular damage and toxicity, asthma, cancer, and extrapulmonary systemic effects.

Lung inflammation. The introduction of MWCNTs into the lungs of rats and mice has been associated with an innate immune response characterized by the influx and activation of macrophages and neutrophils (Ma-Hock *et al.*, 2009; Pauluhn, 2010b; Tabet *et al.*, 2011; Muhlfeld *et al.*, 2012; Bonner *et al.*, 2013). This neutrophilia is often accompanied by an increase in pro-inflammatory signaling detectable in lung mRNA expression and BALF levels of pro-inflammatory cytokines TNF-α (Tabet *et al.*, 2011; Tkach *et al.*, 2011; Muhlfeld *et al.*, 2012; Pothmann *et al.*, 2015) and IL-1β (Muller *et al.*, 2005; Muller *et al.*, 2008; Tkach *et al.*, 2011). While increased levels of eosinophils (Fenoglio *et al.*, 2012; Poulsen *et al.*, 2015b) and lymphocytes (Fenoglio *et al.*, 2012; Pothmann *et al.*, 2015) have also been reported, neutrophilia is the most consistent response across numerous studies with different MWCNTs, doses, exposure routes, and rodent models.

In general, this neutrophilia peaked within 24 h of a single exposure—typically via oropharyngeal aspiration (OPA) or intratracheal instillation (ITI)—and diminished within 1 – 4 weeks (Tkach *et al.*, 2011; Bonner *et al.*, 2013; Poulsen *et al.*, 2015b). However, neutrophilia was reported to persist up to 3 weeks after the end of a 90-d inhalation exposure in Wistar rats (Ma-Hock *et al.*, 2009), and up to 4 weeks following an acute dose of 100 µg/mouse delivered by ITI (Tabet *et al.*, 2011). This chronic inflammation—with its persistently activated macrophages and neutrophils, which release reactive oxygen species (Bhattacharya *et al.*, 2013)—may engender oxidative stress and, potentially, lead to further tissue damage, genotoxicity, and cancer (Bauer *et al.*, 2004; Rondini *et al.*, 2010; Sargent *et al.*, 2014; Pothmann *et al.*, 2015).

Oxidative stress. MWCNTs have been reported to both induce oxidative stress and to reduce it by quenching the formation of reactive oxygen species. MWCNTs may induce oxidative stress either directly through the generation of reactive oxygen species, or indirectly through the activation of neutrophils and NADPH oxidase activation in macrophages experiencing frustrated phagocytosis of MWCNT fibers (Nymark *et al.*, 2014).

Supportive evidence for the ability of MWCNTs to engender oxidative stress comes from multiple studies *in vivo*. In mice, exposure to MWCNTs was associated with a 40 – 50% decrease in lung tissue levels of the major cellular tripeptide antioxidant glutathione (GSH) (Shvedova *et al.*, 2008; Ravichandran *et al.*, 2011; Luyts *et al.*, 2014). Exposure was also associated *in vivo* with increased mRNA expression

of the redox-sensitive genes *Hmox1* and *Sod2* (Tabet *et al.*, 2011). Similarly, MWCNT exposure in murine macrophages was observed to decrease GSH levels (Fenoglio *et al.*, 2012), and to increase mRNA expression of *Hmox1* and *Sod2* (Bussy *et al.*, 2012).

Nonetheless, there is conflicting evidence about the ability of MWCNTs to either directly generate or quench reactive oxygen species. The iron catalysts contaminating MWCNTs from the manufacturing process may enable MWCNTs to generate acellular radicals through Fenton reactions (Fenoglio *et al.*, 2008; Madl *et al.*, 2014). This would be similar to iron-rich asbestos, which can generate hydroxyl radicals (Nymark *et al.*, 2014). In support of this, MWCNTs have been reported to generate acellular radicals detectable in electron spin resonance (ESR) spectra (Fenoglio *et al.*, 2008; Nymark *et al.*, 2014) or by the fluorescence reporter assay DCFDA (Fenoglio *et al.*, 2012; Poulsen *et al.*, 2015b). The latter assay is potentially unreliable, however, as MWCNTs have been observed to interfere with fluorescence-based assays (Xia *et al.*, 2013).

In contrast, MWCNTs have been observed to quench acellular radical generation—although this appeared to be contingent on the surface characteristics of the MWCNTs, and the components of the medium for resuspending the MWCNTs (Nymark *et al.*, 2014). While MWCNTs with intact graphene surfaces were observed to produce ESR spectra characteristic of hydroxyl radical generation, MWCNTs with defective surfaces (e.g., broken carbon-carbon bonds) actually produced no such spectra, perhaps indicating that these MWCNTs were capable of scavenging free radicals (Fenoglio *et al.*, 2008). Similarly, MWCNTs which had previously been observed to generate hydroxyl radicals in one medium with bovine serum albumin, were observed to no longer generate radicals in medium without bovine serum albumin (Nymark *et al.*, 2014).

Overall, the capacity for MWCNTs to induce oxidative stress may thus depend on both innate characteristics of the MWCNTs themselves, and the local conditions of the lung where they deposit.

Fibrosis. Lung fibrosis has been observed *in vivo* following MWCNT exposure, and was consequently used by the National Institute for Occupational Safety and Health (NIOSH) as the principal pathological endpoint for developing an inhalation-based recommended exposure limit in 2013 (NIOSH, 2013). As a pathological end stage of tissue repair, lung fibrosis involves the excessive deposition of collagen and extracellular matrix in the pulmonary interstitium, thereby impairing normal gas exchange

(Walkin *et al.*, 2013). Fibrosis is linked to both lung inflammation and oxidative stress, as leukocyte recruitment into the lungs may result in increased levels of cytokines and oxidants that promote fibrosis and epithelial cell hyperplasia (Muller *et al.*, 2005). Given that lung fibrosis is a debilitating disease associated with high mortality typically within 2 – 5 years of diagnosis (Walkin *et al.*, 2013), it is concerning that MWCNTs may be capable of inducing this pathological state.

Conflicting evidence for the association between MWCNT exposure and lung fibrosis comes from multiple studies in rats and several studies in mice. While Ma-Hock *et al.* observed no signs of pulmonary fibrosis or alveolar septal thickening in Wistar rats following a 90-d subchronic inhalation exposure of up to 2.5 mg/m^3 (Ma-Hock *et al.*, 2009), Pauluhn *et al.* reported an increase in soluble collagen, histopathological lesions, and pulmonary fibrosis in Wistar rats similarly exposed for 90 d to ≥ 0.4 mg/m^3 (Pauluhn, 2010b). The difference in outcomes between these two comparable studies may be due to the type of MWCNTs used (Nanocyl vs. Baytubes), or even Pauluhn's use of collagen-sensitive Sirius Red stain to evaluate fibrosis in histopathological samples (Pauluhn, 2010b).

While Pauluhn's study suggested that air concentrations comparable to those reported in a Korean manufacturer (Han *et al.*, 2008) may cause fibrosis, other studies in rats suggest that fibrosis may only be associated with acute exposures. Wistar and Sprague-Dawley rats exposed via ITI to extremely high acute doses (2 – 5 mg/rat) exhibited significantly greater lung levels of hydroxyproline and Type I collagen 60 d post-exposure (Muller *et al.*, 2005; Muller *et al.*, 2008). While there was a trend for lower doses also increasing hydroxyproline and collagen levels, these levels were only significant at the highest doses examined—suggesting that low-concentration exposures in the workplace may not lead to lung fibrosis after all.

In contrast to the conflicting data in rats, fibrosis has been observed in mice exposed to much lower doses of MWCNTs. Within 3 d of exposure via OPA to 18 – 162 µg of MWCNTs, C57BL/6 mice demonstrated perturbations in fibrosis pathways, notably in genes associated with exposure to other pro-fibrotic agents (bleomycin and chrysotile asbestos), as well as pathways regulated by TGFβ1 (Poulsen *et al.*, 2015b). TGFβ1 is a key mediator in promoting fibrosis, as it is involved in fibroblast to myofibroblast conversion and the epithelial-mesenchymal transition; both lead to more myofibroblasts and more collagen deposition (Walkin *et al.*, 2013; Poulsen *et al.*, 2015b). Similarly, C57BL/6 mice exposed via

OPA to 10 – 80 μg MWCNTs developed fibrosis detectable histopathologically within 7 d of exposure (Porter *et al.*, 2010). In another report, C57BL/6 mice exposed via OPA to 10 μg of short—but not long—MWCNTs had developed alveolar septal fibrosis and a thickened interstitium within 28 d of exposure. This difference was attributed to shorter MWCNTs being able to penetrate the interstitium, enter interstitial macrophages, and stimulate release of pro-fibrotic signaling molecules such as PDGF or TGFβ1 (Muhlfeld *et al.*, 2012).

Altogether, these data suggest that at least some individuals may be susceptible to lung fibrosis following MWCNT exposure, although this may depend on the dose and duration of that exposure, as well as physicochemical characteristics of the MWCNTs.

Gross cellular damage and toxicity. MWCNT-induced toxicity may derive from MWCNTs associating with cell membranes and consequent malfunction and damage; MWCNT-protein interactions which may inhibit enzymes; and the induction of oxidative stress (Nymark *et al.*, 2014). In general, gross cellular damage and toxicity *in vivo* has only been associated with acute exposure to MWCNTs.

Among rats, direct cellular damage—indicated by an increase in BALF levels of lactate dehydrogenase—has been observed following a 90-d subchronic inhalation exposure to 5.0 mg/m^3 (Pothmann *et al.*, 2015) or a single bolus dose of 2 mg via ITI (Muller *et al.*, 2008; Fenoglio *et al.*, 2012). *In vitro*, cytotoxicity has been reported in mesothelial cells directly penetrated by thin, rigid MWCNTs (Nagai *et al.*, 2011) and in murine alveolar macrophages (Fenoglio *et al.*, 2012).

In contrast, no evidence for increased BALF levels of lactate dehydrogenase or total protein—an indicator of alveolar/capillary barrier disruption—has been found in most studies. No evidence for toxicity or barrier disruption was found in mice exposed subacutely to 1 mg/m^3 (Mitchell *et al.*, 2009), rats exposed subchronically to concentrations under 5 mg/m^3 (Ma-Hock *et al.*, 2009; Pothmann *et al.*, 2015), or mice exposed once via OPA (Muhlfeld *et al.*, 2012). Among *in vitro* models, minimal cytotoxicity was detected in either exposed primary mouse macrophages (Hamilton *et al.*, 2013), RLE-6TN rat alveolar epithelial cells, BEAS-2B human bronchial epithelial cells, or THP-1 human monocytes/macrophages (Xia *et al.*, 2013). No cytotoxicity was observed in exposed A549 human lung epithelial cells, although in the latter there was a dose-response trend for apoptosis detectable by Hoechst staining (Ursini *et al.*, 2012).

While these results indicate that exposure to MWCNTs can be associated with gross damage to lung cells, it is likely that the damage is a non-specific consequence of acute exposures at high concentrations.

Asthma. In allergic asthma, common environmental antigens such as particulate matter trigger an aberrant immune response involving airway narrowing, eosinophilia, mucous hypersecretion, and fibrosis (Inoue *et al.*, 2009; Ronzani *et al.*, 2014). Data from *in vivo* and *ex vivo* experiments indicate that MWCNT exposure may exert different effects in humans with allergic asthma, compared to non-asthmatic populations.

Multiple experiments in mice sensitized to either ovalbumin or house dust mite extract, and then exposed to MWCNTs, have suggested that MWCNT exposure exacerbates the asthmatic pathology via increased airway fibrosis and eosinophilia. Similarly, pre-existing asthma was observed to exacerbate MWCNT-induced neutrophilia (Inoue *et al.*, 2009; Ryman-Rasmussen *et al.*, 2009; Ronzani *et al.*, 2014). Consistent with these *in vivo* observations, when human peripheral blood mononuclear cells (PBMCs) collected from volunteers with and without mite allergies were exposed *ex vivo* to MWCNTs, the allergic-derived PBMCs demonstrated a dose-dependent increase in lipopolysaccharide-stimulated release of TNF-α, IL-6, and IL-12 (Laverny *et al.*, 2013).

In the absence of ovalbumin or house dust mite sensitization, however, eosinophilia was not observed following MWCNT exposure *in vivo* (Inoue *et al.*, 2009; Ryman-Rasmussen *et al.*, 2009; Bonner *et al.*, 2013; Ronzani *et al.*, 2014).

These reports indicate that workers with allergic asthma or a family history of asthma (Bauer *et al.*, 2004) may be at risk for an exacerbation of allergic symptoms following MWCNT exposure, and that asthma may enhance the lung's inflammatory response to MWCNTs.

Cancer. In 2014, the well-studied Mitsui-7 MWCNTs were classified as possibly carcinogenic to humans (Group 2B) by the International Agency for Research on Cancer (IARC). Although IARC found that there was inadequate evidence to classify other MWCNTs or all SWCNTs (Group 3), it concluded that there was sufficient evidence that Mitsui-7 MWCNTs caused peritoneal mesothelioma in rats and male *p53*$^{+/-}$ mice, and promoted bronchioloalveolar adenoma and carcinoma in male mice following inhalation (Grosse *et al.*, 2014).

Nonetheless, the carcinogenicity of MWCNTs—and the mechanisms by which they may be carcinogenic—remains under investigation. Inflammation induced by MWCNT exposure may lead to angiogenesis promoted by macrophage-released factors, or via oxidative stress secondary to macrophage and neutrophil activation (Bauer *et al.*, 2004; Muller *et al.*, 2005; Nagai *et al.*, 2011; Sargent *et al.*, 2014). Oxidative stress may also result from the direct acellular generation of radical species by MWCNTs, perhaps through Fenton reactions involving residual metal catalysts (Madl *et al.*, 2014). These oxidants may then lead to carcinogenesis via DNA damage, notably through mutations affecting *Kras* and the tumor suppressor *Cdkn2a* (Bauer *et al.*, 2004).

There is conflicting evidence regarding the association between MWCNT exposure and genotoxicity. Supportive evidence comes from several *in vivo* and *in vitro* studies: Notably, C57BL/6 mice exposed via OPA developed DNA damage detectable by comet assays performed on lung tissue within 1 d of exposure to 18 µg MWCNT (Poulsen *et al.*, 2015b). Similarly, rats exposed via intraperitoneal injection of MWCNTs developed an aggressive and malignant mesothelioma, where the majority of tumors contained homozygous deletions of the tumor suppressor *Cdkn2a/2b* (Nagai *et al.*, 2011). DNA damage (e.g., micronucleus formation) was also detected *in vitro* following MWCNT exposure in A549 human alveolar carcinoma epithelial cells (Yamashita *et al.*, 2010; Ursini *et al.*, 2012), immortalized rat lung epithelial cells (Muller *et al.*, 2008), BEAS-2B human respiratory epithelial cells, and primary human small airway epithelial cells (SAECs) (Siegrist *et al.*, 2014).

Intriguingly, this genotoxicity may be due to mechanisms other than oxidant damage. In the BEAS-2B cells, MWCNTs were observed to localize to the nucleus, and to directly associate with DNA and centrosomes (Siegrist *et al.*, 2014). MWCNTs may also act by modulating cellular processes: C57BL/6 mice sacrificed 6 months after an acute dose of 100 µg MWCNT via ITI had increased lung markers of cell proliferation, vascularization, invasion, and autophagy, as well as histopathological indications of tumorigenesis (e.g., adenocarcinoma nodules, hyperplasia) (Yu *et al.*, 2013).

There is also evidence that MWCNTs may be incomplete carcinogens capable of tumor promotion. In support of this, B6C3F1 mice, sacrificed 17 months after a subacute inhalation exposure to 5 mg/m^3, only developed bronchioalveolar adenocarcinomas and adenocarcinomas when given the tumor initiator methylcholanthrene (Sargent *et al.*, 2014).

In contrast to these data supportive of carcinogenesis, Wistar rats exposed for 90 d via inhalation to 0.05 – 5 mg/m^3 Graphistrength C100 MWCNTs had negative results for lung and systemic DNA damage (Pothmann *et al.*, 2015). Similarly, a 2-year carcinogenicity study following a single intraperitoneal injection of MWCNTs into Wistar rats was negative for mesothelioma (Muller *et al.*, 2009).

While the best evidence indicates that MWCNTs may act more as tumor promoters than as complete carcinogens in the lung, this capability may increase the risk for lung cancer among workers exposed to common environmental initiators such as cigarette smoke and radon (Sargent *et al.*, 2014).

Extrapulmonary and systemic effects. While respiratory exposure to MWCNTs has been associated with numerous lung pathologies, there is some evidence for extrapulmonary effects principally involving the cardiovascular system, spleen, and immune function.

MWCNT exposure has been associated *in vivo* with an increase in cardiovascular disease markers, cholesterol dysregulation, and atherosclerosis. Among spontaneously hypertensive rats—a model of human hypertension used to study cardiovascular disease—an acute MWCNT exposure induced systemic inflammation and a significant increase in blood levels of fibrinogen and angiotensin-converting enzyme (Chen *et al.*, 2015). Similarly, C57BL/6 mice exposed via ITI to 18 – 162 µg MWCNT developed persistently elevated serum amyloid A protein levels. These levels correlated strongly with mRNA levels in the lung, but not the liver, thereby indicating a pulmonary origin for this risk marker. Given that serum amyloid A can affect blood lipid homeostasis and the regulation of cholesterol biosynthesis, it was unsurprising that the highest MWCNT exposure was associated with a significant increase in total cholesterol (Poulsen *et al.*, 2015a). Furthermore, among C57BL/6 mice deficient for *ApoE*, MWCNT exposure in conjunction with a high-fat diet significantly accelerated plaque progression, which was likely mediated through pulmonary and systemic inflammation and oxidative stress (Cao *et al.*, 2014).

Both the spleen and the immune system may be affected by respiratory exposure to MWCNTs. Although tracer experiments with MWCNTs injected intravenously into BALB/c mice indicated that MWCNTs distributed within 24 h to the lungs, liver, and spleen (Gao *et al.*, 2011), no spleen deposition was observed in C57BL/6 mice exposed via inhalation (Mitchell *et al.*, 2009). However, lung exposure was reported to exert systemic effects that modulated the immune response in the spleen. Among

C57BL/6 mice exposed subacutely via inhalation to 0.3 – 1.0 mg/m^3, there was no overt lung toxicity, but the spleen had increased expression of the prostaglandin-producing enzymes COX-2 and PTGES2. Furthermore, there was a dose-dependent decrease in the *ex vivo* T-cell-dependent antibody response to sheep erythrocytes among splenic T cells recovered from exposed mice (Mitchell *et al.*, 2009). Immunosuppression was also observed in BALB/c mice exposed via OPA to 40 – 120 µg SWCNTs, with T cell proliferation suppressed in the spleen (Tkach *et al.*, 2011). While the latter study proposed that the lung's activated dendritic cells had migrated to lymphoid tissues and presented SWCNTs—thereby affecting splenic T cells (Tkach *et al.*, 2011)—the former study suggested that alveolar macrophages phagocytizing MWCNTs secreted TGF-β, which entered systemic circulation and had anti-inflammatory effects on the spleen (Mitchell *et al.*, 2009).

In contrast to these reports, other studies in animal models and even humans found no such systemic effects. In a case series involving 9 workers directly handling MWCNTs and 4 controls, no differences in hematology and blood biochemistry were observed (Lee *et al.*, 2015b). Similarly, neither systemic toxicity nor histopathological lesions in the spleen were observed in rats exposed for 90 d via inhalation of MWCNTs (Ma-Hock *et al.*, 2009; Pauluhn, 2010b). However, these studies were not explicitly investigating immune function, and may have thus missed the immunosuppressive effects observed in mice.

1.4. Knowledge gaps in understanding MWCNT-induced lung toxicity.

Role of physicochemical characteristics. The rapid and continuing development of heterogeneous MWCNTs exceeds current abilities to perform animal safety testing (Xia *et al.*, 2013), and even impaired the ability of the IARC working group in 2014 to classify MWCNTs as a group as carcinogenic (Grosse *et al.*, 2014). Given that MWCNTs encompass huge variation in aspect ratio, surface functionalization, and contamination with metals and carbonaceous materials, there is a pressing need to identify key MWCNT characteristics associated with lung toxicity (Muller *et al.*, 2005; Johnston *et al.*, 2010; Bhattacharya *et al.*, 2013; Kim *et al.*, 2014; Poulsen *et al.*, 2015b). To date, while extensive evidence indicates that the lung's pathological response varies with MWCNT characteristics, there is conflicting evidence about the

pathological association with specific characteristics, notably MWCNT length, diameter, surface functionalization, and surface defects

One such disagreement concerns the conflicting reports about the toxicity of longer compared to shorter MWCNTs. Evidence from research into asbestos fibers supports a "long fiber paradigm" of toxicity, where the mesothelium was observed to be more sensitive to longer asbestos fibers (Poland *et al.*, 2008), and that the most carcinogenic fibers were more than 5 μm long (Nagai *et al.*, 2011; Sargent *et al.*, 2014).

In support of this long fiber paradigm for MWCNTs, C57BL/6 mice exposed via ITI to short (0.8 μm) and long (4 μm) MWCNTs developed comparable neutrophilia, but the long MWCNTs induced DNA damage more quickly and at lower doses. Furthermore, the long MWCNTs altered the expression of more genes and pathways associated with fibrosis, and were associated with worse fibrosis histopathologically (Poulsen *et al.*, 2015b). Additional supportive evidence for the long fiber paradigm comes from multiple studies involving direct injection of MWCNTs into the pleural or peritoneal cavities. Among C57BL/6 mice injected into the pleural cavity with long or short MWCNTs, only the mice exposed to long MWCNTs developed significant neutrophilia and increases in the protein levels of pleural lavage fluid (Murphy *et al.*, 2011). Similar results were reported for C57BL/6 mice exposed by intraperitoneal injection (Poland *et al.*, 2008). Furthermore, C57BL/6 mice injected intraperitoneally with long MWCNTs (5 – 15 μm) had significantly greater cell influx into the peritoneal cavity compared to shorter (< 2 μm) MWCNTs, with exposures to these same tubes *in vitro* showing that the long induced the most DNA damage in A549 human alveolar carcinoma epithelial cells (Yamashita *et al.*, 2010).

The enhanced toxicity of longer MWCNTs has been attributed to their increased persistence observed in multiple studies (Muller *et al.*, 2005; Hamilton *et al.*, 2013), perhaps as a consequence of frustrated phagocytosis in macrophages and/or of impaired clearance to the lymph nodes (Johnston *et al.*, 2010; Murphy *et al.*, 2011; Muhlfeld *et al.*, 2012). However, the observed toxicity of longer MWCNTs in the peritoneal or pleural cavities may reflect tissue-specific differences between those cavities and the lungs.

In contrast to this long fiber paradigm, other reports support the argument that shorter MWCNTs may be more toxic to the lung. Among C57BL/6 mice exposed to a panel of MWCNTs, the mice

developed significant neutrophilia following exposure to short but not long MWCNTs (Hamilton *et al.*, 2013). A separate set of investigators found that C57BL/6 mice exposed to short MWCNTs developed significantly more neutrophilia, as well as increased alveolar septal fibrosis and thickened interstitium (Muhlfeld *et al.*, 2012). Similar results were observed in Sprague-Dawley rats exposed by ITI to acute doses of short or long MWCNTs, where exposure to the short MWCNTs was associated with persistently elevated levels of TNF-α and increased levels of hydroxyproline and Type I collagen (Muller *et al.*, 2005).

Shorter MWCNTs may thus be able to disperse better throughout the lung parenchyma (Muller *et al.*, 2005), more effectively penetrate the interstitium to induce fibrosis (Muhlfeld *et al.*, 2012), and better induce inflammasome activation in macrophages by more effectively permeabilizing the phagolysosome (Hamilton *et al.*, 2013).

Similar to the debate over the association between MWCNT length and toxicity, there is conflicting evidence about the role of MWCNT diameter. On the one hand, thicker MWCNTs may be more rigid and therefore more capable of disrupting the phagolysosome membrane following phagocytosis, thereby activating the inflammasome (Hamilton *et al.*, 2013). Consistent with this, MWCNTs with the thickest diameter (30 – 50 nm) provoked more neutrophilia in C57BL/6 mice exposed via OPA to 50 µg, when compared to MWCNTs with a similar length but narrower diameter (10 – 20 nm). These thicker MWCNTs were also retained to a greater extent in the lung than the thinner MWCNTs, indicating that their larger size may impede macrophage clearance (Hamilton *et al.*, 2013).

On the other hand, there is more evidence for thinner MWCNTs inducing inflammation both *in vivo* and *in vitro*. Only thin MWCNTs (9 nm) induced significant neutrophilia, eosinophilia, and lung toxicity indicated by elevated BALF lactate dehydrogenase levels when given at 2 mg/rat via OPA to Wistar rats, compared to thick MWCNTs (70 nm). These same thin MWCNTs were more cytotoxic and depleted more total GSH *in vitro* in murine alveolar macrophages (Fenoglio *et al.*, 2012). Similarly, MWCNT diameter was inversely related to cytotoxicity in mesothelial cells *in vitro*, with the thin, rigid MWCNTs best able to penetrate cells independent of active internalization processes (Nagai *et al.*, 2011).

Pathology may also be influenced by MWCNT surface characteristics. Surface functionalization may influence agglomeration and interactions with cells and cellular receptors, which may alter pathology (Bonner *et al.*, 2013) and clearance from the body. Common surface functionalizations include hydroxyl,

carboxyl, and ammonium groups, as well as much larger moieties (e.g., proteins, drugs) which can be attached to the CNT surface via these smaller groups (Johnston *et al.*, 2010). Unsurprisingly, the pathological effects of these functionalization groups varies.

There are conflicting reports about the effect of hydroxylation and carboxylation on MWCNT toxicity. Carboxylated MWCNTs were observed to be non-inflammogenic in THP-1 cells *in vitro* (Xia *et al.*, 2013), and in primary mouse alveolar macrophages *ex vivo* (Hamilton *et al.*, 2013), when compared to MWCNTs which had not been functionalized or to MWCNTs which had been acid-purified post-synthesis. In contrast, oxidation may shorten MWCNTs and improve the dispersion of MWCNTs throughout the lung (Johnston *et al.*, 2010), which are both characteristics associated with more inflammogenic MWCNTs (Muller *et al.*, 2005; Muhlfeld *et al.*, 2012). Similarly, oxidized MWCNTs were more genotoxic *in vitro* than pristine MWCNTs (Ursini *et al.*, 2012).

Other types of surface groups can modulate toxicity *in vivo*. In a comparison of uncoated, acid-based polymer-coated, and polystyrene-based polymer-coated Graphistrength MWCNTs in BALB/c mice exposed by ITI to 10 – 100 µg, while all three induced significant neutrophilia, only the polystyrene-based coating was associated with increased markers of oxidative stress and fibrosis. These effects may have been mediated by coating-dependent differences in macrophage phagocytosis (Tabet *et al.*, 2011). In a separate study of mice exposed intravenously, ammonium-functionalized MWCNTs accumulated less in the lungs, kidneys, spleen, and liver, indicating improved solubility and excretion from the body (Johnston *et al.*, 2010).

These disagreements within the scientific literature about the roles of MWCNT physicochemical characteristics are likely exacerbated by significant interlaboratory confounders (Bonner *et al.*, 2013). To control for such confounders, we will examine how lung inflammation and oxidative stress are associated with MWCNT length, diameter, surface carboxylation, and acid purification in a panel of systematically different MWCNTs. **Aim 1 will therefore elucidate which physicochemical characteristics of nine well-characterized MWCNTs are associated with acute lung pathology in A/J mice.**

Role of genetic variability and context of C57BL/6 mouse response. Numerous investigations into MWCNT-associated lung pathology have used the ubiquitous C57BL/6 strain (Shvedova *et al.*, 2007;

Poland *et al.*, 2008; Shvedova *et al.*, 2008; Mitchell *et al.*, 2009; Ryman-Rasmussen *et al.*, 2009; Porter *et al.*, 2010; Yamashita *et al.*, 2010; Murphy *et al.*, 2011; Pacurari *et al.*, 2011; Wang *et al.*, 2011; Muhlfeld *et al.*, 2012; Shvedova *et al.*, 2012a; Bonner *et al.*, 2013; Hamilton *et al.*, 2013; Yu *et al.*, 2013; Cao *et al.*, 2014; Sargent *et al.*, 2014; Poulsen *et al.*, 2015a; Sun *et al.*, 2015). By relying exclusively upon the C57BL/6 strain to model respiratory pathology, MWCNT toxicity studies may be biased by this strain's particular combination of susceptibilities and resistances. The C57BL/6 mouse's immune response is skewed towards a pro-inflammatory, Th1 response; this strain is less susceptible to tumors; and this strain fails to recapitulate human asthma-like airway hyperreactivity following ovalbumin exposure (Rivera and Tessarollo, 2008). Thus, the use of predominantly C57BL/6 mice may underestimate potential pathologies associated with MWCNT exposure, including eosinophilic Th2 responses, asthma, and lung carcinogenesis.

While using the isogenic C57BL/6 strain improves study reproducibility, limits cost, and offers experimental advantages in mechanistic studies (King-Herbert and Thayer, 2006), previous investigations have demonstrated that the choice of strain significantly modulates the respiratory pathology observed. Furthermore, strains can demonstrate differential susceptibility across studies and toxicants. For example, while A/J mice resisted lung neutrophilia induced by ozone (Vancza *et al.*, 2009) and zinc oxide (Wesselkamper *et al.*, 2001b), they were sensitive to neutrophilia induced by vanadium pentoxide (Rondini *et al.*, 2010) and quantum dots (Scoville *et al.*, 2015). Similarly, 129 mice resisted lung inflammation induced by asbestos (Jun *et al.*, 2011) but not zinc oxide (Wesselkamper *et al.*, 2001b).

Furthermore, susceptibility to one form of pathology does not automatically confer susceptibility to others. While C57BL/6 mice were highly susceptible to fibrosis induced by bleomycin (Walkin *et al.*, 2013) and asbestos (Jun *et al.*, 2011), they resisted inflammation and lung toxicity induced by ozone (Vancza *et al.*, 2009) and quantum dots (Scoville *et al.*, 2015).

Evaluating the effects of a toxicant in multiple strains imparts a number of advantages. First, multi-strain studies can identify mouse models with pathological characteristics and susceptibilities which recapitulate human diseases, particularly subpopulations of patients (Montagutelli, 2000). Second, the use of multiple strains can better capture the range of potential pathological responses in a genetically heterogeneous human population, thereby improving risk assessments (King-Herbert and Thayer, 2006;

Rivera and Tessarollo, 2008). And third, multi-strain studies can provide data to identify genetic polymorphisms underlying the differential response to environmental toxicants in humans (King-Herbert and Thayer, 2006).

These differences in strain susceptibility and genetics have been exploited for quantitative trait loci (QTL) analyses, which can identify genetic regions accounting for differences in phenotype (Montagutelli, 2000; Bauer *et al.*, 2004). QTL analyses have identified the locus for susceptibility to ozone inflammation on mouse chromosome 17, which contains the genes for the major histocompatibility complexes and *Tnfα*. This region is homologous to human chromosomes 6 and 21. Furthermore, susceptibility to toxicant-induced inflammation and tumor promotion has been identified on mouse chromosome 18, while susceptibility to bleomycin-induced fibrosis has been localized to mouse chromosome 11 (Bauer *et al.*, 2004). QTL analyses—which require multiple strains—can thus be used to identify genes to be further studied in knockout experiments, or to corroborate knockout experiments conducted with toxicants similar to MWCNTs (e.g., asbestos, carbon black).

In Aim 2 we will determine if there is a differential response to MWCNT-induced acute lung inflammation across ten isogenic mouse strains. This aim will identify mouse models best suited for further investigations into different forms of MWCNT-induced pathology; for understanding the potential range of responses in a genetically heterogeneous worker population; and to select strains with the most disparate responses for use in future QTL studies to identify loci associated with respiratory susceptibility to MWCNTs.

Role of glutathione status and gender. Glutathione (GSH), a major cellular antioxidant composed of glutamic acid, cysteine, and glycine, is involved in regulation of the cell's redox state, cell signaling, and the immune response (Townsend *et al.*, 2003; Ghezzi, 2011). Numerous lung diseases are associated with GSH deficiency in lung tissue and epithelial lining fluid (ELF), including chronic bronchitis, chronic obstructive pulmonary disease, and idiopathic pulmonary fibrosis (Ghezzi, 2011). Exposure to MWCNTs may in turn lead to oxidative stress and GSH deficiency as a consequence of either the direct generation of oxidative radicals from Fenton reactions (Madl *et al.*, 2014) or through immune activation (Rondini *et al.*, 2010).

MWCNT exposure in humans has been reported to induce oxidative stress, and even to alter GSH-associated enzymes. In a case series of workers from the largest Korean MWCNT manufacturing firm, workers who handled MWCNTs had increased levels of oxidative stress markers (malondialdehyde, n-hexanal, and 4-HHE) in exhaled breath condensate (Lee *et al.*, 2015b). In one of the first epidemiological studies of MWCNT workers, an increased risk for exposure was associated with lung dysfunction and a decrease in glutathione peroxidase activity (Liao *et al.*, 2014). While preliminary, these studies suggest that oxidative stress—and potentially GSH depletion—may accompany occupational exposure to MWCNTs.

Multiple studies *in vitro* and *in vivo* have established that MWCNT exposure induces oxidative stress and alters GSH levels. When murine alveolar macrophages were exposed to narrow, short MWCNTs, they were observed to lose total GSH reserves (Fenoglio *et al.*, 2012). Similarly, total GSH was decreased by 40 – 50% in mice exposed to CNTs (Shvedova *et al.*, 2008; Ravichandran *et al.*, 2011; Luyts *et al.*, 2014).

Given that MWCNT depletes GSH levels, other studies have investigated the effects of increasing GSH levels through N-acetylcysteine supplementation. In mice, N-acetylcysteine supplementation increased their GSH levels and protected the animals against MWCNT-induced fibrosis and neutrophilia (Sun *et al.*, 2015). Similarly, N-acetylcysteine administration ameliorated the effects of MWCNT exposure in murine macrophages (Bussy *et al.*, 2012).

While these studies suggest that GSH is affected by MWCNT exposure—and that increasing GSH may mitigate the consequences of exposure—none have examined the effects of pre-existing alterations to GSH levels on susceptibility to MWCNT exposure.

GSH levels can be perturbed through multiple means, from genetic polymorphisms in related enzymes to nutritional status impacting cysteine reserves. GSH can either be regenerated from oxidized GSH (GSSG) by glutathione reductase, or synthesized *de novo* in a two-step reaction. The first step is the rate-limiting synthesis of γ-glutamylcysteine by glutamate cysteine ligase (GCL), a heterodimer composed of a catalytic (GCLC) and modifier (GCLM) subunits. The second step is the addition of glycine to γ-glutamylcysteine to form reduced GSH, which is carried out by glutathione synthetase (Townsend *et al.*, 2003; McConnachie *et al.*, 2007). Multiple factors influence cellular GSH levels, from

nutrition to oxidative stress arising from toxicant exposure or health disorders. Oxidative stress can trigger increased GSH production by, for example, depleting GSH levels—which induces increased production by itself—and by activating the transcription factor Nrf2, which increases GCL subunit transcription (Townsend *et al.*, 2003). For experimental purposes, GSH can also be depleted through treatment with the GCL inhibitor buthionine sulfoximine or by genetic manipulation of either *Gclc* (Dalton *et al.*, 2000) or *Gclm* (McConnachie *et al.*, 2007; Johansson *et al.*, 2010).

Mice deficient for the *Gclm* subunit are greatly impaired in their ability to synthesize GSH; *Gclm* knockouts thus have approximately 5 – 17% of the lung's total GSH compared to *Gclm* wild-types. *Gclm* heterozygous mice have approximately 77 – 90% of the lung's total GSH compared to wild-types (Weldy *et al.*, 2011; McConnachie *et al.*, 2013).

Unsurprisingly, *Gclm* genetic status in mice influences the pathological response to multiple respiratory toxicants. For example, following nasal instillation of diesel particles, male *Gclm* heterozygous mice had significantly greater lung neutrophilia and levels of pro-inflammatory cytokines compared to wild-type and knockouts (Weldy *et al.*, 2011). Nasal instillation of quantum dot nanoparticles significantly increased neutrophilia and TNF-α levels in male *Gclm* wild-type and heterozygotes compared to knockouts (McConnachie *et al.*, 2013). Similarly, ozone provoked lung inflammation in *Gclm* wild-type and knockout mice, although the knockouts generally had less neutrophilia. This ameliorated inflammation was attributed to compensatory upregulation of radical scavengers (e.g., metallothionein, α-tocopherol transporter protein, sodium-dependent vitamin C transporter) (Johansson *et al.*, 2010).

Intriguingly, the influence of GSH levels may differ by gender. Male mice overexpressing the GCL enzyme were better protected against acetaminophen-induced liver injury, compared to wild-type males and females overexpressing the GCL enzyme (Botta *et al.*, 2006). While this study would suggest that female mice are less dependent on GSH, it was also reported that female *Gclm* heterozygotes and knockouts were more susceptible to acetaminophen-induced liver injury (McConnachie *et al.*, 2007)—suggesting that GSH deficiency has greater negative effects on females than males.

Given the importance of GSH and related enzymes in regulating oxidative stress and inflammation within the lung, as well as the potential modifying factor of gender, **it is the goal of Aim 3 to investigate how *Gclm* status modulates susceptibility to MWCNT-induced acute lung pathology in**

male and female mice. By investigating susceptibility in *Gclm* heterozygote mice, we will gain information about the vulnerability of human subpopulations with moderate GSH deficiencies due to health conditions and genetic polymorphisms. By comparing susceptibility in *Gclm* wild-type to knockout mice, we will gain further mechanistic understanding of GSH's role in the acute inflammatory and toxic response to MWCNT exposure.

Chapter 2 : Aim 1

2.1. Introduction

The rapid expansion of carbon nanotube (CNT) research and development poses a health risk to the growing population of workers manufacturing and handling CNTs (Han *et al.*, 2008; Lee *et al.*, 2010; Dahm *et al.*, 2012). Data on the effects of multi-walled carbon nanotube (MWCNT) exposure *in vivo* and in human studies indicate that workers may be at risk for lung inflammation, oxidative stress, fibrosis, and dysfunction (Shvedova *et al.*, 2008; Ma-Hock *et al.*, 2009; Pauluhn, 2010b; Liao *et al.*, 2014; Lee *et al.*, 2015b). Recently, an International Agency for Research on Cancer working group classified one well-studied MWCNT, Mitsui-7, as possibly carcinogenic to humans (Group 2B). However, the working group designated all other CNTs as not classifiable (Group 3), because the lack of coherent evidence across different types of CNTs impeded generalization (Grosse *et al.*, 2014).

This lack of coherent evidence is unsurprising in light of the diversity of CNTs. MWCNTs vary in physical dimension, surface functionalization, graphene bonding defects, and the degree of contamination with metals and carbonaceous materials leftover from manufacturing. This diversity impedes risk assessments, as it is uncertain if a pathological response to one MWCNT can be extrapolated to other, dissimilar MWCNTs (Poulsen *et al.*, 2015b). Because not every MWCNT can be tested for toxicity, there is a pressing need to identify which physicochemical characteristics are most associated with lung pathology (Kim *et al.*, 2014; Nymark *et al.*, 2014). Nonetheless, there is disagreement over the pathological roles that specific characteristics play.

One disagreement concerns whether shorter or longer MWCNTs are more toxic. Several head-to-head comparisons of shorter (≤ 5 μm) to longer MWCNTs *in vivo* suggest that shorter MWCNTs may exacerbate cellular toxicity, neutrophil influx, and fibrosis (Muller *et al.*, 2005; Muhlfeld *et al.*, 2012; Hamilton *et al.*, 2013). However, these data contradict the "long fiber" paradigm drawn from asbestos research (Poland *et al.*, 2008). In support of this paradigm, longer MWCNTs have been reported to induce lung eosinophilia and exacerbate fibrosis (Poulsen *et al.*, 2015b). Further support comes from studies directly injecting MWCNTs into the pleural or peritoneal cavities; these found that longer (≥ 5 μm) MWCNTs induced greater cell influx (Yamashita *et al.*, 2010), neutrophil influx, and cell toxicity (Poland *et al.*, 2008; Murphy *et al.*, 2011).

Length is unlikely to be the sole determinant of toxicity, however, given existing data about surface functionalization and contamination. Carboxylated MWCNTs have been observed to induce greater cytotoxicity (Jain, 2012) and pro-inflammatory cytokine production *in vitro*, potentially because they interacted with the mannose receptor—which can promote inflammation—as well as with scavenger receptors during macrophage internalization processes (Gao *et al.*, 2011). However, oxidized MWCNTs were reported to induce less IL-1β production than non-oxidized MWCNTs *in vitro* (Xia *et al.*, 2013) and *in vivo* (Bonner et al., 2013), although these results were confounded by nickel contamination. In contrast to the disagreements about length and functionalization, most studies have found that contamination with transition metals (e.g., iron) enabled MWCNTs to generate more reactive oxygen species, provoke more inflammation, and promote fibrosis (Bussy *et al.*, 2012; Muhlfeld *et al.*, 2012; Bonner *et al.*, 2013; Xia *et al.*, 2013).

Given that these disagreements are likely exacerbated by interlaboratory confounders (Bonner *et al.*, 2013; Xia *et al.*, 2013), it is this aim's goal to control for these confounders while determining which physicochemical characteristics are associated with acute lung toxicity in a mouse model of respiratory exposure. By comparing nine MWCNTs that systematically differ in length, diameter, surface carboxylation, and post-synthesis acid treatment, it will be possible to identify the pathological role of these characteristics.

For this aim, I hypothesize that (1.1) within each of the three aspect ratios examined, the unpurified (stock), non-carboxylated class of MWCNTs will the most pro-inflammatory and toxic; and (1.2) within each of the three chemical classes examined, the MWCNT series #12, which has the shortest length and narrowest width, will be the most pro-inflammatory and toxic.

2.2. Materials and Methods

Reagents.

All reagents were obtained from Sigma-Aldrich (St. Louis, MO), unless otherwise indicated.

MWCNT source and generation.

To reduce the risk of MWCNT exposure to personnel, we followed the National Research Council's recommendations for personal protective equipment and engineering controls when handling nanomaterials (NRC, 2011b).

For these experiments, we used MWCNTs manufactured via catalytic chemical vapor deposition by Cheap Tubes, Inc., and purchased for use by the National Institute of Environmental Health Sciences (NIEHS) Centers for Nanotechnology Health Implications Research Consortium (NCNHIRC). The manufacturer supplied three MWCNTs with different aspect ratios: #12 (outer diameter, 10-20 nm; length, 0.5-2.0 μm); #13 (outer diameter, 30-50 nm; length, 0.5-2.0 μm); and #14 (outer diameter, 10-20 nm; length, 10-30 μm) (NCI, 2012).

For each of these MWCNTs, three chemical classes were derived, thereby giving us a panel of nine total MWCNTs. Stock samples were received as-is from the manufacturer, and presumably contained residual metal catalysts from manufacture as well as non-graphene carbonaceous materials. Carboxylated samples were generated from each stock sample by NCNHIRC collaborators at the New Jersey Institute of Technology. In brief, the stock sample was incubated with a solution of 1:1 concentrated H_2SO_4 and HNO_3 at 140°C for 20 min, cooled to room temperature, vacuum filtered (pore size 10 μm), and washed with deionized water until the wash water was a neutral pH. This carboxylated, washed sample was dried in a vacuum oven at 70°C.

Purified samples were also generated from each stock sample by NCNHIRC collaborators at the New Jersey Institute of Technology. Purification presumably would remove residual metal catalysts and non-graphene carbonaceous materials leftover from manufacture. The stock sample was incubated with HNO_3 (1 M) at 100°C for 10 min, cooled to room temperature, vacuum filtered (pore size 10 μm), and washed with deionized water until the wash water was a neutral pH. This purified, washed sample was dried in a vacuum oven at 65°C (NCI, 2012).

MWCNT characterization.

The physicochemical properties of these nine MWCNTs have been extensively characterized (NCI, 2012; Hamilton *et al.*, 2013; Xia *et al.*, 2013). In addition to the work reported by other investigators, we have also characterized properties of these MWCNTs when in liquid suspension, and captured images of the dry #12 stock and #12 purified MWCNTs using helium ion microscopy.

In brief, the Nanotechnology Characterization Laboratory (Frederick National Laboratory for Cancer Research, Frederick, MD) was tasked by NIEHS to conduct physicochemical characterizations. These characterizations included analyses of elemental composition by inductively coupled plasma mass spectrometry (ICP-MS) for 6/9 MWCNTs, and energy dispersive x-ray spectroscopy (EDS) for all nine MWCNTs, as well as analyses of endotoxin contamination for 3/9 MWCNTs through a kinetic turbidity Limulus Amoebocyte Lysate assay (NCI, 2012). Hamilton *et al.* similarly examined elemental composition through EDS, and also used scanning electron microscopy (SEM) to determine the average lengths and outer diameters for 6/9 MWCNTs (Hamilton *et al.*, 2013).

To characterize the aggregative properties of these nine MWCNTs in solution, we resuspended each sample to a concentration of 0.5 mg/ml in either distilled water or dispersion medium dosing vehicle [phosphate buffered saline (PBS) + 0.6 mg/ml mouse serum albumin + 10 µg/ml 1,2-dipalmitoyl-sn-glycero-3-phosphocholine surfactant in ethanol (0.1% v/v)] (Bonner *et al.*, 2013), sonicated the solution for 19 seconds in a Branson 2510 bath sonicator, and vortexed the solution for 1 second. We then measured the sample's equivalent hydrodynamic radii and zeta potentials via dynamic light scattering with a Zetasizer (Malvern Instruments Ltd., Malvern, UK).

To image the #12 stock and #12 purified MWCNTs, we resuspended the dry powder to 0.5 mg/ml in distilled water, sonicated the solution for 19 s in a Branson 2510 bath sonicator, and vortexed the solution for 1 second. The MWCNT solution was then drop-cast onto a transmission electron microscopy grid, and the images captured with a Helium Ion Microscope (ZEISS, Oberkochen, Germany).

Mice.

All animal experiments were conducted according to the guidelines provided in the National Institutes of Health Guide for the Care and Use of Laboratory Animals (NRC, 2011a), and with the approval of the University of Washington Institutional Animal Care and Use Committee. We made all efforts to minimize animal distress and suffering.

For these studies, we used 8-week-old male A/J mice obtained from The Jackson Laboratory. Mice were group housed in a modified specific pathogen free vivarium on a 12-hour light/dark cycle with nesting materials and access to water and chow provided *ad libitum*.

Experimental design.

To determine how the physicochemical characteristics of MWCNTs may influence lung pathology, we randomly assigned the A/J mice to receive 50 µl dispersion medium dosing vehicle only, or 50 µl vehicle containing 40 µg MWCNT, by oropharyngeal aspiration (n ≥ 3 mice/group, for a total of 39 mice). By comparison, a 10 µg MWCNT/mouse bolus dose was reported to approximate human lung deposition after one month of light work in an environment with an ambient MWCNT concentration of 400 µg/m^3, a level reported in Korean manufacturing settings (Han *et al.*, 2008; Porter *et al.*, 2010). Thus, our dose approximates four times the human lung deposition experienced under these conditions.

Thirty minutes prior to exposing the mice, we prepared fresh dispersion medium dosing vehicle (described under ***MWCNT characterization***), and resuspended the MWCNTs to 0.5 mg/ml in this fresh vehicle. Both the vehicle control and MWCNT solutions were sonicated for 19 seconds in a Branson 2510 bath sonicator, and then vortexed for 1 second.

Immediately before exposure, each mouse was weighed and anesthetized with 4% Isoflurane. The mouse was exposed via oropharyngeal aspiration (OPA) of 50 µl dispersion medium only, or 50 µl dispersion medium containing 40 µg MWCNTs, as previously described (Bonner *et al.*, 2013). OPA was selected as the means of exposure because it is quick, the dose is well-controlled, and the dose distributes well throughout the lung; furthermore, OPA reduces risk to personnel compared with inhalation exposure regimes (Poulsen *et al.*, 2015b).

Following OPA, we monitored the mice until they recovered from anesthesia, and then for any signs of distress (e.g., weight loss, huddling, unkempt fur) over the next 24 h. We observed neither distress nor mortality associated with treatment and handling.

Twenty-four h after exposure, each mouse was weighed to determine its post-treatment weight, and then humanely euthanized through CO_2 narcosis followed by cervical dislocation. We performed bronchoalveolar lavage (BAL) with two serial lavages of sterile PBS (1.2 ml, 0.6 ml), using previously described methods (McConnachie *et al.*, 2013). From the first lavage, we removed aliquots for cytospin/differential staining of the recovered cells, and for fluorescent labeling of the recovered cells for flow cytometry. The remainder was centrifuged and the acellular supernatant (bronchoalveolar lavage fluid, BALF) was saved for future measurements of total protein concentration and lactate dehydrogenase concentration.

Along with BALF, we collected blood via cardiac puncture for serum isolation via serum separator tubes (Becton, Dickinson and Company, Franklin Lakes, NJ). We removed a lung tissue sample from the right caudal lobe and immersed this sample in RNA*later*® Stabilization Solution (Ambion via Thermo Fisher Scientific Inc., Waltham, MA) for 24 h at 4 °C. The stabilized sample was then frozen at -80 °C for later RNA extraction. The remainder of the right lung was snap-frozen in liquid nitrogen and stored at -80 °C for future measurements of glutathione (GSH) content and total protein.

Differential staining of cytospin slides to assess lung neutrophilia.

To quantify the percentage of neutrophils among cells recovered through BAL, we performed differential scoring of the cells recovered in the first BAL. We centrifuged the cells onto cytospin slides, and then differentially stained them using the Hema 3™ system (Thermo Fisher Scientific, Waltham, MA), which is a derivative of the Wright-Giemsa staining method. We determined the percentage of specific inflammatory cell types (eosinophils, lymphocytes, macrophages/monocytes, and neutrophils) by counting at least 500 cells per slide.

Flow cytometry assessment of lung neutrophilia.

To quantify the percentage of neutrophils among cells recovered through BAL, we performed flow cytometry using a Cytopeia Influx flow cytometer (BD Biosciences, San Jose, CA) as previously described (McConnachie *et al.*, 2013). In brief, we stained BAL cells with an anti-F4/80 antibody conjugated to Alexa Fluor 488 (eBioscience, San Diego, CA), which stains murine macrophages, and an anti-CD11b antibody conjugated to phycoerythrin (eBioscience), which preferentially stains murine neutrophils. After gating to exclude small particles (e.g., the membranes of lysed erythrocytes), we identified neutrophils as having high CD11b expression and low F4/80 expression. Macrophages were identified as having intermediate CD11b expression and high F4/80 expression. We gated cytograms to exclude cells with low-intermediate staining, and therefore ambiguous, phenotypes. The flow cytometry data were further analyzed using FlowJo software (FlowJo, LLC, Ashland, OR).

Assessment of MWCNT internalization by alveolar macrophages.

To evaluate how MWCNT physicochemical characteristics may affect uptake and retention by macrophages, we scored macrophages for visible MWCNT inclusions under a light microscope (20x), as previously described (Silva *et al.*, 2014). We counted at least 500 macrophages for each sample.

Measurement of total glutathione in lung tissue.

We evaluated the association between severe oxidative stress and MWCNT physicochemical characteristics by measuring levels of the major cellular antioxidant glutathione in lung tissue. In the lung tissue, we quantified the total glutathione (reduced and oxidized glutathione) content of clarified lung homogenates using methods described previously (McConnachie *et al.*, 2013). The total GSH content was normalized to the total protein concentration of the lung homogenates, which we determined using a commercial Bradford protein assay kit (Bio-Rad Laboratories, Inc., Hercules, CA).

Quantification of mRNA levels for genes associated with early pathological responses through quantitative real-time PCR.

Using methods previously described, the University of Washington's Center for Ecogenetics and Environmental Health Functional Genomics and Proteomics Core measured the mRNA levels of ten target genes and one normalizing gene using fluorogenic 5' nuclease-based assays (McConnachie *et al.*, 2013). In brief, we extracted total RNA from the RNA*later*®-stabilized lung sample with the miRNeasy Mini Kit (Qiagen, Venlo, The Netherlands), and then generated cDNA from 1 µg total RNA using the SuperScript® III First-Strand Synthesis System (Life Technologies, Carlsbad, CA). This PCR reaction mix contained TaqMan Gene Expression Master Mix (Applied Biosystems, Inc., Foster City, CA), primers, and dual-labeled probes for each gene. The primers and probes were designed using ABI Primer Express v1.5 (Applied Biosystems), and the targets amplified and detected on an ABI PRISM 7900 system (Applied Biosystems) using a previously published reaction profile (McConnachie *et al.*, 2013). The mRNA levels were calculated using a linear regression formula derived from *Gapdh* amplification plots with serial dilutions of an established reference.

We analyzed the following mRNAs: cystic fibrosis transmembrane regulator (*Cftr*), glutamate cysteine ligase catalytic subunit (*Gclc*), glutamate cysteine ligase modifier subunit (*Gclm*), granulocyte-macrophage colony stimulating factor (*Gmcsf*), heme oxygenase-1 (*Hmox1*), interleukin-1β (*Il1β*), Cxcl1/keratinocyte-derived cytokine, (*Kc*), monocyte chemotactic protein-1 (*Mcp1*), transforming growth factor-β 1 (*Tgfb1*), and tumor necrosis factor-α (*Tnfα*). We used *Gapdh* mRNA levels to normalize the expression of these ten genes.

Evaluation of lung toxicity using bronchoalveolar lavage fluid.

We evaluated the association between MWCNT physicochemical characteristics and lung toxicity by measuring BALF concentrations of total protein and acellular lactate dehydrogenase in the first BAL. These respectively reflect disruption of the alveolar/capillary barrier's integrity, and cellular death (Wesselkamper *et al.*, 2001a).

To measure the concentration of total protein, we used a commercial Bradford protein assay kit (Bio-Rad Laboratories). To measure the concentration of lactate dehydrogenase, we used the enzyme activity CytoTox 96® Non-Radioactive Cytotoxicity Assay (Promega Corporation, Madison, WI).

Generation of heatmap summarizing pathological responses to MWCNT panel.

To summarize and compare all pathological responses to each of the nine MWVNTs, we created a heatmap of the log(fold-change) value for each endpoint. The fold-change compares the mean for each MWCNT-exposed group to the mean of the control group. The heatmap was created using the heatmap.2() function available in the R package, gplots, with the clustering options disabled.

Statistical analyses.

We analyzed the data using a one- or two-way analysis of variance (ANOVA) and, when these tests indicated significant associations, performed post-hoc analyses using unpaired, two-tailed *t*-tests. The resulting *p*-values were adjusted with Bonferroni corrections for multiple comparisons. When determining the correlation between variables, we calculated Pearson's correlation coefficients and report the two-tailed *p*-values for significance. Significance was set at $\alpha = 0.05$. Data were managed in Excel 2013 (Microsoft, Redmond, WA), and analyzed in Prism 5 for Windows, v.5.02 (GraphPad Software, Inc., La Jolla, CA).

2.3. Results

Characterization of physicochemical and aggregative characteristics of MWCNT panel.

For these experiments, we used a panel of nine MWCNTs (Table 2.1) developed from three unmodified MWCNTs with different aspect ratios. These original three MWCNTs were provided to NCNHIRC by Cheap Tubes, Inc. (Cambridgeport, VT). For each aspect ratio, an NCNHIRC collaborator (Dr. Somenath Mitra, New Jersey Institute of Technology) derived three different chemical classes: a stock sample (unmodified); a carboxylated sample (outer surface functionalized with carboxyl groups);

and a purified sample (acid-treated to remove residual metals and non-graphene carbonaceous materials). Thus, our panel consists of the thin/short #12 series (#12 stock, #12 carboxylated, #12 purified); a wide/short #13 series (#13 stock, #13 carboxylated, #13 purified); and a thin/long #14 series (#14 stock, #14 carboxylated, #14 purified).

On behalf of the NCNHIRC, the Nanotechnology Characterization Laboratory characterized the physicochemical traits of these nine MWCNTs (Table 2.2). Imaging via SEM confirmed that all nine samples consisted of CNTs of varying lengths and diameters (NCI, 2012). We verified this observation by capturing images via helium ion microscopy of the #12 stock and #12 purified MWCNTs (Figure 2.1) with collaborators at the Environmental Molecular Sciences Laboratory in the Pacific Northwest National Laboratory (PNNL). Hamilton *et al.* quantified the dimensions of the #12 and #13 series through SEM, but did not collect data on the dimensions of the #14 series due to its excessive tangling (Hamilton *et al.*, 2013). These measurements for all three stock samples fell within the dimensions specified by Cheap Tubes, Inc. (Table 2.1). These results also suggested that surface carboxylation had increased the outer diameter of the MWCNTs in each series (Table 2.2).

In addition to imaging, the Nanotechnology Characterization Laboratory examined the elemental composition of all nine MWCNTs using SEM EDS. Four elements were quantified: carbon, oxygen, nickel, and iron (Table 2.2). Unsurprisingly, carbon constituted the vast majority of the elements (88.6 – 95.9% by weight), followed by oxygen (2.9 – 8.0%), nickel (0.2 – 2.3%), and iron (0.3 – 0.9%). Within each series, the carboxylated MWCNT had more oxygen than the stock or purified MWCNTs, consistent with successful surface carboxylation. However, acid purification had not reduced the residual metals, nickel and iron, contaminating the stock samples (NCI, 2012).

The Nanotechnology Characterization Laboratory also attempted to quantify endotoxin contamination of the #12 series using the kinetic turbidity Limulus Amoebocyte Lysate assay (Table 2.2). However, spike-and-recovery experiments suggested that endotoxin binds to the MWCNTs. Instead of direct measurements, the #12 series were resuspended to 1 mg/ml in distilled water, centrifuged, and the supernatant recovered for performing the assay (NCI, 2012). Using this indirect approach, it was determined that the #12 carboxylated MWCNT was significantly contaminated with 11.7 EU/mg of endotoxin. This was likely introduced during the carboxylation procedure, and endotoxin may similarly

contaminate the #13 and #14 carboxylate MWCNTs; by comparison, #12 stock only had 0.06 EU/mg, which was reduced 12-fold by the acid purification to 0.005 EU/mg in the #12 purified MWCNT.

Our collaborators at PNNL used Raman spectroscopy to examine surface defects and the presence of non-graphene carbonaceous material in the #12 stock and purified samples. Acid purification did not introduce significant surface defects, based on the intensity ratio—a ratio of the intensity of the signature peak corresponding to defective bonding, I_D, to the signature peak corresponding to intact graphene, I_G. Indeed, the I_D/I_G ratios were comparable between the samples: The #12 stock I_D/I_G was 0.7596, and the #12 purified I_D/I_G was 0.7869. However, Raman spectroscopy did detect a more intense G-band signal in the #12 purified MWCNT (23.778 arbitrary units) compared to the #12 stock MWCNT (21.842 arbitrary units). This suggested that the #12 purified contains slightly fewer non-nanotube carbonaceous impurities (Miyata *et al.*, 2011).

Along with our collaborators in the University of Washington's Chemical Engineering department, we characterized the aggregative properties of all nine MWCNTs when resuspended in distilled water or dispersion medium vehicle (Table 2.3). Using the Zetasizer (Malvern Instruments Ltd., Malvern, UK), we performed dynamic light scattering to measure the equivalent hydrodynamic radii of the aggregates formed by these MWCNTs in liquid suspension. When resuspended in distilled water, the MWCNTs formed aggregates with equivalent hydrodynamic diameters from 202.8 – 340.3 nm. MWCNT aggregates in dispersion medium tended to have larger diameters, which ranged from 425.4 – 1,206.0 nm. By comparison, MWNCTs in manufacturing settings form complex bundles of nanotubes, metal catalysts, and other carbonaceous material (Maynard *et al.*, 2004) which reach sizes of 400 – 2,000 nm in diameter (Lam *et al.*, 2006); similar sizes of 1,000 – 3,000 have been reported from a rodent inhalation study (Pauluhn, 2010b).

We also measured each MWCNT's zeta potential, which reflects a particle's propensity to aggregate in solution; particles with zeta potentials from -30 to 30 mV tend to aggregate, while particles with zeta potentials outside of this range tend to form stable colloidal suspensions (Heurtault *et al.*, 2003). Consistent with our observations of MWCNTs forming aggregates with smaller equivalent diameters in water, we observed that the zeta potentials of all MWCNTs in water ranged from -52.7 to -36.1 mV—values consistent with less aggregative behavior, and therefore smaller aggregates. In contrast, the

MWCNTs formed larger aggregates in dispersion medium, and we correspondingly observed that the zeta potentials ranged from -15.4 to -9.2 mV—values consistent with pro-aggregative behavior. However, we observed no significant correlation between the zeta potentials and equivalent diameters in either water (Pearson's $r = 0.5583$, $p = 0.1182$) or dispersion medium ($r = -0.2981$, $p = 0.4359$), suggesting that other variables more significantly influence aggregation within these different media.

Lung neutrophilia.

To examine the association between the innate inflammatory response and MWCNT physicochemical characteristics, we quantified the proportion of neutrophils among cells recovered through BAL 24 h post-exposure using two methods: cytospins and flow cytometry (Figure 2.2 and Figure 2.3). These two methods produced results that were significantly correlated (Figure 2.2, B; Pearson's $r = 0.9409$, $p < 0.0001$). Thus, we are only presenting the cytospin data (Figure 2.2, A).

For the #12 and #13 series, the stock MWCNTs provoked the most neutrophilia, followed by the carboxylated and then the purified samples. Within the #14 series, the stock and carboxylated provoked comparable neutrophilia, followed by the purified sample. When comparing the same chemical class across the different series, the #13 stock and carboxylated MWCNTs provoked the most neutrophilia, followed by the #12 and then the #14 series. This trend was reversed for the purified samples, where the #14 purified provoked more neutrophilia than the #12 purified or #13 purified MWCNT.

Overall, when comparing the mean neutrophilia values for each aspect ratio across its three chemical classes, the #13 series had the greatest neutrophilia (16.10%), followed by the #12 series (10.50%) and then the #14 series (7.59%). When the nine MWCNTs were ranked from most inflammogenic to most inert based on neutrophilia, they ranked as follows: #13 stock > #12 stock > #13 carboxylated > #12 carboxylated > #14 carboxylated > #14 stock > #14 purified > #12 purified > #13 purified.

These results partially support hypothesis 1.1, because within two out of three aspect ratios, the stock MWCNT was the most inflammogenic. However, these results do not fully support hypothesis 1.2, because the #13 series—the short/wide MWCNT with the lowest aspect ratio—provoked the most neutrophilia overall.

Correlation between lung neutrophilia and bulk nickel content of MWCNTs.

Nickel contamination of carbonaceous particulate matter has been associated with increased cardiovascular- and respiratory-associated hospitalizations (Bell *et al.*, 2009), perhaps related to cardiopulmonary inflammation associated with increased NADPH oxidase activity (Cuevas *et al.*, 2015). Furthermore, nickel contamination of MWCNTs was associated with increased NLRP3 inflammasome activation *in vitro*, as well as worse lung pathology scores for C57BL/6 mice exposed to acute doses of nickel-contaminated MWCNTs (Hamilton *et al.*, 2012). Thus, we examined the association between lung neutrophilia and the dose of bulk nickel administered with the MWCNTs. Bulk nickel data were available for the #13 and #14 series, but due to concerns about endotoxin contamination, we omitted the #13 and #14 carboxylated MWCNTs from the analysis.

Lung neutrophilia was significantly correlated with the dose of bulk nickel administered to individual mice (Figure 2.4; Pearson's $r = 0.8358$, $p = 0.0007$). The dose-response slope was very steep, covering approximately a 40-ng difference in bulk nickel dose between the purified vs. the stock #13 and #14 MWCNTs. While these results suggest that greater contamination with bulk nickel may be one of the factors contributing to the stock MWCNTs inducing greater neutrophilia, these results cannot address either hypothesis 1.1 or 1.2, because the data were not stratified by aspect ratio or chemical class.

MWCNT internalization by alveolar macrophages.

To examine how MWCNT physicochemical characteristics may affect alveolar macrophage uptake and retention, we quantified the proportion of macrophages with visible MWCNT inclusions on cytospin slides (Figure 2.5 and Figure 2.6).

Both MWCNT aspect ratio and chemistry were significantly associated with the extent of MWCNT internalization by macrophages (two-way ANOVA aspect ratio $p = 0.0002$, chemistry $p = 0.0006$). Post-hoc analyses further indicated that within the stock chemical class, the mice exposed to the #12 and #13 MWCNTs had a significantly greater proportion of macrophages with internalized MWCNTs than the mice exposed to the #14 stock MWCNT. Similarly, mice exposed to the #13 carboxylated MWCNT had a significantly greater proportion of macrophages with internalized MWCNTs than did those exposed to the #14 carboxylated MWCNT; mice exposed to #12 also had a greater proportion than those exposed to #14, although this was statistically non-significant. Within mice exposed to the #12 and #13 series, there

was a non-significant trend of the stock and carboxylated MWCNT having a greater proportion of MWCNT with internalized MWCNTs than the purified MWCNT.

We further observed that across all nine MWCNTs, the proportion of macrophages with internalized MWCNTs significantly correlated with lung neutrophilia (Pearson's $r = 0.6161$, $p < 0.0001$).

These results indicate that the degree of MWCNT uptake and retention by alveolar macrophages is significantly associated with the physicochemical characteristics of the MWCNT. The most influential characteristic appears to be aspect ratio, as the #14 thin/long series had the lowest proportion of MWCNT internalization for all three of its chemical classes. MWCNT length, therefore, may play the most significant role in determining the extent of MWCNT internalization. As more MWCNT internalization correlated significantly with greater neutrophilia, this suggests that shorter MWCNT may induce greater inflammation.

These results support hypothesis 1.2, but not hypothesis 1.1, because we did not observe significant differences between chemical classes within the same aspect ratio.

Quantification of mRNA levels of chemoattractant and pro-inflammatory genes.

We determined how the exposure to MWCNTs with different physicochemical characteristics altered the expression of genes associated with immune cell recruitment and pro-inflammatory signaling. To do this, we measured the mRNA levels of genes associated with granulocyte production (granulocyte-macrophage colony stimulating factor, *Gmcsf*), neutrophil chemoattraction (Cxcl1/keratinocyte-derived cytokine, *Kc*), monocyte recruitment (monocyte chemotactic protein-1, *Mcp1*), and pro-inflammatory signaling (interleukin-1β, *Il1β*; tumor necrosis factor-α, *Tnfα*).

Exposure to any of the nine MWCNTs was only associated with a change in the mRNA levels of *Gmcsf* 24 h post-exposure (Table 2.4). The mRNA levels of *Gmcsf* were significantly increased among the groups exposed to the #13 carboxylated, #13 purified, #14 stock, and #14 purified MWCNTs. The expression of no other gene was significantly associated with MWNCT exposure.

Altogether, these results do not support hypothesis 1.1, because the expression of only one pro-inflammatory gene, *Gmcsf*, was associated with only one stock MWCNT. These results also do not support hypothesis 1.2, because the expression of most genes was unaltered. Furthermore, *Gmcsf* expression significantly increased for the #13 and #14 series, not the #12 series.

Total glutathione content in lung tissue.

To evaluate how oxidative stress may be associated with different MWCNT physicochemical characteristics, we measured the total glutathione content in lung tissue 24 h after exposing the mice to MWCNTs. We observed no significant differences between the three aspect ratios or between the three chemical classes of MWCNTs (Table 2.5). Therefore, these negative results do not support either hypothesis 1.1 or 1.2; instead, these results indicate that none of the nine MWCNTs evaluated induced severe oxidative stress measurable within 24 h of exposure.

mRNA expression of oxidative stress- and fibrosis-associated genes.

In addition to evaluating how different MWCNT characteristics may induce severe oxidative stress, we also examined how these characteristics may more subtly alter the expression of redox-sensitive and pro-fibrotic genes. Using qRT-PCR, we measured the mRNA levels of genes associated with glutathione synthesis (glutamate cysteine ligase catalytic subunit, *Gclc*; glutamate cysteine ligase modifier subunit, *Gclm*), oxidative stress (heme oxygenase-1, *Hmox1*), glutathione transport into lung epithelial lining fluid (cystic fibrosis transmembrane regulator protein, *Cftr*), and fibrosis (transforming growth factor-β 1, *Tgfb1*).

Exposure to any of the nine MWCNTs examined was not associated with a change in the mRNA levels of these genes 24 h after exposure (Table 2.6). When we examined the correlations between lung total glutathione levels and the mRNA levels of the redox-sensitive genes, we found that *Gclc* expression was significantly correlated with lung total glutathione (Pearson's $r = 0.3738$, $p = 0.0321$), consistent with GCLC's critical role in *de novo* glutathione synthesis (Franklin *et al.*, 2009).

Altogether, these results do not support either hypothesis 1.1 or 1.2, as there were no observed differences in the expression levels of genes associated with oxidative stress and fibrosis. Instead, these results indicate that at 24 h post-exposure, none of the MWCNTs was inducing subtle changes in the cell's redox status that would alter expression of redox-sensitive genes. These results also indicate that none of the physicochemical characteristics examined promoted early perturbations in TGFβ1-associated fibrosis pathways, such as the conversion of fibroblasts to myofibroblasts, or the epithelial-mesenchymal transition (Poulsen *et al.*, 2015b).

Lung toxicity.

Along with subtler forms of pathology, we also examined how MWCNT characteristics may be associated with gross lung toxicity and cellular damage. To evaluate the integrity of the lung's alveolar/capillary barrier and the extent of cell death, we measured BALF total protein levels and BALF acellular lactate dehydrogenase levels, respectively (Table 2.5).

We found that an interaction between MWCNT aspect ratio and chemistry was significantly associated with BALF total protein levels (two-way ANOVA $p = 0.0274$). When we further compared the three MWCNTs in each aspect ratio to the control group, our one-way ANOVA analyses were all non-significant. However, within each aspect ratio the stock MWCNT tended to have the highest levels of BALF total protein.

We similarly found that an interaction between MWCNT aspect ratio and chemistry was significantly associated with BALF lactate dehydrogenase levels (two-way ANOVA $p = 0.0015$). When we further compared each series to the control group using one-way ANOVA, only the results for the #14 series were significant ($p = 0.0013$). Post-hoc analyses indicated that lactate dehydrogenase levels were significantly higher for the #14 stock sample compared to the control group (t-test $p = 0.0054$). Within the other two aspect ratios, the stock MWCNT also tended to have generally higher lactate dehydrogenase levels. This trend in increased lactate dehydrogenase levels may account for the corresponding trend of increased BALF total protein levels, as these variables were significantly correlated (Pearson's $r = 0.5893$, $p < 0.0001$).

These results overall support hypothesis 1.1, because the stock samples for each aspect ratio generally had the highest lactate dehydrogenase and total protein levels, consistent with greater toxicity. However, these results do not support hypothesis 1.2, because the #14 series had the highest levels of lactate dehydrogenase and total protein.

Heatmap summarizing pathological responses to MWCNT panel.

To compare the pathological responses observed for each MWCNT, we created a heatmap of the log(fold-change) values for each endpoint (Figure 2.7). The fold-change compares the mean for each MWCNT-exposed group to the control group.

These data show that an innate inflammatory response was the most common pathological outcome following exposure to MWCNTs with different physicochemical properties. This innate

inflammatory response consists of a significant increase in neutrophilia for 4/9 MWCNTs, and a significant increase in mRNA levels of *Gmcsf* for 4/9 MWCNTs, although these endpoints were significantly increased together for only 2/9 MWCNTs. All three stock MWCNTs, 2/3 of carboxylated MWCNTs, and none of the purified MWCNTs significantly increased neutrophilia, although 2/3 of the purified MWCNTs did significantly increase *Gmcsf* expression.

We found no evidence for perturbations in redox-sensitive gene expression or the induction of severe oxidative stress associated with exposure to any of these MWCNTs. With the exception of the #14 stock MWCNT, which significantly increased BALF levels of lactate dehydrogenase, we observed no evidence for exposure to these MWCNTs being associated with lung toxicity.

Overall, our data indicate that all aspect ratios of MWCNTs are capable of inducing an acute inflammatory response, and that the stock and carboxylated classes of MWCNTs are more inflammogenic than the purified class.

2.4. Discussion

In this aim, we examined the association between specific physicochemical characteristics of MWCNTs and acute lung pathology in a mouse model of human respiratory exposure. Towards this end, we exposed adult male A/J mice via OPA to 40 μg of one of nine MWCNTs which differed in aspect ratio, surface carboxylation, and post-synthesis acid treatment. We sacrificed the mice 24 h later to evaluate the innate inflammatory response, oxidative stress, gross toxicity, and perturbations in related gene expression. We hypothesized that (1.1) within each of the three aspect ratios in our panel, the unpurified (stock), non-carboxylated class of MWCNT would be the most pro-inflammatory and toxic; and (1.2) within each of the three chemical classes (stock, carboxylated, acid-purified), the MWCNT with the shortest length would be the most pro-inflammatory and toxic.

Our results from examining the innate inflammatory response partially support hypotheses 1.1 and 1.2. Using both differential staining of cytospin slides and flow cytometry to analyze the types of cells recovered through BAL, we found that 4/9 MWCNTs significantly increased the percentage of neutrophils above that of the control group. Consistent with hypothesis 1.1, the #12 and #13 stock samples provoked the most neutrophilia in their series, followed by their carboxylated samples. The #14 stock provoked

neutrophilia comparable to the #14 carboxylated MWCNT. In contrast to hypothesis 1.2, the short/wide series #13 provoked the most neutrophlia overall, followed by #12 and then #14. Overall, these results indicate that the most inflammogenic MWCNTs are short and wide—characteristics which may make them stiffer and more needle-like—and have not been treated post-synthesis to remove metal or carbonaceous contaminats.

Our results suggest that bulk nickel contamination may influence MWCNT-induced inflammation. Without adjusting for aspect ratio or chemical class, we found that lung neutrophilia significantly and positively correlated with increasing amounts of bulk nickel administered along with MWCNTs. These results are consistent with previous observations that nickel exacerbates cardiopulmonary inflammation *in vivo* (Cuevas *et al.*, 2015), and that greater nickel contamination in particulate matter are associated with increased hospitalizations (Bell *et al.*, 2009). Indeed, *in vitro* and *in vivo* data suggest that increasing amounts of nickel contamination in MWCNTs may promote greater lung pathology, potentially by disrupting macrophage phagolysosomes and promoting inflammasome activation (Hamilton *et al.*, 2012). However, it is possible that this correlation may be spurious: the majority of bulk nickel may be embedded within the inner lumen of MWCNTs, and therefore biologically unavailable. Furthermore, because we pooled our data to examine this correlation, our results may have been confounded by other MWCNT physicochemical characteristics.

Our results do not support the long fiber paradigm of toxicity originating from asbestos research (Poland *et al.*, 2008). Instead, they are consistent with previous reports that shorter MWCNTs induce more lung neutrophilia than longer MWCNTs in mice (Muhlfeld *et al.*, 2012; Hamilton *et al.*, 2013). This inflammogenicity may relate to how size affects the extent of MWCNT internalization by alveolar macrophages. We found that shorter MWCNTs (#12 and #13) were internalized by a greater proportion of alveolar macrophages than the longer MWCNT (#14). This is consistent with a previous report that only MWCNTs up to 3 μm were recovered from rat alveolar macrophages (Pauluhn, 2010b). Indeed, the proportion of macrophages with internalized MWCNTs correlated significantly with the degree of lung neutrophilia in our study. This implies that these macrophages may have greater inflammasome activation with concommitant pro-inflammatory signaling (Bhattacharya *et al.*, 2013), resulting in increased neutrophil influx.

However, we observed no change in mRNA levels of pro-inflammatory and chemotactic genes for #12 or #13. Indeed, our gene expression results support neither hypothesis 1.1 or 1.2. Of the five inflammation-related genes we examined (*Gmcsf*, *Il1β, Kc*, *Mcp1*, *Tnfα*), only *Gmcsf* expression was increased in 2/3 chemical classes for the #13 and #14 series. It is possible that, by examining gene expression 24 h after exposure, we may have not captured the time period during which expression would be perturbed. In support of this, it was previously reported that the exposure of murine macrophages *in vitro* to shorter MWCNTs induced a significant increase in mRNA levels of *Tnfα* and *Mip2α* within 6 h of exposure, but that this increase had disappeared by 24 h (Bussy *et al.*, 2012). Similar observations have been made in *in vitro* and *ex vivo* models. Murine bone marrow-derived macrophages achieved peak mRNA expression of *Kc* and *Il6* with 4 h of exposure to quantum dot nanoparticles, but these mRNA levels had diminished to baseline by 24 h post-exposure—even though elevated KC protein was detected 24 h post-exposure (Lee *et al.*, 2015c). Similarly, in human whole blood, exposure *ex vivo* to lipopolysaccharide stimulated a peak in *Tnfα* and *Il6* mRNA levels within 2 – 4 hours, while the protein levels of these cytokines increased and stabilized within 4 – 6 hours of exposure (DeForge and Remick, 1991). Exposure to diesel exhaust particules in mice was also associated with a transient increase in *Kc* and *Il6* mRNA levels within 1 h of exposure, which had returned to baseline by 3 h post-exposure (Saber *et al.*, 2006).

Our results examining the oxidative stress response did not support hypothesis 1.1 or 1.2. Surprisingly, when we measured the total glutathione content in lung tissue and the mRNA levels of redox-sensitive genes, we found no evidence for either severe oxidative stress or subtler perturbations in redox status induced by any of the nine MWCNTs.

In studies *in vivo* where pathological endpoints were examined 24 h after CNT exposure, lung glutathione levels have been variably reported to decrease (Ravichandran *et al.*, 2011; Luyts *et al.*, 2014), to significantly increase (Wang *et al.*, 2010), and to not change (Shvedova *et al.*, 2008). Comparison between these reports is limited by numerous interlaboratory confounders (e.g., different CNTs, doses, strains of mice, age of mice, gender of mice). When these interlaboratory confounders were eliminated in our study, we found no evidence for significant alterations in total glutathione levels associated with any of our nine MWCNTs.

Furthermore, we found no alterations in the expression of redox-sensitive genes (*Gclc*, *Gclm*, *Hmox1*) or a gene associated with glutathione transport into the lung's epithelial lining fluid (*Cftr*), indicating that none of these MWCNTs subtly perturbed the lung's GSH redox state. This is surprising because MWCNT exposure *in vitro* was reported to increase the expression of redox-sensitive genes *Hmox1*, *Sod2*, and *Gpx1* within 24 h of exposure (Bussy *et al.*, 2012). Moreover, a case series of workers in the largest Korean MWCNT manufacturing firm found that workers directly handling MWCNT had increased levels of oxidative stress markers (e.g., malondialdehyde) in breath condensate, compared to office workers (Lee *et al.*, 2015b). The discrepancy between our results and these observations may arise from obvious differences between mouse models, *in vitro* cultures, and humans. In support of this, *Hmox1* mRNA levels were only reported to increase in mice exposed to acute bolus doses of ≥ 52 μg MWCNT (Poulsen *et al.*, 2015b). Oxidative stress associated with MWCNT exposure may only emerge with chronic exposure, or may require at least seven days to measurably deplete lung total glutathione in mouse models following a single exposure (Shvedova *et al.*, 2008).

The lack of oxidative stress may also stem from the low levels of transition metals contaminating our nine MWCNTs. Transition metals such as iron can generate acellular reactive oxygen species through Fenton reactions (Bussy *et al.*, 2012). Acellular radical formation has been reported to be highly sensitive to iron concentration; Muhlfeld *et al.* reported that MWCNTs contaminated with 0.34% (w/w) iron did not generate radicals, while MWCNTs with 1.76% did generate radicals (Muhlfeld *et al.*, 2012). Given that none of our MWCNTs had more than 0.9% iron, they may therefore have been less capable of generating radical species that could induce oxidative stress in the lung within 24 h of exposure.

Our results on gross lung and cellular toxicity support hypothesis 1.1, but do not support hypothesis 1.2. To assess lung toxicity, we examined the integrity of the alveolar/capillary barrier by measuring BALF total protein levels, and we evaluated the extent of cell death by measuring BALF lactate dehydrogenase levels. In support of hypothesis 1.1, we observed a general trend of increased lactate dehydrogenase levels in the stock samples for each aspect ratio, which reached statistical significance for only #14 stock. While this observation supported hypothesis 1.1, it contradicted hypothesis 1.2, as the long/thin #14 stock sample was the most toxic. Intriguingly, this toxicity did not correlate with either lung neutrophilia or oxidative stress, potentially because lung toxicity was reported

only at very high exposure levels (5.0 mg/m^3) in rats exposed via inhalation to MWCNT (Pothmann *et al.*, 2015). Gross toxicity of MWCNTs may be a non-specific response unrelated to the physicochemical characteristics of MWCNTs.

There are several limitations to our study. First, we used a relatively high dose of MWCNTs (40 µg/mouse), and exposed the mice via OPA. While OPA is an artificial and experimental method of human inhalation exposure, the pathology induced by OPA of CNTs in mice was previously reported to be comparable to that induced by inhalation exposure (Shvedova *et al.*, 2008; Silva *et al.*, 2014). We elected to use OPA because it is a safe substitute for inhalation exposures, in that it reduces risk to personnel and allows for a rapid, well-controlled means of exposure (Poulsen *et al.*, 2015b). A second limitation to our study is the use of male A/J mice; we may have missed important gender differences in susceptibility to MWCNTs by failing to examine female mice. And third, while a previous study in our laboratory found that A/J mice were more susceptible to quantum dot-induced lung toxicity than C57BL/6 mice (Scoville *et al.*, 2015), the use of the A/J strain limits comparison between our study's results and other studies using the more common C57BL/6 mice.

In conclusion, we found that the physicochemical characteristics of MWCNT were associated with different degrees of lung neutrophilia, but not oxidative stress. Consistent with hypothesis 1.1, we found that the unpurified, stock MWCNTs were the most inflammogenic and most toxic to the lung. However, our results did not support hypothesis 1.2, in that it was the wide/short #13 series which was the most inflammogenic, while the long/thin #14 series was the most toxic. Altogether, these results indicate that protective measures and risk assessments should prioritize reducing worker exposure while handling unpurified MWCNTs.

2.5. Figures

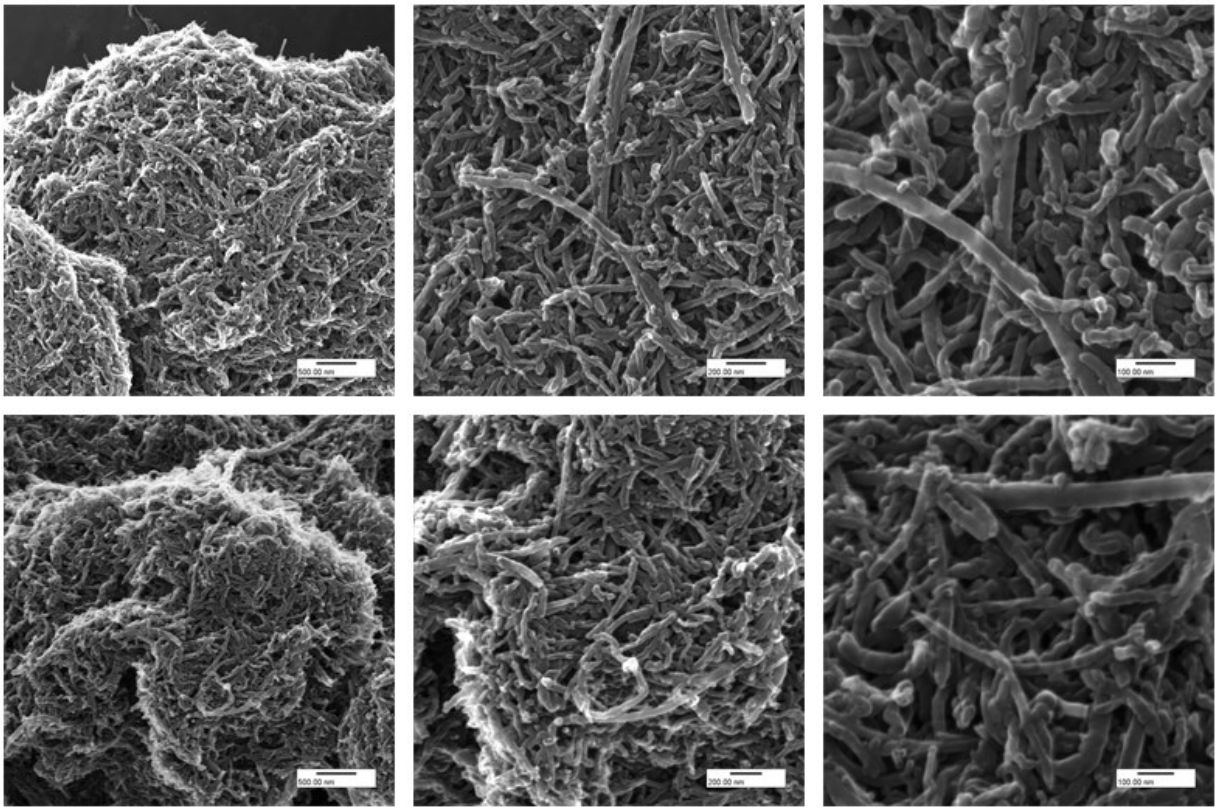

Figure 2.1. Representative Helium Ion Microscope images of MWCNTs.

Images depict #12 stock (upper panels) and #12 purified (lower panels). Scale bars indicate 500 nm (left panels), 200 nm (middle), and 100 nm (right).

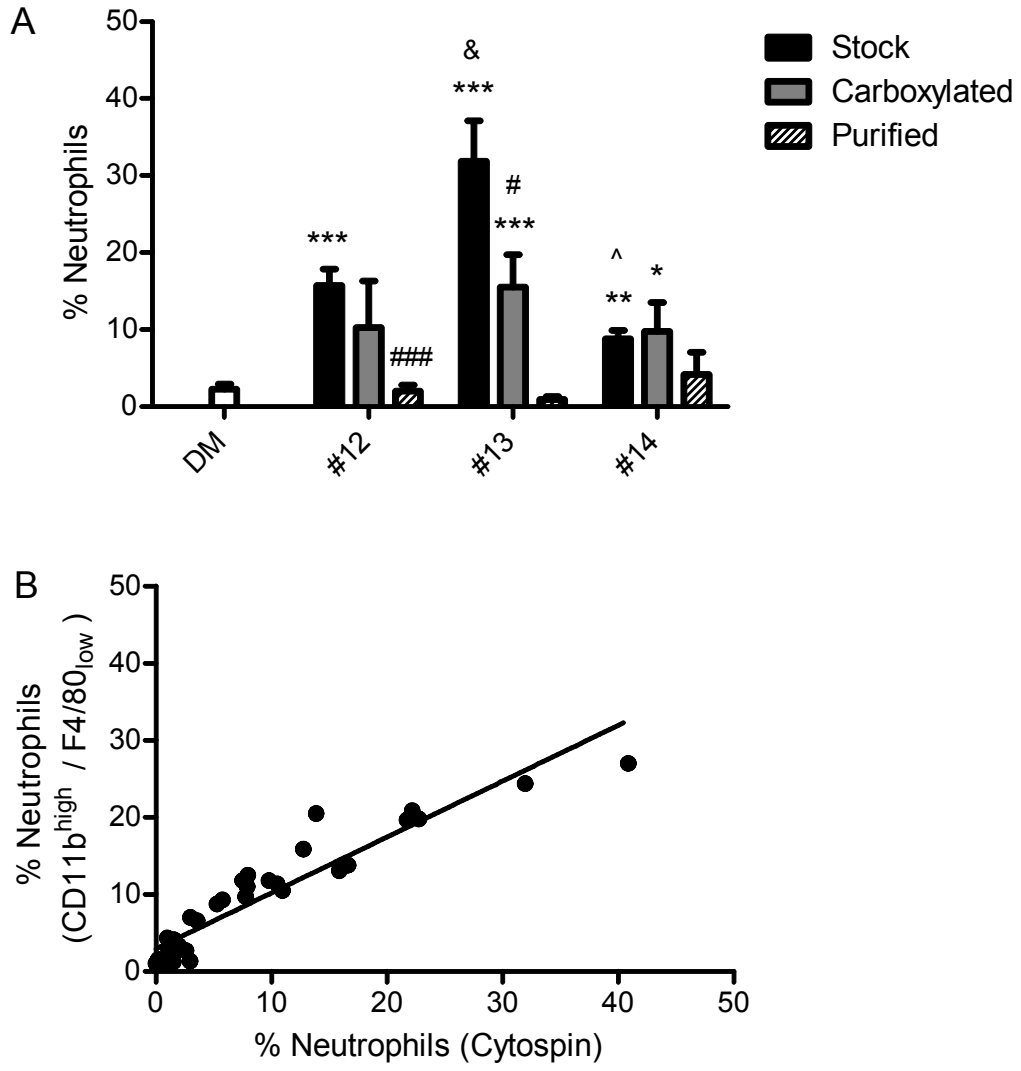

Figure 2.2. Lung neutrophilia.

(A) Percentage of neutrophils on cytospins of cells recovered through bronchoalveolar lavage of male A/J mice, 24 h after aspiration of dispersion medium vehicle (DM) or 40 µg MWCNT. Results are means and SEM (n ≥ 3 mice/group). (B) Linear correlation between neutrophilia determined by flow cytometry and cytospins. * $p < 0.05$, ** $p < 0.01$, *** $p < 0.001$ compared to DM group. # $p < 0.05$, ### $p < 0.001$ compared to same-MWCNT stock. & $p < 0.05$ compared to #12 stock. ^ $p < 0.05$ compared to #13 stock.

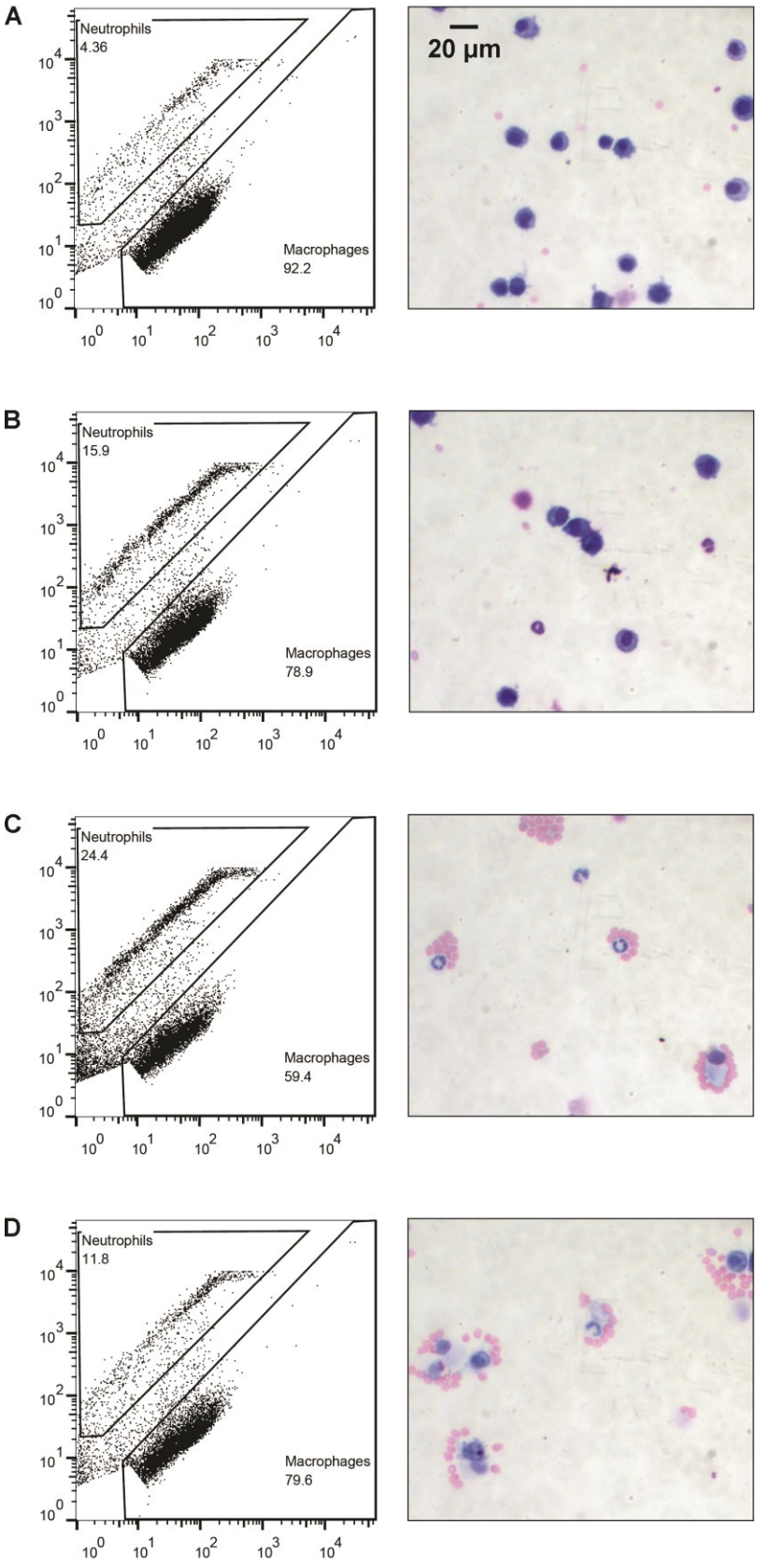
A
Neutrophils
4.36
Macrophages
92.2
20 µm
B
Neutrophils
15.9
Macrophages
78.9
C
Neutrophils
24.4
Macrophages
59.4
D
Neutrophils
11.8
Macrophages
79.6

Figure 2.3. Representative images of lung neutrophilia.

The right column consists of cytospin images (20x) and the left column contains the corresponding flow cytometry analyses of individual mice treated with (C) DM, (D) #12 stock, (E) #13 stock, and (F) #14 stock. Abbreviations: DM, dispersion medium vehicle; E, erythrocyte; M, macrophage; N, neutrophil.

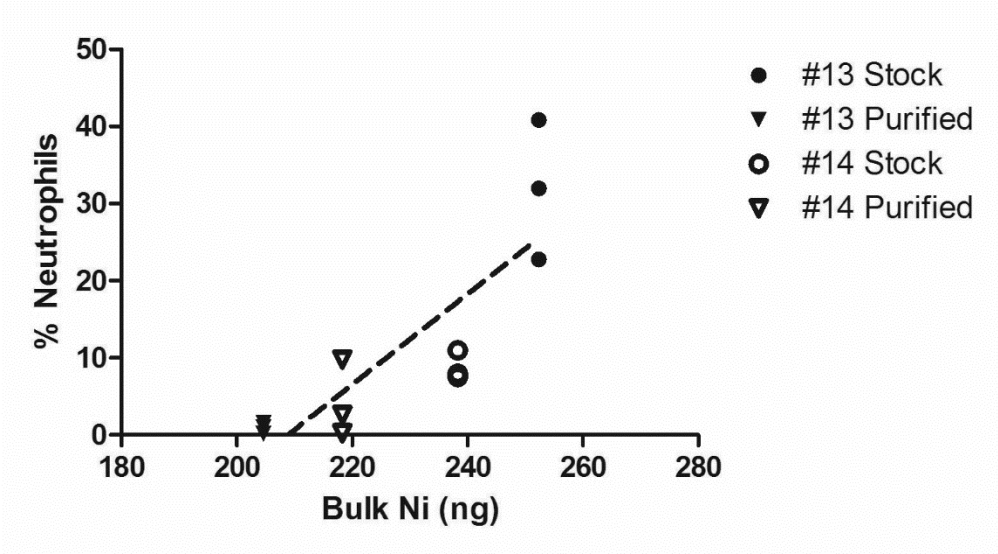

Figure 2.4. Correlation between bulk nickel content and neutrophilia.

Percentage of neutrophils correlated to the amount of contaminant bulk nickel administered with each 40 µg dose of MWCNTs. The percentage of neutrophils was determined by counting cells recovered through bronchoalveolar lavage 24 h post-exposure. Bulk nickel content was determined by inductively-coupled plasma mass spectrometry for the #13 and #14 series of MWCNTs; the #13 and #14 carboxylated MWCNTs were excluded due to concerns over confounding by endotoxin. Each symbol represents an individual mouse.

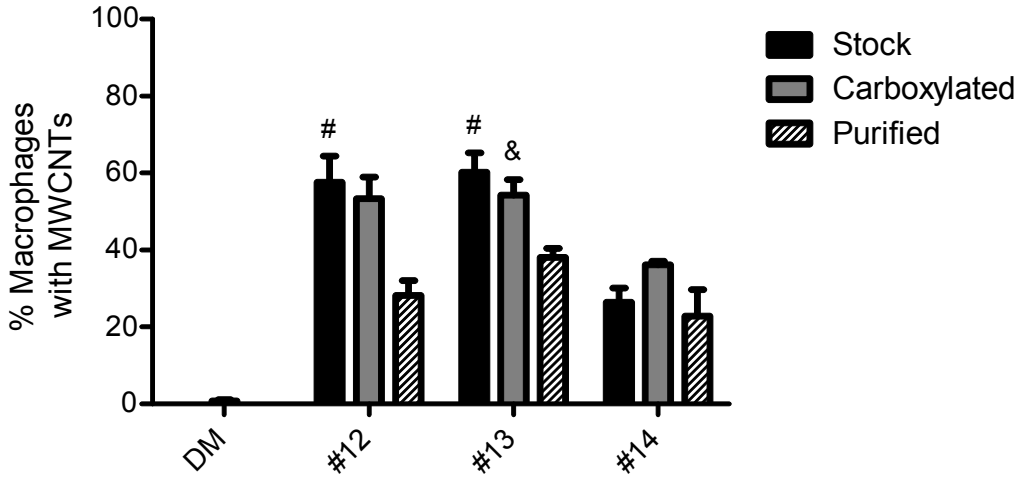

Figure 2.5. MWNCT internalization by alveolar macrophages.

Percentage of macrophages with internalize MWCNTs visible under light microscopy (40x) examination of cytospins. Cells were recovered through bronchoalveolar lavage of male A/J mice, 24 h after aspiration of dispersion medium vehicle (DM) or 40 µg MWCNT. Results are means and SEM (n ≥ 3 mice/group). # $p < 0.05$ compared to #14 stock. & $p < 0.05$ compared to #14 carboxylated. Abbreviation: MWCNT, multi-walled carbon nanotube.

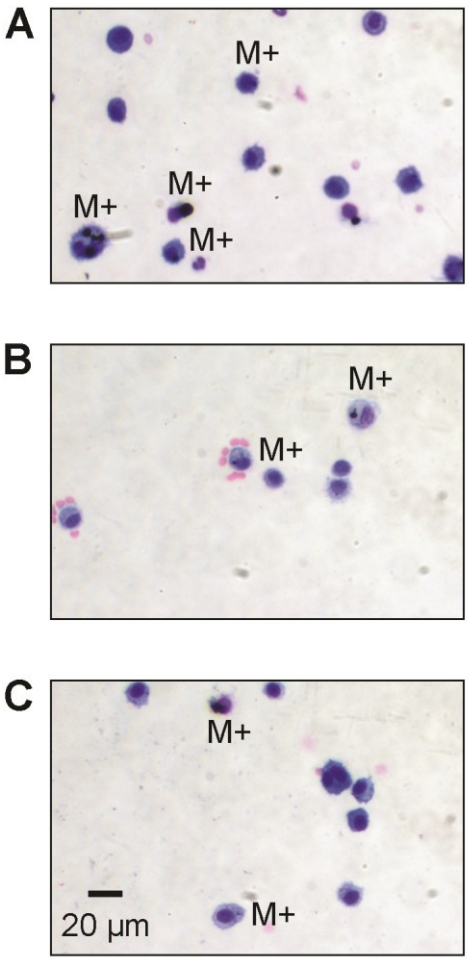

Figure 2.6. Representative images of MWCNT internalization by alveolar macrophages.

Images captured of cytospins (20x) of individual mice treated with (A) DM, (B) #12 stock, (C) #12 carboxylated, and (D) #12 purified. Abbreviations: DM, dispersion medium vehicle; M+, macrophage with internalized multi-walled carbon nanotubes.

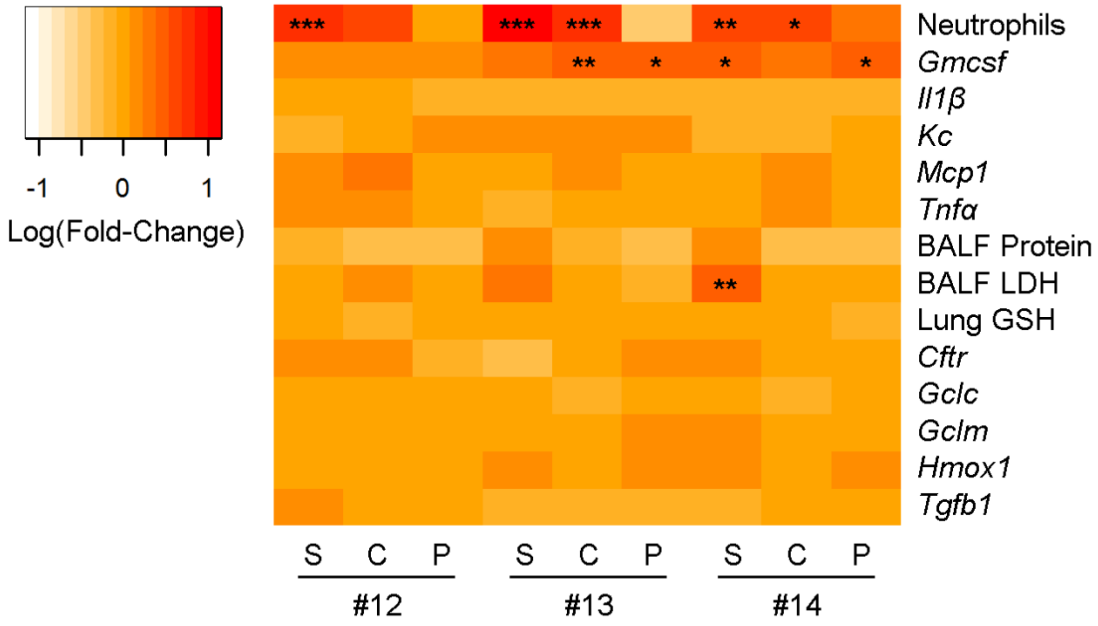

Figure 2.7. Heatmap of MWCNT panel with pathological endpoints.

The log(fold-change) compares the fold-change for each endpoint's MWCNT-exposed mean value to its control (DM) mean value. * $p < 0.05$, ** $p < 0.01$, *** $p < 0.001$ compared to the DM group.

Abbreviations: BALF, bronchoalveolar lavage fluid; C, carboxylated; GSH, glutathione; LDH, lactate dehydrogenase; MWCNT, multi-walled carbon nanotube; P, purified; S, stock.

2.6. Tables

Table 2.1

Manufacturer's Specifications of MWCNT Physical Dimensions.

MWCNT	Length (μm)	OD* (nm)	Aspect Ratio
#12 (Thin/Short)			
Stock	0.5 - 2.0	10 - 20	25 - 200
Carboxylated	0.5 - 2.0	10 - 20	25 - 200
Purified	0.5 - 2.0	10 - 20	25 - 200
#13 (Wide/Short)			
Stock	0.5 - 2.0	30 - 50	17 - 67
Carboxylated	0.5 - 2.0	30 - 50	17 - 67
Purified	0.5 - 2.0	30 - 50	17 - 67
#14 (Thin/Long)			
Stock	10 - 30	10 - 20	500 - 3,000
Carboxylated	10 - 30	10 - 20	500 - 3,000
Purified	10 - 30	10 - 20	500 - 3,000

*OD = outer diameter.

Table 2.2

Measured Physicochemical Characteristics of MWCNT Panel.

MWCNT	Length[a] (µm)	OD[a] (nm)	Endotoxin[b] (EU/mg)	Elemental Composition[b] (%) Carbon	Oxygen	Nickel	Iron
#12 (Thin/Short)							
Stock	1.108	17.8	0.060	94.1	4.7	0.8	0.4
Carboxylated	0.898	24.5	11.700	92.2	6.7	0.7	0.4
Purified	1.007	18.9	0.005	93.5	4.6	1.4	0.5
#13 (Wide/Short)							
Stock	1.199	31.2	nd	94.1	4.5	1.1	0.3
Carboxylated	0.761	32.5	nd	88.6	8.0	2.3	0.9
Purified	0.811	30.2	nd	94.9	3.3	1.2	0.7
#14 (Thin/Long)							
Stock	nd	15.5	nd	95.8	3.4	0.5	0.3
Carboxylated	nd	22.7	nd	91.8	7.4	0.5	0.3
Purified	nd	16.7	nd	95.9	2.9	0.2	0.3

Data presented as means. Abbreviations: DM, dispersion medium; EU, endotoxin units; nd, not done; OD, outer diameter.
[a]Data published in a separate report (Hamilton *et al.*, 2013).
[b]Data collected by the Nanotechnology Characterization Laboratory on behalf of the NCNHIRC (NCI, 2012).

Table 2.3

Aggregative Characteristics of MWCNT Panel.

MWCNT	Hydrodynamic Diameter (nm) Water	DM*	Zeta Potential (mV) Water	DM
#12 (Thin/Short)				
Stock	294.5	425.4	-44.6	-12.4
Carboxylated	221.0	461.9	-52.7	-14.7
Purified	309.6	544.0	-45.8	-9.9
#13 (Wide/Short)				
Stock	340.3	567.2	-40.7	-9.2
Carboxylated	247.6	1206.0	-50.3	-15.4
Purified	320.7	907.3	-40.8	-10.5
#14 (Thin/Long)				
Stock	261.0	910.3	-36.1	-13.9
Carboxylated	202.8	591.3	-47.3	-14.7
Purified	275.8	727.5	-43.1	-11.3

Data presented as means. *DM = dispersion medium.

Table 2.4

Effects of MWCNT Exposure on mRNA Expression of Chemoattractant and Pro-Inflammatory Genes.

MWCNT	*Gmcsf*	*Kc*	*Il1β*	*Mcp1*	*Tnfα*
Control	0.22 (0.06)	0.21 (0.07)	0.76 (0.12)	0.11 (0.02)	0.41 (0.05)
#12 (Thin/Short)					
Stock	0.29 (0.08)	0.17 (0.04)	0.66 (0.08)	0.15 (0.04)	0.62 (0.13)
Carboxylated	0.38 (0.12)	0.22 (0.08)	0.74 (0.20)	0.21 (0.13)	0.53 (0.18)
Purified	0.36 (0.10)	0.27 (0.09)	0.51 (0.09)	0.10 (0.02)	0.47 (0.13)
#13 (Wide/Short)					
Stock	0.48 (0.12)	0.26 (0.11)	0.54 (0.10)	0.11 (0.04)	0.34 (0.06)
Carboxylated	0.70 (0.08)**	0.26 (0.06)	0.53 (0.08)	0.14 (0.02)	0.43 (0.08)
Purified	0.64 (0.05)*	0.27 (0.03)	0.52 (0.10)	0.13 (0.03)	0.43 (0.06)
#14 (Thin/Long)					
Stock	0.63 (0.04)*	0.15 (0.02)	0.53 (0.00)	0.11 (0.03)	0.45 (0.11)
Carboxylated	0.41 (0.08)	0.14 (0.04)	0.54 (0.10)	0.17 (0.02)	0.57 (0.15)
Purified	0.61 (0.08)*	0.18 (0.03)	0.46 (0.07)	0.11 (0.02)	0.36 (0.04)

Data presented as mean (SEM). All gene expression levels (x 10^3) normalized to expression of housekeeping gene *Gapdh*. * $p < 0.05$, ** $p < 0.01$ compared to control mice.

Table 2.5

Effects of MWCNT Exposure on Lung Injury and Oxidative Stress.

MWCNT	BALF [Protein] (mg/ml)	BALF [LDH] (ng/ml)	Lung GSH (nmol/mg protein)
Control	0.306 (0.071)	160.8 (31.1)	12.9 (1.3)
#12 (Thin/Short)			
Stock	0.207 (0.044)	179.4 (29.6)	11.6 (1.8)
Carboxylated	0.174 (0.035)	218.7 (9.6)	10.6 (1.1)
Purified	0.131 (0.006)	135.4 (11.4)	11.4 (2.0)
#13 (Wide/Short)			
Stock	0.433 (0.028)	276.2 (54.5)	11.6 (1.9)
Carboxylated	0.220 (0.055)	147.9 (9.2)	12.2 (0.0)
Purified	0.162 (0.001)	133.4 (13.8)	12.4 (2.2)
#14 (Thin/Long)			
Stock	0.508 (0.107)	453.1 (79.3)**	14.4 (2.0)
Carboxylated	0.180 (0.017)	164.1 (30.1)	12.4 (0.4)
Purified	0.178 (0.005)	136.4 (5.5)	9.5 (0.9)

Data presented as mean (SEM). ** $p < 0.01$ compared to control mice.
Abbreviations: BALF, bronchoalveolar lavage fluid; GSH, glutathione; LDH, lactate dehydrogenase

Table 2.6

Effects of MWCNT Exposure on mRNA Expression of Oxidative Stress- and Fibrosis-Associated Genes.

MWCNT	*Cftr*	*Gclc*	*Gclm*	*Hmox1*	*Tgfb1*
Control	1.98 (0.48)	11.62 (1.36)	2.71 (0.36)	6.13 (0.88)	8.43 (0.92)
#12 (Thin/Short)					
Stock	2.66 (0.62)	11.37 (0.83)	3.12 (0.48)	6.21 (0.43)	10.84 (2.14)
Carboxylated	2.54 (0.68)	11.34 (0.15)	3.09 (0.30)	6.78 (0.94)	7.49 (1.72)
Purified	1.58 (0.31)	9.95 (0.80)	2.74 (0.34)	6.16 (0.16)	7.90 (0.82)
#13 (Wide/Short)					
Stock	1.11 (0.46)	13.02 (0.45)	3.01 (0.07)	7.60 (0.01)	6.60 (0.73)
Carboxylated	1.95 (0.42)	9.46 (0.19)	2.59 (0.22)	6.47 (0.11)	6.96 (0.45)
Purified	2.65 (0.33)	10.76 (1.48)	3.30 (0.41)	8.17 (1.38)	6.79 (0.73)
#14 (Thin/Long)					
Stock	3.09 (0.51)	13.80 (1.87)	3.64 (0.28)	7.71 (1.10)	6.96 (0.40)
Carboxylated	1.81 (0.91)	8.88 (0.19)	3.01 (0.53)	7.00 (0.30)	8.79 (1.79)
Purified	1.85 (0.43)	11.54 (1.60)	3.03 (0.25)	7.94 (0.86)	7.85 (0.93)

Data presented as mean (SEM). All gene expression levels (x 10^3) normalized to expression of housekeeping gene *Gapdh*.

Chapter 3 : Aim 2

3.1. Introduction

While carbon nanotube-like nanoparticles have been recovered from the lungs of first responders to the World Trade Center terrorist attacks (Wu *et al.*, 2010) and more recently from asthmatic French children (Kolosnjaj-Tabi *et al.*, 2015), no human disease has been conclusively linked to multi-walled carbon nanotube (MWCNT) exposure (Bonner *et al.*, 2013). Risk assessments for recommending inhalation-based occupational exposure limits have thus relied on *in vivo* animal data (Pauluhn, 2010a; Kuempel *et al.*, 2012; NIOSH, 2013). Data from rodent models indicate that inhaled CNTs may induce neutrophilic inflammation, oxidative stress, and fibrosis in the lungs. However, these CNT-associated pathologies have been predominantly examined in C57BL/6 inbred mice, a common laboratory strain (Shvedova *et al.*, 2008; Porter *et al.*, 2010; Muhlfeld *et al.*, 2012; Shvedova *et al.*, 2012b; Bonner *et al.*, 2013).

Even though using the isogenic C57BL/6 strain improves study reproducibility, limits cost, and offers experimental advantages in mechanistic studies (King-Herbert and Thayer, 2006), previous investigations with other respiratory toxicants have demonstrated that the choice of mouse strain significantly affects the lung pathology observed. Multi-strain studies into lung pathologies induced by ozone (Vancza *et al.*, 2009), zinc oxide (Wesselkamper *et al.*, 2001a), and cigarette smoke (Gordon and Bosland, 2009) all found that heritable genetic factors significantly modulate pathology. It is highly probable that strain and genetic factors will similarly affect the observed pathology induced by MWCNT.

However, these studies suggested that strain sensitivity does not necessarily extrapolate across toxicants. Indeed, the range of the pathological response—and the relative sensitivities of the examined strains—significantly differed between toxicants. For example, isogenic A/J mice were resistant to zinc oxide-induced lung neutrophilia (Wesselkamper *et al.*, 2001a), but were susceptible to ozone (Vancza *et al.*, 2009) or quantum dot induced lung neutrophilia (Scoville *et al.*, 2015). By contrast, C57BL/6 mice were sensitive to neutrophilia induced by zinc oxide exposure (Wesselkamper *et al.*, 2001a) and ozone (Vancza *et al.*, 2009), but were resistant to quantum dot-induced neutrophilia (Scoville *et al.*, 2015).

The reliance on isogenic C57BL/6 mice may therefore fail to adequately capture the variety and extent of pathological responses possible among an outbred population of human workers (Festing, 1995;

Rusyn *et al.*, 2010). To our knowledge, there have been no studies examining the role that genetic variability among mouse strains plays in modulating the form and extent of MWCNT-induced toxicity. Therefore, the goal of this aim is to examine early lung pathological responses (inflammation, oxidative stress, gene expression, and cytokine expression) in ten inbred mouse strains exposed via oropharyngeal aspiration (OPA) to a chemically unmodified, unpurified MWCNT sample.

By examining the pathological responses of multiple inbred mouse strains, we will improve understanding of the range of pathological responses in a genetically variable population, which can then better inform risk assessors setting occupational exposure limits. Furthermore, comparing multiple strains for susceptibility will enable better understanding of the results from toxicity studies in C57BL/6 mice by placing this strain's responsiveness in the context of other strains. Finally, evaluating multiple strains will allow for identification of a highly resistant and a highly susceptible strain. These differentially-susceptible strains may then be crossed, and their offspring used for performing linkage analyses to identify susceptibility loci associated with the disparate responses between the strains (Wesselkamper *et al.*, 2001a; Rusyn *et al.*, 2010).

For this aim, I hypothesize that (2.1) there is a strain-dependent differential response in acute lung pathology to the #12 stock MWCNT, and given previous work done in our lab with other nanoparticles, that (2.2) A/J mice will be the strain most susceptible to inflammation and oxidative stress.

3.2. Materials and Methods

Reagents.

Unless otherwise noted, we purchased all reagents from Sigma-Aldrich (St. Louis, MO).

MWCNT characterization.

For comprehensive characterization of this MWCNT (#12 stock), please see **Aim 1: Materials and Methods → *MWCNT characterization.***

Mice.

We performed all animal experiments in accordance with the National Institutes of Health Guide for the Use and Care of Laboratory Animals (NRC, 2011a) and with the approval of the University of Washington Institutional Animal Care and Use Committee. We made all efforts to minimize animal

distress and suffering. No mortality or distress (e.g., weight loss, huddling, unkempt fur) was observed in our experimental animals.

For our experiments, we purchased 7-week-old male mice from ten inbred strains from The Jackson Laboratory. This work was conducted as a collaboration between our laboratory and that of Dr. Terry Gordon (Department of Environmental Medicine, New York University School of Medicine). Both the Gordon and Kavanagh laboratories worked with the 129S1/SvImJ (129), A/J (AJ), and C57BL/6J (C57) strains. Only the Gordon laboratory worked with the AKR/J (AKR), C3H/HeJ (C3H), DBA/2J (DBA), and FVB/NJ (FVB) strains. Only the Kavanagh laboratory worked with the NOD/ShiLtJ (NOD), NZO/HiLtJ (NZO), and WSB/EiJ (WSB) strains.

Mice were housed in a modified specific pathogen free (SPF) vivarium on a 12-hour light/dark cycle with nesting materials and access to food and water *ad libitum*. Except for the wild-derived WSB mice, which were singly housed to reduce the chance for escape during routine care, all other strains were group housed.

All mice were acclimated for 5 – 7 days to the vivarium, and were 8 weeks old at the time of MWCNT exposure.

Experimental design.

To assess how mouse strain modulates the lung's pathological response to MWCNT exposure, we randomly assigned mice from ten strains to receive either 50 µl/mouse dosing vehicle or 50 µl vehicle + 25 µg/mouse MWCNT by oropharyngeal aspiration (minimum n = 3 mice/exposure/strain, for a total of 122 mice). In the context of human workplace exposures, a 10 µg/mouse bolus of MWCNT approximates human lung deposition after one month of full-time work with an ambient environmental MWCNT concentration of 400 µg/m^3, a concentration detected in Korean manufacturing environments (Han *et al.*, 2008; Porter *et al.*, 2010).

Thirty minutes prior to exposing the mice, we prepared fresh dispersion medium (DM) dosing vehicle [PBS + 0.6 mg/ml mouse serum albumin + 10 µg/ml DPPC (1,2-dipalmitoyl-sn-glycero-3-phosphocholine) surfactant in ethanol (0.1% v/v)] (Bonner *et al.*, 2013), and resuspended the MWCNT to 0.5 mg/ml in DM. For the Kavanagh laboratory exposures, both control and MWCNT solutions were sonicated for 19 seconds in a Branson 2510 bath sonicator, and vortexed for 1 second.

For exposures performed in the Kavanagh laboratory, we weighed each mouse and anesthetized it with 4% Isoflurane. The mouse was exposed via OPA of 50 µl dispersion medium only for the controls, or 50 µl dispersion medium + 25 µg MWCNT, using previously described methods (Bonner *et al.*, 2013). The mice were monitored for recovery from anesthesia and for signs of distress over the next 24 hours. We did not observe exposure-associated distress or mortality.

Twenty-four hours after exposure, we weighed each mouse to determine its post-exposure weight and then humanely euthanized it through CO_2 narcosis and cervical dislocation. We performed bronchoalveolar lavage (BAL) with two sequential lavages of sterile PBS (1.2, 0.6 ml) using previously described methods (McConnachie *et al.*, 2013). From the first lavage, we removed 100 µl for differential staining of cells, and centrifuged the remaining lavage. The acellular bronchoalveolar lavage fluid (BALF) was saved for future measurements of cytokines, glutathione (GSH) content of epithelial lining fluid (ELF), total protein concentration, and urea concentration. We also collected blood via cardiac puncture for serum isolation using serum separator tubes (Becton, Dickinson and Company, Franklin Lakes, NJ). The right lung was snap-frozen in liquid nitrogen and stored at -80°C until processing to measure GSH content and total protein. For the mice used in the Gordon laboratory, a sample of this snap-frozen right lung was used for later RNA extraction. For the mice used in the Kavanagh laboratory, a sample of the right lung's caudal lobe was removed at necropsy and immersed in RNA*later*® Stabilization Solution (Ambion/Thermo Fisher Scientific Inc., Waltham, MA) for at least 24 hours at 4 °C, and then frozen at -80 °C for later RNA extraction.

Measurement of lung inflammation through cell differentials.

To determine each strain's inflammatory response to MWCNT aspiration, we differentially scored the immune cells recovered from the first of two BALs. The lavaged cells in a 100-µl aliquot were centrifuged onto a microscopy slide (Cytospin 3, Shandon Life Sciences International Ltd., Cheshire, England) and differentially stained using the Hema 3™ system (Thermo Fisher Scientific, Waltham, MA), a commercial modification of the Wright-Giemsa method. The percentage of neutrophils among the recovered immune cells was determined by counting at least 100 cells from each mouse.

Because of significant interlaboratory variability in the number of total cells recovered even with standardized lavage techniques (Bonner *et al.*, 2013), we report the percentage of neutrophils rather than the total number of neutrophils.

Measurement of total protein in bronchoalveolar lavage fluid to assess lung injury.

To assess the extent of each strain's susceptibility to MWCNT-induced damage to the alveolar/capillary barrier of the lung, we measured the concentration of total protein in BALF (Wesselkamper *et al.*, 2001a). We centrifuged the first of two BALs (500 *g*, 10 min, 4°C), and determined the total protein concentration in this acellular BALF using a commercial protein assay (Bio-Rad Laboratories, Inc., Hercules, CA) derived from Bradford's method (Bradford, 1976).

Measurement of total glutathione in lung tissue and epithelial lining fluid.

To evaluate strain differences in vulnerability to MWCNT-induced oxidative stress, we measured the major antioxidant glutathione (GSH) in lung tissue and ELF. In the tissue, we measured total glutathione (reduced glutathione + oxidized glutathione) content as previously reported (McConnachie *et al.*, 2013). In brief, in clarified lung homogenates we reduced the oxidized glutathione using tris-carboxyethyl phosphine, and then derivatized the reduced glutathione using napthelene-2,3-dicarboxyaldehyde. We then measured the relative fluorescence intensity of this derivatized product and calculated total GSH levels by interpolating from a standard curve [0.01 – 0.75 mM]. The amount of total GSH was normalized to the total protein content of the lung homogenate as noted above for BALF, with appropriate dilutions. We determined both the total GSH and protein levels using triplicate homogenate samples.

We similarly determined the concentration of ELF GSH in BALF, but with interpolation from a less-concentrated standard curve [0.25 – 5 µM]. To adjust for the dilution of ELF in BALF, we calculated a dilution factor by measuring urea in BALF and serum with the QuantiChrom™ Urea Assay Kit (BioAssay Systems, Hayward, CA), as previously described (Gould *et al.*, 2010).

Measurement of cytokines in bronchoalveolar lavage fluid.

The University of Washington's Center for Ecogenetics and Environmental Health Functional Genomics and Proteomics Core (CEEH FGPC) measured cytokine levels in AJ and C57 BALF samples using the V-PLEX Proinflammatory Panel 1 Mouse Kit (Meso Scale Discovery, Rockville, MD), a multiplex

sandwich immunoassay. The samples were analyzed following manufacturer's specifications for a subset of analytes: CXCL1 (KC), IL-1β, IL-6, and TNF-α. For this assay (lot #K0080292-166134), the dynamic range for KC was 0.408 – 1670 pg/ml; for IL-1β, 0.339 – 1390 pg/ml; for IL-6, 1.04 – 4260 pg/ml; and for TNF-α, 0.127 – 522 pg/ml. None of the samples were outside the range for KC and TNF-α. For IL-1β and IL-6, more than 90% of BAL samples were below the limit of detection (LOD); these cytokines were omitted from further analysis.

RNA extraction and Real-time PCR measurement of mRNA levels for genes associated with inflammation, oxidative stress, and fibrosis.

In order to measure mRNA expression, we first extracted total RNA from a sample of the right lung using the miRNeasy Mini Kit (Qiagen, Venlo, The Netherlands), and generated cDNA from 1 µg of total RNA using the SuperScript® III First-Strand Synthesis System (Life Technologies, Carlsbad, CA). Using this cDNA, the University of Washington's CEEH FGPC quantified mRNA expression of specific genes using fluorogenic 5' nuclease-based assays as previously described (McConnachie *et al.*, 2013). In brief, the mix for each PCR reaction contained TaqMan Gene Expression Master Mix (Applied Biosystems Inc., Foster City, CA) and primers and dual-labeled probes for each gene target, designed using ABI Primer Express v.1.5 software (Applied Biosystems). We then amplified and detected the targets using the ABI PRISM 7900 system (Applied Biosystems) with the following reaction profile: 1 cycle at 95°C for 10 minutes; 40 cycles at 95°C for 30 seconds; 1 cycle at 62°C for 1 minute. To calculate mRNA expression, we derived a linear regression formula from *Gapdh* amplification plots using serial dilutions of an established reference sample.

The analyzed mRNAs consisted of cystic fibrosis transmembrane regulator, *Cftr*; glutamate cysteine ligase catalytic subunit, *Gclc*; glutamate cysteine ligase modifier subunit, *Gclm*; granulocyte-macrophage colony stimulating factor, *Gmcsf*; heme oxygenase-1, *Hmox1*; interleukin-1β, *Il1β*; Cxcl1/keratinocyte-derived cytokine, *Kc*; monocyte chemotactic protein-1, *Mcp1*; transforming growth factor- β 1, *Tgfβ1*; and tumor necrosis factor-α, *Tnfα*. Expression for each target was normalized to *Gapdh* expression. The primer and probe sequences for these genes were previously published (McConnachie *et al.*, 2013).

Semi-quantitative Western immunoblotting for redox-sensitive protein expression and protein nitration.

To evaluate redox-sensitive protein expression and protein nitration in homogenates of the right lung in the six strains examined in the Kavanagh laboratory, we used SDS-PAGE and Western immunoblot analyses as previously described (Thompson *et al.*, 1999). We detected the expression of GCLC and GCLM using rabbit polyclonal anti-GCLC and -GCLM peptide antisera (Thompson *et al.*, 1999); the expression of HMOX1 using rabbit polyclonal Heme Oxygenase 1 Antibody (Santa Cruz Biotechnology, Dallas, TX); and nitrotyrosine modifications using anti-3-nitrotyrosine antibody (Takakusa *et al.*, 2012). We detected β-actin as the loading control using β-actin Rabbit Antibody (Cell Signaling Technology, Danvers, MA). To evaluate the extent of protein nitration, we ran on each SDS-PAGE gel a positive control (untreated lung homogenate incubated for 1 minute at room temperature in 1.0 mM peroxynitrite (Takakusa *et al.*, 2012)) and negative control (untreated lung homogenate incubated in an equivalent volume of distilled water). For each Western blot, we detected the bound secondary Goat Anti-Rabbit IgG Antibody, HRP-conjugate (EMD Millipore, Billerica, MA), using an enhanced chemiluminescence system (GE Healthcare UK, Buckinghamshire, UK) with X-ray film exposure. The optical densities of the appropriate-sized bands were then analyzed using NIH Image J software v1.48 (National Institutes of Health, Bethesda, MD). The optical density of each band was adjusted to the density of the β-actin band, and the fold-change expression for each sample was calculated compared to the mean value for the dispersion medium vehicle-exposed control mice.

Creation of heatmap summarizing each strain's response to all pathological endpoints.

To summarize each strain's responsiveness to all of the above pathological endpoints, we generated a heatmap of the log(fold-change) values. The fold-change compares the mean for each strain's MWCNT-exposed group to the mean of its control group.

The heatmap was created using the heatmap.2() function available in the R package, gplots, with the clustering options disabled. Our R code is publicly available at https://gist.github.com/mcartwri/16b8119016cac3471ca1#file-cartwright-heatmap-r.

Normalization of data for interlaboratory variability.

It has been previously demonstrated that significant interlaboratory variation exists in lung pathology endpoints, even with standardization of protocols, MWCNT, dose, and animal strain (Bonner *et al.*, 2013). To adjust for this interlaboratory variability, we calculated a unique normalization factor for each endpoint, so that the data across our two laboratories could be pooled for analysis.

To calculate this endpoint-unique normalization factor, we used the mean values from the control and exposed groups of the three strains of mice (129, A/J, and C57) common to both laboratories. For each endpoint, we performed linear regression with the intercept set to 0 on these six mean values (2 exposure groups x 3 strains), where for each data point the Gordon laboratory mean value provided the y-coordinate and the Kavanagh laboratory the x-coordinate. The resulting linear regression equation $y = mx$ yielded an endpoint-unique normalization factor, m. Perfect agreement with no interlaboratory variability would therefore yield a linear regression equation of $y = x$.

We applied this normalization factor m to the Kavanagh laboratory data to normalize it to the Gordon laboratory data. After normalizing the data, we analyzed the pooled data.

Statistical analyses.

To analyze the normalized data, we used two-way analysis of variance (ANOVA) for exposure, strain, and interactions. When the two-way ANOVA results indicated significant associations, we performed post-hoc analyses using unpaired, two-tailed *t*-tests, and adjusted the resulting *p*-values for multiple comparisons using Bonferroni corrections. For determining correlations, we calculated Pearson's correlation coefficients and report two-tailed *p*-values for significance. Data were managed in Excel 2013, part of Microsoft Office Professional Plus 2013 (Microsoft, Redmond, WA), and analyzed in Prism 5 for Windows, v.5.02 (GraphPad Software, Inc., La Jolla, CA).

3.3. Results

Lung inflammation and injury.

To investigate strain-dependent susceptibility to lung inflammation, we determined the percentage of neutrophils relative to other types of cells (macrophages/monocytes, eosinophils, and lymphocytes) recovered through BAL 24 hours after the mice aspirated 50 µl of dispersion medium vehicle (control) or 25 µg MWCNT in 50 µl vehicle (Figure 3.1).

MWCNT exposure induced neutrophilia in an exposure- and strain-dependent manner (two-way ANOVA $p < 0.0001$ for exposure, $p = 0.0019$ for strain). For all strains, the control groups had a percentage of neutrophils below 6%, indicating low inflammogenic potential for the dispersion medium vehicle (Figure 3.1). The overall mean for all controls was 1.89%; the strain closest to this overall mean was AJ, followed by C3H. For the exposed groups, the percentage of neutrophils ranged from 7.49 – 43.04%, a five-fold difference potentially attributable to genetic differences between the ten isogenic strains. The exposed mice had an overall mean of 23.52%; the strain closest to this overall mean was NOD, followed by AJ.

Compared to each strain's control group, MWCNT exposure significantly increased the proportion of neutrophils for 8/10 of the inbred strains. When ordered from highest to lowest by each strain's mean percentage of neutrophils in its exposed group, the strains ranked as follows: 129 ($p = 0.0045$, compared to control); C3H ($p < 0.0001$); AKR ($p < 0.0001$); DBA ($p = 0.0002$); NOD ($p = 0.3121$); AJ ($p < 0.0001$); FVB ($p = 0.0001$); NZO ($p = 0.2049$); C57 ($p = 0.0479$); and WSB ($p = 0.0114$). Despite their intermediate rankings, the NZO and NOD strains did not have significant differences between their control and exposed groups. The lack of significance may be due to high variability in individual animal response to MWCNT exposure for these two strains; furthermore, the NOD control group had a relatively high mean percentage of neutrophils (4.1%).

While this MWCNT induced significant neutrophilia in most strains, we found no evidence for its capacity to severely injure the lung and disrupt the integrity of the alveolar/capillary barrier (Table 3.1). Protein concentration in BAL fluid was not significantly associated with either MWCNT exposure or strain. However, there was a small but statistically significant correlation between the percentage of neutrophils and the concentration of protein in BAL fluid across all strains and exposure groups (Pearson's $r = 0.1821$, $p = 0.0456$).

Altogether, our data indicate that susceptibility to MWCNT-induced neutrophilia is significantly associated with mouse strain. These data also show that MWCNTs can induce inflammation in the absence of significant lung injury and barrier disruption. Furthermore, the strain closest to the overall mean percentage of neutrophils for both control and exposed groups is AJ, rather than the commonly-used C57BL/6.

These data support hypothesis 2.1, in that they show a strain-dependent differential response in acute lung inflammation. However, these data do not support hypothesis 2.2; rather than being the most susceptible strain, the AJ mice were actually the strain with neutrophilia values closest to the overall mean for both the control and MWCNT-exposed groups.

Total glutathione content in lung tissue and epithelial lining fluid.

CNTs can engender severe oxidative stress within *in vitro* and *in vivo* models of respiratory exposure (Inoue *et al.*, 2010; Shvedova *et al.*, 2012b; Moller *et al.*, 2014). This oxidative stress is reported to significantly alter levels of the major antioxidant GSH (Shvedova *et al.*, 2007; Wang *et al.*, 2010; Ravichandran *et al.*, 2011). Thus, we investigated strain-dependent susceptibility to oxidative stress, as reflected by the levels of total GSH measured in clarified lung homogenates and total GSH in lung ELF of control and MWCNT-exposed mice (Table 3.1).

The total GSH content of lung tissue was significantly associated with an interaction between exposure and strain (two-way ANOVA $p = 0.0330$ for interaction, $p = 0.3853$ for exposure, $p < 0.0001$ for strain). An example of this interaction is the contrasting trends for the FVB strain compared with the NOD and NZO strains. The FVB strain had a significant decrease ($p = 0.0300$), while the NOD and NZO strains had non-significant increases in total GSH.

When we examined total GSH levels in the lungs of all strains' control groups, we observed significant strain differences (one-way ANOVA $p < 0.0001$). These baseline GSH levels ranged from a low in the NOD strain (mean 8.13 nmol GSH/mg protein) to a high in the FVB strain (24.39 nmol/mg protein), with an overall mean of 12.04 nmol/mg protein. The strain closest to this overall mean was AJ, followed by C3H.

In contrast to total GSH in lung tissue, we observed that GSH content in ELF was not associated with MWCNT exposure or strain. Across all strains and exposure groups, the levels of total GSH in ELF and lung tissue did not correlate (Pearson's $r = 0.07283$, $p = 0.4273$).

Taken together, these data indicate that the response to MWCNT-induced oxidative stress varies across strains, as indicated by the total GSH content in lung tissue. This may be associated with baseline variation in strain differences, as reflected in total GSH levels in the control groups. However, these data also indicate that this MWCNT did not generate sufficient oxidative stress within 24 h of exposure to

significantly alter GSH levels in either lung tissue or ELF for most strains. Therefore, while these data indicate strain differences in the lung's total GSH levels and therefore support hypothesis 2.1, they do not support hypothesis 2.2, as the AJ mice did not have the most significant change in response to MWCNT exposure.

Real-time PCR measurement of mRNA levels of inflammation-, oxidative stress-, and fibrosis-associated genes.

We evaluated strain differences in the early pathological response to MWCNT exposure by measuring the mRNA levels of genes associated with inflammation, oxidative stress, and fibrosis. Inflammation genes include those associated with inflammasome activation (interleukin-1β, *Il1β*), pro-inflammatory signaling (tumor necrosis factor-α, *Tnfα*), granulocyte production (granulocyte-macrophage colony stimulating factor, *Gmcsf*), neutrophil chemoattraction (keratinocyte-derived cytokine, *Kc*), and monocyte recruitment (monocyte chemotactic protein-1, *Mcp1*).

Except for *Il1β*, the mRNA levels of these inflammation-associated genes were all significantly associated with both MWCNT exposure and strain (two-way ANOVA $p < 0.05$ for exposure, $p < 0.05$ strain) (Table 3.2). Post-hoc analyses indicated that, compared to each strain's respective control, MWCNT exposure significantly increased mRNA levels of *Tnfα* in 2/10 strains (AKR, FVB); of *Gmcsf* in 1/10 strains (DBA); of *Kc* in 2/10 strains (C3H, DBA); and of *Mcp1* in 1/10 strains (FVB). Overall, the percentage of neutrophils across all strains and exposure groups was significantly correlated with the mRNA levels of three of these genes: *Il1β* (Pearson's $r = 0.3740$, $p < 0.0001$); *Kc* ($r = 0.2755$, $p = 0.0022$); and *Tnfα* ($r = 0.1964$, $p = 0.0308$).

We also examined MWCNT-induced changes in mRNA levels of genes associated with GSH transport into lung ELF (cystic fibrosis transmembrane regulator protein, *Cftr*), GSH synthesis (glutamate cysteine ligase catalytic subunit, *Gclc*; glutamate cysteine ligase modifier subunit, *Gclm*), oxidative stress (heme oxygenase-1, *Hmox1*), and fibrosis (transforming growth factor-β 1, *Tgfβ1*). The mRNA levels of these five genes were not associated with either MWCNT exposure or strain (Table 3.3). However, across all strains and exposure groups, the GSH levels in lung tissue significantly correlated with *Gclm* (Pearson's $r = 0.2725$, $p = 0.0024$), consistent with its role in *de novo* GSH synthesis.

Altogether, these data indicate that 24 h after exposure to MWCNT, we can detect significant strain differences in the mRNA levels of genes related to an innate inflammatory response closely tied with neutrophil recruitment. The negative data on the mRNA levels of redox-sensitive genes is consistent with our data on total GSH, indicating that this MWCNT does not engender oxidative stress 24 h post-exposure. Consistent with our previous results on neutrophilia and total GSH, these data support hypothesis 2.1 in that they show clear strain differences in response to MWCNT exposure, but do not support hypothesis 2.2, in that the AJ strain is not the most sensitive to exposure.

Heatmap summarizing each strain's response to all pathological endpoints.

To summarize and compare each strains' responsiveness to all of the pathological endpoints examined, we created a heatmap of the log(fold-change) values for each endpoint within each strain (Figure 3.2). The fold-change compares the mean for each MWCNT-exposed group to its control group.

Our data across the ten strains show an overall pathological pattern of MWCNTs inducing an acute inflammatory response, but not an oxidative stress response. This acute inflammatory response was characterized by a statistically significant increase in lung neutrophilia for 8/10 strains, and by an associated increase in mRNA levels of pro-inflammatory genes *Gmcsf* (1/10 strains), *Kc* (2/10), *Mcp1* (1/10), and *Tnfα* (2/10). In contrast, only one strain had a statistically significant response for one oxidative stress-related endpoint: the FVB strain had lower levels of lung GSH in its MWCNT-exposed group compared to its control group.

BAL cytokines.

To better characterize the lung's inflammatory response across strains, we measured the levels of pro-inflammatory and chemoattractant cytokines (KC, TNF-α) in BALF in the AJ and C57 strains (Figure 3.3). While the C57 strain is more commonly used for MWCNT toxicity studies, the AJ strain had a response to MWCNT exposure closest to the overall mean of all strains for neutrophilia.
Both AJ and C57 mice had significantly higher levels of these two cytokines compared to their control group. However, exposed AJ mice had significantly higher levels of these two cytokines than did exposed C57 mice (KC, $p < 0.0001$; TNF-α, $p = 0.0340$).

When the data for both strains were pooled, we found that each cytokine correlated significantly with the percentage of neutrophils (KC: $r = 0.5353$, $p = 0.0002$; TNF-α: $r = 0.7138$, $p < 0.0001$).

Overall, these results were consistent with our hierarchical ranking of strains based on endpoint responsiveness: the AJ mice were more sensitive and responsive to MWCNT exposure compared with the C57 mice, as reflected in BAL levels of pro-inflammatory and chemoattractant cytokines.

Western immunoblot analysis.

To investigate if MWCNT exposure alters the expression of redox-sensitive proteins (GCLC, GCLM, and HMOX1) in a strain-specific manner, we used semi-quantitative Western immunoblotting to measure each of these proteins in lung homogenates in the six strains examined in the Kavanagh laboratory (129, AJ, C57, NOD, NZO, and WSB). We adjusted each sample's densitometry value to its β-actin loading control, and then calculated the fold-change by normalizing the adjusted values for the MWCNT-exposed groups to the mean of their respective dispersion medium-only control group.

We observed a mild (< 2-fold) but statistically significant increase in protein levels for at least one of these three proteins in 5/6 strains; only the WSB strain had no significant changes (Figure 3.4, A). Overall, there was no consistent pattern for the increased expression of these proteins. GCLC levels were significantly increased for 2/6 strains (AJ, NOD); GCLM levels for 3/6 strains (129, AJ, NOD); and HMOX1 levels for 2/6 strains (AJ, C57). We observed no significant correlations between the expression levels of these proteins and neutrophilia, glutathione in lung tissue, or glutathione in ELF.

To determine if strain altered susceptibility to severe nitrative stress, we determined if MWCNT exposure increased the generation of reactive nitrogen species (e.g., peroxynitrite) and consequent nitration of tyrosine residues on proteins in lung homogenates (Takakusa *et al.*, 2012). While Western immunoblotting readily detected 3-nitrotyrosine in our positive control (a peroxynitrite-treated lung homogenate of an unexposed mouse), it did not detect 3-nitrotyrosine residues in the homogenates of any control or exposed mice for any strain, even after exposing the film to the immunoblot for 1 h (Figure 3.4, B).

These Western blotting data indicated that MWCNT aspiration induced mild increases in the levels of redox-sensitive proteins, although these levels were not significantly correlated with neutrophilia or glutathione levels. Furthermore, these data indicated that MWCNT aspiration was not associated with nitrative stress. These results support hypothesis 2.1, because there was a strain-differential response in

protein levels, and they partially support hypothesis 2.2, because only the AJ strain had significant increases in the levels of all three redox-sensitive proteins.

3.4. Discussion

To evaluate the potential variety and extent of MWCNT-induced lung pathologies—and to contextualize the pathological response of the ubiquitous C57 strain—we characterized the inflammatory and oxidative stress responses in the lungs of ten strains of mice 24 h after aspiration of 25 μg MWCNT. Overall, our data demonstrate that this MWCNT sample induced an innate inflammatory response, but that it did not engender a response consistent with oxidative stress. Our data also indicate that the C57 strain was more resistant to MWCNT-induced inflammation than most other strains.

In support of hypothesis 2.1—that there would be a strain-dependent differential response to MWCNTs—we observed an innate inflammatory response characterized by an increase in lung neutrophilia for all strains, and which reached statistical significance for 8/10 strains. The strains ranged in susceptibility from the resistant WSB, which had a mean of only 7.49% neutrophils among cells recovered through BAL, to the susceptible 129, which had a neutrophil percentage of 43.04%. However, when we ranked the strains based on neutrophil percentage, the AJ strain was the closest to the overall mean for the control groups, and second-closest to the overall mean for the MWCNT-exposed groups. In contrast, the C57 strain was among the more resistant strains, as indicated by percentage of neutrophils in the MWCNT-exposed groups. These rankings clearly do not support hypothesis 2.2—that the AJ strain would be the sensitive and responsive to MWCNT exposure.

Our observation that CNT exposure provokes an innate inflammatory response dominated by neutrophilia is consistent with other reports. Previously, an interlaboratory study reported the male C57BL/6 mice that had aspirated 40 μg MWCNT had a percentage of neutrophils that ranged from approximately 10 – 40% across four collaborating institutions (Bonner *et al.*, 2013). These results are comparable to the range of responses we observed in our ten strains after adjusting for interlaboratory differences. Our results also agree with other studies, although the comparison is not perfect because these groups reported total cell numbers—a value reported to vary significantly between laboratories, even with standardized protocols (Bonner *et al.*, 2013). Cao *et al.* reported that two MWCNT samples

triggered an 8- and 20.8-fold increase in total BAL neutrophils 24 h after instillation of 32 μg MWCNT in female *ApoE*$^{+/+}$ C57BL/6 mice (Cao *et al.*, 2014). Similarly, Shvedova *et al.* reported that aspiration of 10 μg single-walled carbon nanotubes (SWCNTs) triggered a 51-fold increase in total BAL neutrophils among female C57BL/6 at 24 h after exposure (Shvedova *et al.*, 2008). This aim's results reinforces these reports in indicating that neutrophilia is the most prominent and consistent pathological response following acute CNT exposure. Furthermore, this aim's results add to this understanding by indicating that genetic variation can significantly affect the extent of neutrophilia induced by the same MWCNT.

While the extent of lung neutrophilia varied across mouse strains, we observed that it was significantly correlated with the expression of three pro-inflammatory and chemotactic genes: *Il1β*, *Kc*, and *Tnfα*. Similarly, when we measured BALF cytokine levels in AJ and C57 mice, we found that MWCNT exposure was associated with a significant increase in levels of KC and TNF-α for AJ and C57 mice. However, the exposed AJ mice had significantly higher cytokine levels than the exposed C57 mice. These cytokine results are consistent with our observation that C57 are more resistant to MWCNT-induced inflammation. These results are also consistent with other studies, which reported that MWCNT exposure in male C57BL/6 mice was associated with a significant increase in these two cytokines 24 to 40 h post-exposure (Cao *et al.*, 2014; Sun *et al.*, 2015).

In contrast to several previous studies, we did not observe consistent evidence for oxidative stress as indicated by changes in total GSH levels in lung tissue and ELF. However, one strain did demonstrate a significant decrease in total GSH levels in lung tissue following MWCNT exposure. CNT exposure has variously been reported to decrease lung GSH levels by 30% in juvenile BALB/c mice (Ravichandran *et al.*, 2011); to decrease total GSH by nearly 50% in female C57BL/6 mice (Luyts *et al.*, 2014); to increase total GSH by almost 1,500% in male CD-1 mice (Wang *et al.*, 2010); and to not alter total GSH in female C57BL/6 mice (Shvedova *et al.*, 2008) at 24 h post-exposure.

In addition to examining GSH levels, we also measured changes in mRNA levels for all ten strains and protein levels of redox-sensitive genes for six strains. At 24 h post-exposure, we found no changes in gene expression for any strain, while we observed a modest (< 2-fold) but statistically significant increase in levels of the proteins for 5/6 strains. This discrepancy may arise from the rapid and transient upregulation of these genes, which has been reported for *Hmox1* (Stocker and Perrella, 2006),

and post-translational regulation of proteins such as GCLC (Wild and Mulcahy, 2000; Krejsa *et al.*, 2010; Vogel and Marcotte, 2012). Given that the modest increases we observed did not significantly correlate with lung neutrophilia or glutathione levels, these data are at best weakly suggestive of MWCNT exposure inducing oxidative stress. Overall, these data support hypothesis 2.1, in that we observed one strain that was susceptible to GSH depletion induced by MWCNT exposure; however, they do not support hypothesis 2.2, in that this sensitive strain was not the AJ mice.

There are several possible explanations for why we did not observe oxidative stress. First, by measuring total GSH rather than the ratio of oxidized to reduced GSH, we may have missed subtler changes in redox status. However, we did not detect changes in the mRNA levels of redox-sensitive genes (e.g., *Gclc*, *Gclm*, *Hmox1*). Second, the MWCNT sample we used in this aim may not generate sufficient acellular radical species to induce oxidative stress. Our MWCNT was contaminated with relatively little metal (0.8% Ni, 0.4% iron); previously, Muhlfeld *et al.* reported that MWCNTs contaminated with 0.34% iron generated significantly fewer acellular radicals than did MWCNTs contaminated with 1.76% iron (Muhlfeld *et al.*, 2012). Indeed, another study reported that MWCNTs contaminated with 0.32% iron did not generate acellular radicals detectable through electron spin resonance (Porter *et al.*, 2010). Given that our MWCNT sample is contaminated with a comparable amount of iron, this MWCNT may be innately less capable of engendering the oxidative stress reported in other toxicity studies.

While our GSH data differ from some studies, our data on mRNA levels of redox-sensitive genes are consistent with other previous studies. In a subacute inhalation study of MWCNTs, Mitchell *et al.* observed no changes in lung mRNA expression of the oxidative stress-associated gene *Nqo1* (NADPH oxidoreductase 1) (Mitchell *et al.*, 2007). Similarly, Pacurari *et al.* observed no change at 7 days post-exposure in expression of the oxidative stress-associated genes for plasma GSH peroxidase-3 or superoxide dismutase-1, -2, or -3 (Pacurari *et al.*, 2011). In contrast, Cao *et al.* observed a significant increase in lung *Hmox1* expression following MWCNT exposure; however, as this exposure was a 5-week-long regimen with a cumulative exposure of 128 µg/mouse (Cao *et al.*, 2014), this elevated *Hmox1* expression may reflect severe oxidative stress resulting from a more toxic exposure regimen.

There were several limitations to this aim's approach. First, by examining only male mice in our multi-strain panel, we have likely missed important differences in susceptibility between the genders,

even as we have limited variables which may influence pathological differences across strains. Second, by using OPA of a MWCNT bolus to expose our mice, our results imperfectly represent the consequences of chronic inhalation of dry MWCNTs in an occupational setting. However, it was reported that aspiration of CNTs recapitulates the pathology associated with CNT inhalation, although to a lesser degree (Shvedova *et al.*, 2008).

In conclusion, we found support for hypothesis 2.1, in that there was a consistent strain-dependent differential response to MWCNTs, but no support for hypothesis 2.2, in that the AJ strain was not the most sensitive to MWCNT exposure. We found that MWCNT exposure was most consistently associated with lung neutrophilia, although the extent of response varied significantly with strain. These results are consistent with previous multi-strain studies, and indicate that the pathological response to MWCNT exposure has a significant genetic component. Furthermore, this study's results indicate that the common use of C57BL/6 mice for investigating MWCNT-induced toxicity may underestimate the range of responses possible in a genetically-heterogeneous human worker population, as the C57BL/6 mice was one of the strains more resistant to MWCNT-induced neutrophilia. To further explore strain differences and to identify the loci involved with inflammation susceptibility, future studies could involve crossing the neutrophilia-resistant WSB mice with the neutrophilia-sensitive 129 mice to generate offspring for performing quantitative trait loci analyses.

3.5. Figures

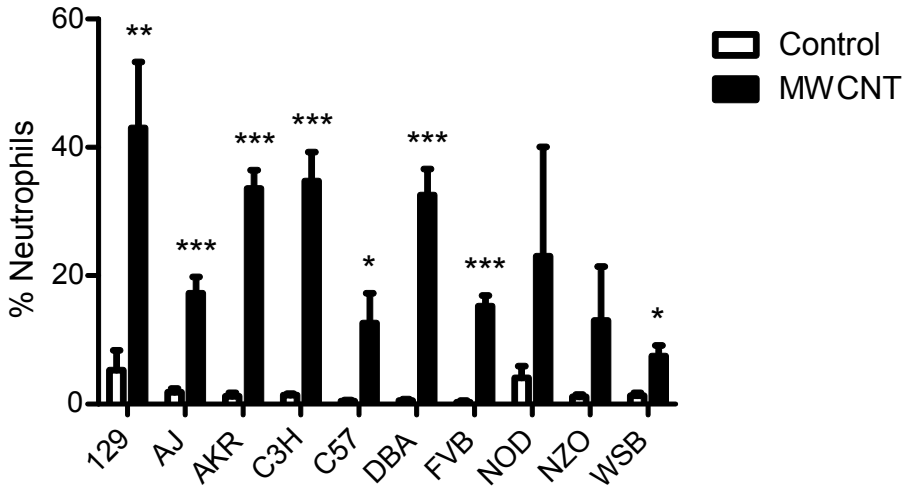

Figure 3.1. Neutrophilia varies by mouse strain.

Percentage of neutrophils in cells recovered through bronchoalveolar lavage of ten inbred mouse strains, 24 h after aspiration of dispersion medium vehicle (Control) or 25 µg MWCNT. Results are means and SEM (n ≥ 3 mice/group). * $p < 0.05$, ** $p < 0.01$, *** $p < 0.001$ compared to same-strain control.

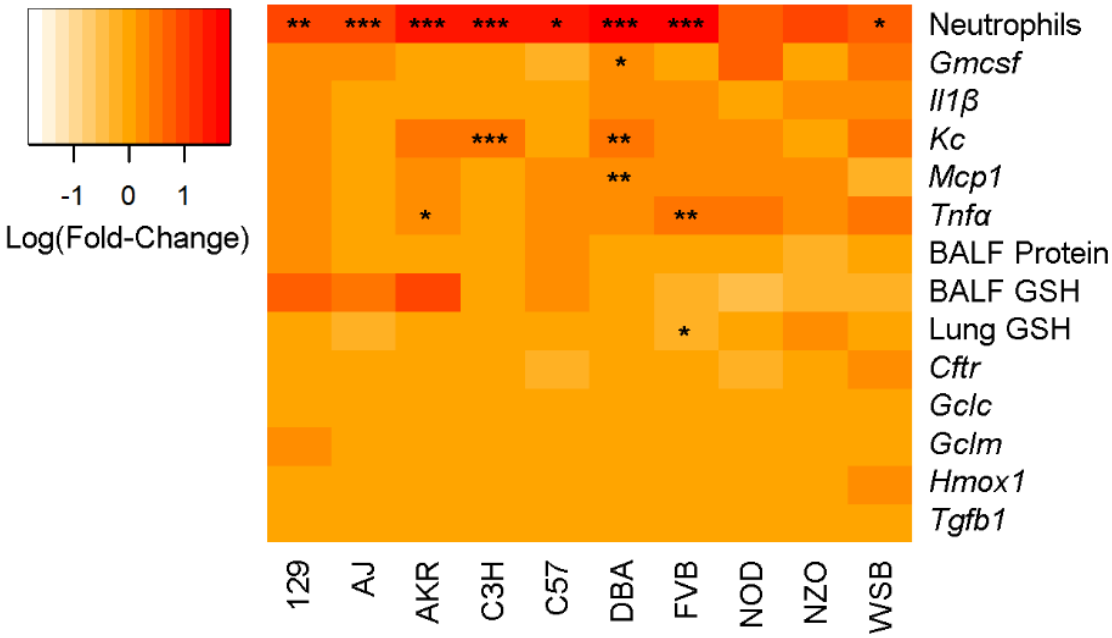

Figure 3.2. Heatmap of each strain's log(fold-change) values for all pathological endpoints.

The log(fold-change) compares the fold-change for each endpoint's MWCNT-exposed mean value to its control mean value. * $p < 0.05$, ** $p < 0.01$, *** $p < 0.001$ compared to the control group. Abbreviations: BALF, bronchoalveolar lavage fluid; GSH, glutathione; MWCNT, multi-walled carbon nanotube.

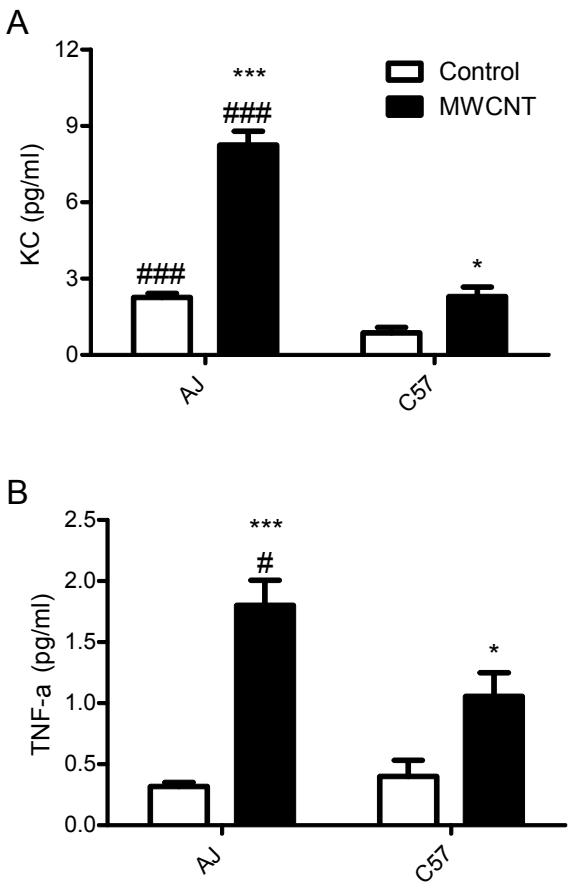

Figure 3.3. BALF cytokine levels in AJ vs. C57 mouse strains.

Levels of inflammation-associated cytokines in BALF recovered 24 h after aspiration of dispersion medium vehicle (Control) or 25 µg MWCNT. Results are means and SEM (n ≥ 3 mice/group). * $p < 0.05$, *** $p < 0.001$ compared to same-strain control. # $p < 0.05$, ### $p < 0.001$ compared to same-treatment group for C57 mice. Abbreviations: BALF, bronchoalveolar lavage fluid; MWCNT, multi-walled carbon nanotube.

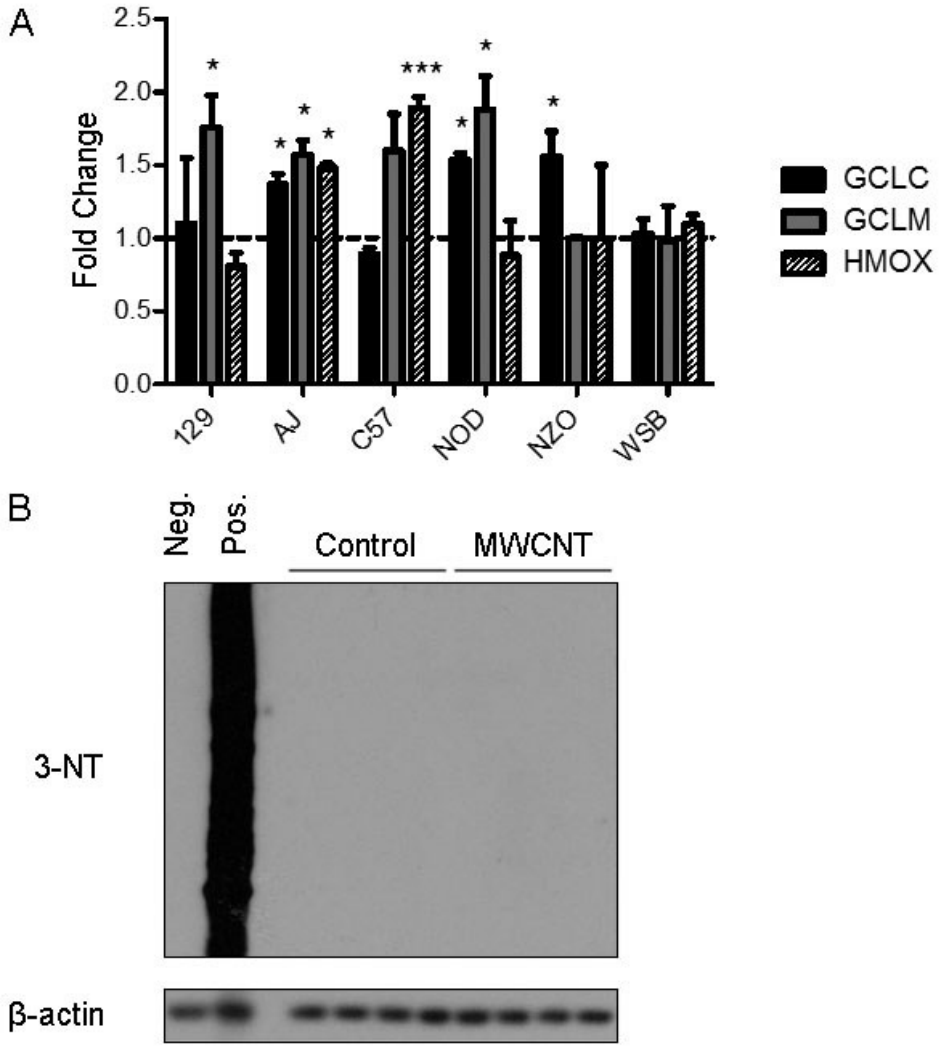

Figure 3.4. Semi-quantitative Western blotting for redox-sensitive protein expression and nitrated residues.

For the six strains examined in the Kavanagh laboratory, we examined the expression of redox-sensitive proteins using (A) densitometry analyses of Western blots for GCLC, GCLM, and HMOX1 in lung homogenates collected 24 h after aspiration of dispersion medium vehicle (Control) or 25 μg MWCNT. The results are means and SEM (n = 5 – 6 mice/group), adjusted to the loading control, β-actin, and calculated as the fold-change relative to the mean of each genotype's control. We also examined lung homogenates for nitrated residues; a representative blot from the NZO strain is shown (B). * $p < 0.05$, ** $p < 0.01$, *** $p < 0.001$ compared to same-strain control. Abbreviations: 3-NT, 3-nitrotyrosine; MWCNT,

multi-walled carbon nanotube; Neg., negative control (an untreated lung homogenate incubated with distilled water); Pos., positive control (an untreated lung homogenate incubated with peroxynitrite).

3.6. Tables

Table 3.1

Effects of MWCNT Exposure on Lung Injury and Oxidative Stress in Multiple Strains.

Strain	BALF Protein (mg/ml) Mean (SEM)	BALF GSH (μM) Mean (SEM)	Lung GSH (nmol/mg protein) Mean (SEM)
Control			
129	0.097 (0.012)	1.39 (0.22)	11.19 (1.52)
AJ	0.124 (0.018)	3.23 (0.28)	11.77 (1.54)
AKR	0.123 (0.006)	1.59 (0.38)	9.04 (0.54)
C3H	0.105 (0.005)	6.07 (0.65)	11.26 (0.84)
C57	0.125 (0.016)	4.68 (0.56)	13.01 (2.06)
DBA	0.177 (0.005)	4.41 (0.57)	13.68 (0.90)
FVB	0.201 (0.032)	9.66 (0.23)	24.39 (2.06)
NOD	0.264 (0.155)	10.34 (0.63)	8.13 (0.73)
NZO	0.208 (0.069)	6.01 (0.62)	8.79 (0.69)
WSB	0.216 (0.108)	2.81 (0.16)	10.15 (0.90)
MWCNT (25 μg)			
129	0.170 (0.032)	9.55 (25.20)	12.29 (0.71)
AJ	0.149 (0.030)	10.25 (25.72)	7.96 (0.82)
AKR	0.143 (0.014)	19.01 (25.78)	9.13 (0.79)
C3H	0.106 (0.018)	4.83 (25.27)	12.63 (1.09)
C57	0.167 (0.040)	7.67 (25.44)	12.31 (0.80)
DBA	0.181 (0.015)	5.36 (25.42)	11.91 (1.87)
FVB	0.237 (0.024)	5.58 (25.64)	16.39 (1.94)*
NOD	0.284 (0.186)	3.84 (25.02)	9.46 (1.31)
NZO	0.134 (0.055)	3.00 (25.85)	12.91 (1.57)
WSB	0.199 (0.031)	2.04 (25.55)	10.34 (1.14)

* $p < 0.05$ compared to same-strain control mice.
Abbreviation: BALF, bronchoalveolar lavage fluid; GSH, glutathione; MWCNT, multi-walled carbon nanotubes.

Table 3.2

Effects of MWCNT Exposure on mRNA Expression of Chemoattractant and Pro-Inflammatory Genes in Multiple Strains.

Strain	*Gmcsf* Mean (SEM)	*Il1β* Mean (SEM)	*Kc* Mean (SEM)	*Mcp1* Mean (SEM)	*Tnfα* Mean (SEM)
Control					
129	0.86 (0.29)	3.51 (0.64)	0.45 (0.16)	0.54 (0.13)	1.17 (0.13)
AJ	1.02 (0.20)	3.67 (0.80)	1.04 (0.18)	0.62 (0.08)	1.64 (0.20)
AKR	3.79 (0.41)	7.32 (0.39)	1.48 (0.13)	0.05 (0.27)	2.07 (0.22)
C3H	0.40 (0.02)	9.02 (0.85)	1.02 (0.18)	0.48 (0.09)	1.58 (0.21)
C57	1.86 (0.33)	4.90 (1.02)	0.45 (0.10)	0.73 (0.13)	1.38 (0.23)
DBA	0.64 (0.11)	4.30 (0.28)	1.12 (0.12)	0.56 (0.15)	1.52 (0.12)
FVB	3.13 (0.30)	3.49 (1.20)	1.94 (0.12)	0.00 (0.10)	1.60 (0.22)
NOD	0.36 (0.31)	6.35 (2.61)	0.82 (0.16)	0.96 (0.22)	1.49 (0.37)
NZO	1.00 (0.39)	1.43 (0.45)	1.05 (0.14)	0.68 (0.17)	2.54 (0.77)
WSB	0.32 (0.13)	1.77 (0.51)	0.15 (0.15)	0.32 (0.28)	1.27 (0.28)
MWCNT (25 µg)					
129	1.54 (0.67)	6.27 (2.70)	0.88 (0.31)	0.79 (0.26)	1.73 (0.44)
AJ	1.41 (0.28)	3.56 (0.62)	0.98 (0.21)	0.67 (0.13)	1.72 (0.12)
AKR	4.72 (0.60)	8.18 (0.91)	4.67 (1.41)	0.91 (0.65)	2.92 (0.24)*
C3H	0.44 (0.12)	8.26 (0.67)	2.86 (0.21)***	0.58 (0.03)	1.58 (0.16)
C57	1.26 (0.25)	5.93 (0.64)	0.53 (0.11)	0.97 (0.13)	1.87 (0.19)
DBA	1.14 (0.16)*	6.43 (0.75)	3.97 (0.64)**	0.11 (0.22)**	2.06 (0.41)
FVB	3.19 (0.47)	6.16 (0.93)	3.92 (2.27)	0.96 (0.24)	3.78 (0.54)**
NOD	1.69 (1.03)	5.49 (0.39)	1.37 (0.66)	0.05 (0.87)	3.68 (0.82)
NZO	1.05 (0.37)	2.00 (0.49)	0.80 (0.18)	0.28 (0.25)	3.47 (0.88)
WSB	1.09 (0.76)	2.84 (1.87)	0.41 (0.35)	2.96 (0.37)	3.63 (2.02)

All gene expression levels (x 10^3) normalized to expression of housekeeping gene *Gapdh*.
* $p < 0.05$, ** $p < 0.01$, *** $p < 0.001$ compared to the gene's same-strain expression in control mice.
Abbreviation: MWCNT, multi-walled carbon nanotubes.

Table 3.3

Effects of MWCNT Exposure on mRNA Expression of Oxidative Stress- and Fibrosis-Associated Genes in Multiple Strains.

Strain	*Cftr* Mean (SEM)	*Gclc* Mean (SEM)	*Gclm* Mean (SEM)	*Hmox1* Mean (SEM)	*Tgfb1* Mean (SEM)
Control					
129	11.89 (2.70)	99.98 (11.31)	48.38 (5.93)	33.31 (1.83)	79.13 (5.04)
AJ	22.78 (2.69)	176.54 (12.39)	78.44 (8.14)	71.59 (6.24)	100.47 (7.90)
AKR	32.73 (2.57)	117.28 (13.99)	74.89 (4.40)	61.84 (3.61)	128.49 (5.97)
C3H	18.26 (0.76)	195.24 (13.19)	70.90 (2.23)	81.37 (12.38)	75.97 (4.66)
C57	14.54 (1.46)	193.74 (14.64)	79.31 (5.20)	49.78 (5.07)	78.50 (8.90)
DBA	13.79 (0.52)	184.44 (9.63)	66.68 (5.03)	68.52 (4.70)	83.40 (10.29)
FVB	41.78 (1.59)	180.93 (20.63)	92.14 (4.46)	57.38 (3.86)	110.93 (14.64)
NOD	8.46 (4.30)	135.75 (28.15)	69.00 (15.60)	67.75 (5.27)	126.55 (17.91)
NZO	26.48 (8.46)	86.31 (20.82)	58.01 (20.76)	84.60 (20.70)	87.45 (16.07)
WSB	9.29 (2.58)	115.64 (17.57)	60.23 (9.85)	64.95 (10.29)	111.99 (15.05)
MWCNT (25 µg)					
129	9.63 (2.96)	81.41 (10.77)	74.72 (15.10)	31.48 (8.65)	68.95 (14.68)
AJ	19.65 (1.18)	169.21 (7.36)	65.04 (3.61)	76.73 (3.96)	77.51 (3.54)
AKR	29.40 (1.07)	125.48 (6.93)	68.12 (4.04)	66.18 (3.95)	139.58 (8.04)
C3H	15.66 (0.91)	169.19 (4.22)	67.46 (5.04)	104.95 (24.48)	76.61 (4.14)
C57	10.86 (1.51)	202.48 (21.76)	78.46 (7.20)	54.64 (2.57)	82.38 (8.58)
DBA	14.07 (0.76)	183.71 (15.79)	70.68 (4.89)	75.22 (8.49)	75.92 (2.45)
FVB	32.12 (9.70)	207.10 (7.09)	89.26 (8.77)	63.77 (18.31)	98.80 (19.65)
NOD	4.92 (1.60)	120.01 (30.45)	65.51 (10.63)	64.95 (4.75)	126.69 (17.69)
NZO	22.88 (8.67)	102.49 (15.71)	60.28 (18.64)	75.23 (12.92)	104.84 (8.18)
WSB	20.75 (13.85)	133.22 (46.97)	50.70 (20.27)	146.23 (76.93)	114.49 (26.29)

All gene expression levels (x 10^3) normalized to expression of housekeeping gene *Gapdh*. Abbreviation: MWCNT, multi-walled carbon nanotubes

Chapter 4 : Aim 3

4.1. Introduction

In the absence of human data, risk assessors at the National Institute for Occupational Safety and Health relied on *in vivo* animal toxicology studies to recommend an inhalation-based occupational exposure limit of 1 μg/m^3 for carbon nanotubes (CNTs) in 2013 (NIOSH, 2013). However, this risk assessment was limited by a lack of *in vivo* data on potentially sensitive subpopulations (NIOSH, 2013), who may be at greater risk of multi-walled CNT (MWCNT)-induced lung inflammation, fibrosis, or oxidative stress (Shvedova *et al.*, 2008; Ma-Hock *et al.*, 2009; Pauluhn, 2010b; Porter *et al.*, 2010; Wang *et al.*, 2011; Muhlfeld *et al.*, 2012).

CNTs may induce oxidative stress in the lung through acellular or cellular means. Radicals may be generated via acellular Fenton reactions with residual metals (e.g., nickel and iron), which are commonly used to manufacture CNTs (Madl *et al.*, 2014). Reactive oxygen/nitrogen species and oxidative stress may also result from the activation of immune cells, notably neutrophils and macrophages (Ma-Hock *et al.*, 2009; Shvedova *et al.*, 2012b; Bhattacharya *et al.*, 2013; Madl *et al.*, 2014). This CNT-induced oxidative stress was severe enough *in vivo* to deplete the major cellular tripeptide antioxidant glutathione (GSH) by 40 – 50% (Shvedova *et al.*, 2008; Ravichandran *et al.*, 2011; Luyts *et al.*, 2014). Conversely, elevated GSH levels may protect against such stress. For example, supplementation with the GSH precursor N-acetylcysteine in mice raised their GSH levels and rendered the animals resistant to MWCNT-induced fibrosis and neutrophilia (Sun *et al.*, 2015).

Taken together, these reports indicate that GSH deficiency is a potential consequence of CNT exposure, and that GSH supplementation is a potential protection against CNT-induced pathologies. However, there have been no investigations into how pre-existing GSH deficiency may modulate the lung's pathological response to MWCNTs. In humans, GSH can be depleted because of inadequate dietary intake of cysteine or methionine, or because of pre-existing lung diseases (e.g., chronic bronchitis, chronic obstructive pulmonary disease, idiopathic pulmonary fibrosis) (Biswas and Rahman, 2009; Ghezzi, 2011). GSH levels can also be affected by polymorphisms in *Gclc* and *Gclm*, which respectively encode the catalytic and modifier subunits for glutamate cysteine ligase (GCL), the rate-limiting enzyme in *de novo* GSH synthesis (Townsend *et al.*, 2003; Franklin *et al.*, 2009). Functional genetic

polymorphisms in *Gclc* and *Gclm* have been reported in 30% and 20% of humans, respectively (Nakamura *et al.*, 2002; Siedlinski *et al.*, 2008).

GSH deficiency can dramatically alter toxicant-induced lung pathology. The genetic manipulation of *Gclm* in a mouse model of human GSH deficiency indicated that even the moderate GSH deficiency observed in *Gclm* heterozygous mice significantly enhanced lung inflammation in response to diesel exhaust particle exposure (Weldy *et al.*, 2011). Furthermore, the severe GSH deficiency observed in *Gclm* null mice significantly impaired the lung's inflammatory response to ozone (Johansson *et al.*, 2010) and quantum dot nanoparticles (McConnachie *et al.*, 2013)—underscoring the role of GSH in modulating the immune response, as well as oxidative stress (Ghezzi, 2011).

Intriguingly, gender may modulate the effects of GSH deficiency. While male mice were found to be more sensitive than female mice to acetaminophen-induced liver injury, only female mice were rendered more susceptible to liver injury by *Gclm* manipulation. Following acetaminophen exposure, the female *Gclm* null mice demonstrated twice the amount of liver damage of wild-type mice; in contrast, male *Gclm* null mice only demonstrated 20% more injury than did wild-type mice (McConnachie *et al.*, 2007). In humans, gender also influences susceptibility to lung diseases. Interstitial lung diseases are approximately 20% more prevalent in men (Coultas *et al.*, 1994; Gribbin *et al.*, 2006), while asthma is 34% more prevalent in women (CDC, 2013).

Given that humans can have reduced levels of GSH for genetic, environmental, nutritional, or health status-related reasons, it is the first goal of this aim to investigate the role that GSH may play in MWCNT-induced acute lung pathology using mice with genetic modification of *Gclm*, which simulate moderate and severe deficiencies in GSH levels and GSH synthesis. Furthermore, given the evidence of gender modulating lung diseases, it is the second goal of this aim to investigate how gender influences susceptibility to MWCNT-induced lung inflammation. Finally, because both GSH and gender may interact to modify such responses, it is our third goal to examine the interdependency of gender and *Gclm* genotype in male and female mice exposed to MWCNTs. Such information could be used to better inform the assessment of risks associated with MWCNT exposure in subpopulations of workers who may be more or less susceptible to MWCNT-induced lung pathology, based on their gender and/or GSH status.

For this aim, I hypothesize that (3.1) *Gclm* heterozygous mice are more susceptible than wild-type and null mice to MWCNT-induced lung pathology, and (3.2) female *Gclm* heterozygous and null mice are more susceptible than their male counterparts.

4.2. Materials and Methods

Reagents.

Except where noted, we obtained all reagents from Sigma-Aldrich (St. Louis, MO).

MWCNT characterization.

For comprehensive characterization of this MWCNT (#12 stock), please see **Aim 1: Materials and Methods → *MWCNT characterization.***

Gclm mice.

We conducted all animal experiments in accordance with the National Institutes of Health Guide for the Use and Care of Laboratory Animals (NRC, 2011a), and with the approval of the University of Washington Institutional Animal Care and Use Committee. We made all efforts to minimize animal distress and suffering.

For these studies, we used male and female *Gclm* wild-type (*Gclm*$^{+/+}$), *Gclm* heterozygous (*Gclm*$^{+/-}$), and *Gclm* null (*Gclm*$^{-/-}$) mice which had been backcrossed onto a C57BL/6 background (McConnachie *et al.*, 2007). The mice were group housed in a modified specific pathogen free vivarium on a 12-hour light/dark cycle with nesting materials and access to water and chow provided *ad libitum*. At the time of MWCNT exposure, the mice were 3 – 5 months old with no significant difference in mean age between any of the experimental groups.

Experimental design.

To determine if gender and genetic manipulation of GSH levels modulate the lung's pathological response to MWCNTs, we randomly assigned 3- to 5-month-old mice of all *Gclm* genotypes to receive dispersion medium dosing vehicle only, or 25 µg MWCNTs/mouse by oropharyngeal aspiration (n = 5 – 6 mice per exposure, gender, and genotype, for a total of 71 mice). For purposes of comparison, a 10 µg MWCNT/mouse bolus dose is reported to approximate human deposition after one month of light work in an environment with an ambient MWCNT concentration of 400 µg/m^3, a level reported in Korean

manufacturing settings (Han *et al.*, 2008; Porter *et al.*, 2010). Thirty minutes prior to exposing the mice, we prepared fresh dispersion medium (DM) dosing vehicle [PBS + 0.6 mg/ml mouse serum albumin + 10 µg/ml DPPC (1,2-dipalmitoyl-sn-glycero-3-phosphocholine) surfactant in ethanol (0.1% v/v)] (Bonner *et al.*, 2013), and used it to resuspend the MWCNTs to 0.5 mg/ml. Both the dispersion vehicle and MWCNT solutions were sonicated for 19 seconds in a Branson 2510 bath sonicator, and then vortexed for 1 second.

Immediately before exposure, we weighed each mouse and anesthetized it with 4% Isoflurane. The mouse was exposed via oropharyngeal aspiration (OPA) of 50 µl DM only, or 50 µl of DM containing 25 µg MWCNTs, as previously described (Bonner *et al.*, 2013). We then monitored the mice until they had recovered from anesthesia, and for any signs of distress (e.g., weight loss, huddling, unkempt fur) over the next 24 h. Neither treatment was associated with distress or mortality.

Twenty-four h after exposure, we weighed each mouse to determine its post-treatment weight, and humanely euthanized each mouse through CO_2 narcosis followed by cervical dislocation. We performed bronchoalveolar lavage (BAL) with two serial lavages of sterile PBS (1.2 ml, 0.6 ml) as previously described (McConnachie *et al.*, 2013). From the first lavage, we aliquoted 100 µl for cytospins/differential staining of the recovered cells, and centrifuged the remainder. This acellular supernatant, or bronchoalveolar lavage fluid (BALF), was saved for measurements of cytokines, GSH content of the epithelial lining fluid (ELF), urea, total protein concentration, and lactate dehydrogenase concentration. In addition to BALF, we collected blood via cardiac puncture for serum isolation using serum separator tubes (Becton, Dickinson and Company, Franklin Lakes, NJ). We also removed a lung tissue sample from the right caudal lobe and immersed it in RNA*later*® Stabilization Solution (Ambion via Thermo Fisher Scientific Inc., Waltham, MA) for 24 h at 4 °C, and then froze this stabilized sample at -80 °C for later RNA extraction. The remainder of the right lung was snap-frozen in liquid nitrogen and stored at -80 °C until it could be processed for the measurement of GSH content, total protein, and the levels of oxidative stress responsive proteins via Western immunoblotting.

Assessment of lung inflammation through cell differentials.

To determine the lung's inflammatory responses to MWCNT aspiration, we performed differential scoring of the cells recovered in the first BAL. The cells in a 100-µl aliquot of the first lavage were

centrifuged (Cytospin 3, Shandon Life Sciences International Ltd., Cheshire, England) and then differentially stained using the Hema 3™ system (Thermo Fisher Scientific, Waltham, MA), a modification of the Wright-Giemsa method. The percentage of specific inflammatory cell types (eosinophils, lymphocytes, macrophages/monocytes, and neutrophils) was determined by counting at least 500 cells from each mouse. We report the percentage of cell types instead of the total number, because a multi-center study using standardized protocols demonstrated significant interlaboratory variation in the total number of recovered cell types, despite standardization (Bonner *et al.*, 2013).

Measurement of cytokines in bronchoalveolar lavage fluid.

The University of Washington's Center for Ecogenetics and Environmental Health Functional Genomics and Proteomics Core (CEEH FGPC) measured levels of BALF cytokines using the V-PLEX Proinflammatory Panel 1 Mouse Kit (Meso Scale Discovery, Rockville, MD), a multiplex sandwich immunoassay. The BALF samples were analyzed per manufacturer's directions for the levels of CXCL1 (KC), IL-1β, IL-6, and TNF-α. For this assay (lot #K0080292-166134), the dynamic range for KC was 0.408 – 1670 pg/ml; for IL-1β, 0.339 – 1390 pg/ml; for IL-6, 1.04 – 4260 pg/ml; and for TNF-α, 0.127 – 522 pg/ml. No samples were outside the range for KC and TNF-α analyses. For IL-1β, 69 out of 71 BAL samples (97.2%) were below the limit of detection (LOD), and further analysis was not possible for this cytokine. For IL-6, 14 out of 71 BAL samples (19.7%) were below the LOD. For the samples below the LOD, we replaced these values with the analyte's LOD divided by the square root of 2. This replacement method reportedly minimizes bias when samples with non-detectable levels represent fewer than 50% of all samples, and when the number of observations ranges from 20 – 100 (Hewett and Ganser, 2007; Ogden, 2010).

Measurement of total glutathione in lung tissue and epithelial lining fluid.

To assess the effects of MWCNT exposure, gender, and *Gclm* status, we measured levels of the major cellular antioxidant glutathione in lung tissue and ELF. In lung tissue, we measured the total glutathione (GSH+GSSG) content in clarified lung homogenates as previously described (McConnachie *et al.*, 2013), using tris-carboxyethyl phosphine to reduce GSSG to GSH, and derivatizing GSH with napthelene-2,3-dicarboxaldehyde. We then measured the relative fluorescence intensity of the derivatized GSH and calculated the GSH levels by interpolating from a standard curve [0.01 mM – 0.75

mM]. The total GSH content was normalized to the total protein content of the lung homogenate, which was determined using a commercial Bradford protein assay (Bio-Rad Laboratories, Inc., Hercules, CA). The total GSH and protein contents were both determined using triplicate samples of each homogenate.

To determine the concentration of total GSH in ELF, we used essentially the same procedure in BALF as described above for clarified lung homogenates, but with interpolation from a less-concentrated standard curve [0.25 μM – 5 μM]. To adjust this concentration for the dilution of ELF during lavage, we calculated the dilution factor by measuring urea in BALF and serum using the QuantiChrom™ Urea Assay Kit (BioAssay Systems, Hayward, CA). The use of urea to calculate a dilution factor assumes that urea freely diffuses between blood and ELF, thereby equalizing the urea concentrations between these compartments (Gould *et al.*, 2010).

Measurement of mRNA levels for genes associated with early pathological responses through quantitative real-time PCR.

The University of Washington's CEEH FGPC quantified the mRNA levels of specific genes using fluorogenic 5' nuclease-based assays as previously described (McConnachie *et al.*, 2013). In brief, we extracted total RNA from a sample of the caudal lobe of the right lung using the miRNeasy Mini Kit (Qiagen, Venlo, The Netherlands), and then generated cDNA from 1 μg of total RNA using the manufacturer's protocol for the SuperScript® III First-Strand Synthesis System (Life Technologies, Carlsbad, CA). The PCR reaction mix consisted of TaqMan Gene Expression Master Mix (Applied Biosystems Inc., Foster City, CA), along with primers and dual-labeled probes for each gene designed using ABI Primer Express v.1.5 software (Applied Biosystems). The targets were then amplified and detected using the ABI PRISM 7900 system (Applied Biosystems) using the following reaction profile: 1 cycle at 95 °C for 10 min; 40 cycles at 95 °C for 30 sec; 1 cycle at 62 °C for 1 min. To calculate mRNA expression levels, a linear regression formula was derived from *Gapdh* amplification plots using serial dilutions of an established reference sample.

The analyzed mRNAs included cystic fibrosis transmembrane regulator (*Cftr)*, glutamate cysteine ligase catalytic subunit (*Gclc)*, glutamate cysteine ligase modifier subunit (*Gclm),* granulocyte-macrophage colony stimulating factor (*Gmcsf),* heme oxygenase-1 (*Hmox1),* interleukin-1β (*Il1β),* Cxcl1/keratinocyte-derived cytokine, (*Kc)*, monocyte chemotactic protein-1 (*Mcp1)*, transforming growth

factor-β 1 (*Tgfβ1)*, and tumor necrosis factor-α (*Tnfα)*. The expression of these targets was normalized to *Gapdh* mRNA expression. The primer and probe sequences for these genes have been previously published (McConnachie *et al.*, 2013).

Assessment of bronchoalveolar lavage fluid for lung toxicity.

To evaluate MWCNT-induced lung toxicity, we measured in BALF the concentrations of acellular lactate dehydrogenase and total protein, which respectively indicate cytotoxicity and disruption of alveolar/capillary barrier integrity (Wesselkamper *et al.*, 2001a). The first lavage was centrifuged (500 *g*, 10 min, 4°C) and the acellular supernatant decanted to obtain BALF. We determined the concentration of lactate dehydrogenase in BALF using the enzyme activity CytoTox 96® Non-Radioactive Cytotoxicity Assay (Promega Corporation, Madison, WI). We determined the total protein concentration in BALF using a commercial Bradford protein assay (Bio-Rad Laboratories, Inc., Hercules, CA).

Semi-quantitative Western immunoblotting for redox-sensitive protein expression and protein nitration.

To evaluate redox-sensitive protein expression and protein nitration in homogenates of the right lung, we used SDS-PAGE and Western immunoblot analyses as previously described (Thompson *et al.*, 1999). The expression of GCLC and GCLM was detected using rabbit polyclonal anti-GCLC and -GCLM peptide antisera (Thompson *et al.*, 1999); HMOX1 was detected using rabbit polyclonal Heme Oxygenase 1 Antibody (Santa Cruz Biotechnology, Dallas, TX); and nitrotyrosine modifications were detected using anti-3-nitrotyrosine antibody (Takakusa *et al.*, 2012). We detected β-actin as the loading control using β-actin Rabbit Antibody (Cell Signaling Technology, Danvers, MA). To evaluate the extent of protein nitration, we ran on each SDS-PAGE gel a positive control (untreated lung homogenate incubated for 1 minute at room temperature in 1.0 mM peroxynitrite (Takakusa *et al.*, 2012)) and negative control (untreated lung homogenate incubated in an equivalent volume of distilled water). For each Western blot, we detected the bound secondary Goat Anti-Rabbit IgG Antibody, HRP-conjugate (EMD Millipore, Billerica, MA), using an enhanced chemiluminescence system (GE Healthcare UK, Buckinghamshire, UK) with X-ray film exposure. The optical densities of the appropriate-sized bands were then analyzed using NIH Image J software v1.48 (National Institutes of Health, Bethesda, MD). The optical density of each

band was adjusted to the density of the β-actin band, and the fold-change expression for each sample was calculated compared to the mean value for the dispersion medium vehicle-exposed control mice.

Statistical analyses.

We analyzed the data using two-way analysis of variance (ANOVA) for genotypes, treatments, and their interactions. For each genotype, we also analyzed the data using two-way ANOVA for gender, treatments, and interactions. When two-way ANOVA results indicated significant associations, we performed post-hoc analyses using unpaired, two-tailed *t*-tests, and adjusted the resulting *p*-values with Bonferroni corrections for multiple comparisons. For determining correlations, we calculated Pearson's correlation coefficients and report two-tailed *p*-values for significance. We managed our data in Excel 2013, part of Microsoft Office Professional Plus 2013 (Microsoft, Redmond, WA), and analyzed our data in Prism 5 for Windows, v.5.02 (GraphPad Software, Inc., La Jolla, CA).

4.3. Results

Lung inflammation.

To investigate gender- and GSH-dependent susceptibility to acute lung inflammation, we determined the percentage of neutrophils and eosinophils through differential staining of cells recovered through BAL 24 h after MWCNT aspiration. Mice which aspirated an equal volume of dispersion medium served as controls.

MWCNT exposure significantly increased lung neutrophilia in *Gclm*$^{+/+}$ mice of both genders (Figure 4.1), but *Gclm* genotype was significantly associated with neutrophilia only among female mice (two-way ANOVA $p = 0.0191$). When compared to MWCNT-exposed female *Gclm*$^{+/+}$ mice, the MWCNT-exposed female *Gclm*$^{+/-}$ *and Gclm*$^{-/-}$ mice had significantly less neutrophilia. In contrast, MWCNT exposed male *Gclm*$^{+/-}$ and *Gclm*$^{-/-}$ mice developed neutrophilia to an extent comparable to that of MWCNT exposed male *Gclm*$^{+/+}$ mice, although these were statistically non-significant when compared to their respective dispersion medium-alone control groups.

In addition to neutrophilia, MWCNT exposure induced a mild (< 2%) but statistically significant eosinophilia among female mice (two-way ANOVA $p = 0.0022$), although none of the post-hoc analyses were significant when comparing exposure groups within each *Gclm* genotype. In contrast to the

genotype-dependent pattern of neutrophilia among female mice, this mild eosinophilia did not significantly vary by *Gclm* genotype (Figure 4.2).

Taken together, these results do not support either hypothesis 3.1 or 3.2. Instead, these results indicate that moderate and severe GSH deficiencies significantly reduce MWCNT-induced neutrophilia among female, but not male, mice.

BALF cytokines.

To determine if gender and GSH levels alter immune signaling 24 h after MWCNT aspiration, we measured the concentration in BALF of cytokines involved with pro-inflammatory signaling (TNF-α, IL-6) and neutrophil chemoattraction (KC)

MWCNT aspiration significantly increased levels of these cytokines in BALF in both genders (Figure 4.3). MWCNT aspiration but not *Gclm* genotype was significantly associated with higher levels of TNF-α, KC, and IL-6. We did not observe significant differences in cytokine levels between genders.

We found in both genders that BALF cytokine levels correlated significantly with the proportion of neutrophils recovered in BAL. In males, this correlation was significant for TNF-α (Pearson's $r = 0.6974$, $p < 0.0001$) and IL-6 ($r = 0.6164$, $p < 0.0001$), but not for KC. In females, this correlation was significant for TNF-α ($r = 0.7062$, $p < 0.0001$), IL-6 ($r = 0.5649$, $p = 0.0003$), and KC ($r = 0.4496$, $p = 0.0059$).

These results do not support hypothesis 3.1, as we did not observe a significant increase in pro-inflammatory cytokines in the *Gclm*$^{+/-}$ mice compared with other genotypes. Furthermore, these results do not support hypothesis 3.2, as we did not observe a difference in cytokine levels between the genders.

Total glutathione content in lung tissue and epithelial lining fluid.

GSH is a major cellular antioxidant involved in regulating the cell's redox state and the immune response. Total GSH content is sensitive to toxicant exposure, in that CNT exposure depletes GSH from lung tissue (Shvedova *et al.*, 2008; Ravichandran *et al.*, 2011), while cigarette smoke increases glutathione in ELF (Gould *et al.*, 2012). Thus, we examined the effect of MWCNT aspiration on total GSH levels in lung tissue and in ELF.

For any *Gclm* genotype and either gender, MWCNT exposure did not alter the amount of total GSH measured in clarified homogenates of lung tissue (Figure 4.4). As expected, genotype was significantly associated with lung GSH for both genders (two-way ANOVA $p < 0.0001$). Among male

control mice, the *Gclm*$^{+/+}$ and *Gclm*$^{+/-}$ mice had approximately 68% and 11% the levels of *Gclm*$^{-/-}$ mice, respectively. Among female control mice, *Gclm*$^{+/-}$ and *Gclm*$^{-/-}$ mice had 84% and 22% the levels of *Gclm*$^{+/+}$ mice, respectively. While lung GSH levels were comparable between the genders for *Gclm*$^{+/-}$ and *Gclm*$^{-/-}$ mice, exposed female *Gclm*$^{-/-}$ mice had significantly lower levels (approximately 72%) of lung GSH compared to male *Gclm*$^{+/+}$ mice (p = 0.0027). Our data on GSH levels in male mice agree with previous reports for this mouse *Gclm* model; female mice were not examined in these other studies (McConnachie *et al.*, 2007; McConnachie *et al.*, 2013).

The concentration of GSH in ELF was not associated with MWCNT exposure or *Gclm* genotype for either gender (Figure 4.5).

Taken together, our data indicate that MWCNT aspiration did not induce oxidative stress sufficient to alter total GSH levels in the lung 24 h after exposure. Furthermore, these results do not support either hypothesis 3.1 or 3.2.

Real-time PCR measurement of inflammation-, oxidative stress-, and fibrosis-associated gene expression.

To assess the early pathological responses induced by MWCNT aspiration, we measured at 24 h post-exposure the mRNA levels of genes involved in inflammation, oxidative stress, and fibrosis pathways.

We assessed inflammatory and pro-fibrotic responses by measuring mRNA expression of genes associated with granulocyte production (granulocyte-macrophage colony stimulating factor, *Gmcsf*), neutrophil chemoattraction (keratinocyte-derived cytokine, *Kc*), monocyte recruitment (monocyte chemotactic protein-1, *Mcp1*), inflammasome activation (interleukin-1β, *Il1β*), pro-inflammatory signaling (tumor necrosis factor-α, *Tnfα*), and fibrosis (transforming growth factor-β 1, *Tgfβ1*). MWCNT aspiration was not associated with a change in expression detectable 24 h post-exposure (male, Table 4.1; female, Table 4.2), except for increased *Gmcsf* expression in exposed male *Gclm*$^{+/+}$ mice. Intriguingly, gender played a more important role than MWCNT exposure in mRNA expression levels for four of these genes: Female mice of all *Gclm* genotypes expressed significantly higher levels of *Gmcsf*, *Kc*, and *Mcp1* than did male mice. Female *Gclm*$^{+/-}$ and *Gclm*$^{-/-}$ mice also expressed significantly higher levels of *Tgfβ*1 than their male counterparts.

We analyzed the mRNA levels of oxidative stress genes associated with GSH synthesis (glutamate cysteine ligase catalytic subunit, *Gclc*; glutamate cysteine ligase modifier subunit, *Gclm*), oxidative stress (heme oxygenase-1, *Hmox1*), and GSH transport into lung ELF (cystic fibrosis transmembrane regulator protein, *Cftr*). For male and female mice of all *Gclm* genotypes, MWCNT aspiration did not induce oxidative stress sufficient to significantly alter expression of these four mRNAs (male, Table 4.1; female, Table 4.2). As expected, *Gclm* genotype was significantly associated with expression of *Gclm* mRNA (male and female $p < 0.001$). *Gclm* genotype was also significantly associated with *Hmox1* mRNA expression in female mice (two-way ANOVA $p = 0.0268$). For both genders, *Gclm* expression significantly correlated with lung GSH levels (male Pearson's $r = 0.8126$, $p < 0.0001$; female $r = 0.7700$, $p < 0.0001$).

When we compared mRNA expression between genders, we found that *Gclm* mRNA expression was significantly lower in females for control $Gclm^{+/+}$, control $Gclm^{+/-}$, and MWCNT-exposed $Gclm^{+/-}$ mice. Similarly, female $Gclm^{+/-}$ and $Gclm^{-/-}$ mice had significantly lower *Hmox1* mRNA expression compared to their male counterparts. In contrast, female mice of all *Gclm* genotypes had greater *Cftr* expression than did male mice, although this difference was statistically non-significant. *Cftr* expression did not significantly correlate with GSH levels in the ELF for either gender.

Collectively, our mRNA expression data indicate that the expression of inflammation-related genes was unaltered 24 h post-MWCNT-exposure, consistent with reports that gene expression of pro-inflammatory cytokines peaks less than 8 h after lung injury (Lesur *et al.*, 2010; Weldy *et al.*, 2011). Intriguingly, female mice of all genotypes expressed significantly higher levels of neutrophil and monocyte recruitment cytokines than did male mice—indicating that gender, rather than MWCNT exposure or *Gclm* genotype, has a significant influence on mRNA expression of these genes. Consistent with our observations on lung GSH levels, we found that MWCNT aspiration did not induce oxidative stress sufficient to change related gene expression at least at 24 h post-exposure. Consistent with our previous results, these data on mRNA expression do not support either hypothesis 3.1 or 3.2.

Lung toxicity.

To assess how MWCNT-induced lung damage might vary between genders and *Gclm* genotypes, we measured acellular BALF lactate dehydrogenase levels as an indicator of cellular death,

and BALF total protein levels as an indication of the integrity of the alveolar-capillary barrier. We found that MWCNT aspiration did not cause sufficient lung damage at 24 h post-exposure to increase lactate dehydrogenase or protein levels (Table 4.3). Furthermore, these parameters did not significantly differ between genders or *Gclm* genotypes.

These results indicate that neither gender nor GSH deficiency predisposes the lung towards MWCNT-induced cellular damage and alveolar-capillary disruption. Furthermore, they do not support either hypothesis 3.1 or 3.2.

Western immunoblot analysis.

To investigate if MWCNT exposure alters the expression of redox-sensitive proteins (GCLC, GCLM, and HMOX1) in a gender- and/or *Gclm* genotype-dependent manner, we used semi-quantitative Western immunoblotting to measure each of these proteins in lung homogenates. We adjusted each sample's densitometry value to its β-actin loading control, and then calculated the fold-change by normalizing the adjusted values for the MWCNT-exposed groups to the mean of their respective dispersion medium-only control group.

Consistent with our observations for mRNA expression of *Gclc*, *Gclm*, and *Hmox1*, MWCNT aspiration did not significantly alter the expression of these three proteins at 24 h post-exposure (Figure 4.6 and Figure 4.7, A). As expected, we did not detect GCLM protein expression in the lung homogenates prepared from *Gclm*$^{-/-}$ mice (Figure 8, A).

To determine if gender or *Gclm* genotype confer increased susceptibility to severe nitrative stress, we determined if MWCNT exposure increased the generation of reactive nitrogen species (e.g., peroxynitrite) and consequent nitration of tyrosine residues on proteins in lung homogenates (Takakusa *et al.*, 2012). While Western immunoblotting readily detected 3-nitrotyrosine in our positive control (a peroxynitrite-treated lung homogenate of an unexposed mouse), it did not detect 3-nitrotyrosine residues in the homogenates of any control or exposed mice, even after exposing the film to the immunoblot for 1 h (Figure 4.7, B).

These Western blotting data indicate that MWCNT aspiration induces neither subtle alterations in redox-sensitive protein expression nor substantial nitrative stress, not even in *Gclm*$^{-/-}$ mice with substantially lower levels of lung GSH. These results do not support either hypothesis 3.1 or 3.2.

4.4. Discussion

In order to identify potential factors modulating MWCNT-induced acute pathology in the lung, we examined how gender and genetically-induced GSH deficiencies altered lung inflammation and oxidative stress in a mouse model of MWCNT exposure. Overall, I found no support for either hypothesis 3.1—that the *Gclm*$^{+/-}$ mice would be the most susceptible—or hypothesis 3.2—that the female *Gclm*$^{+/-}$ and *Gclm*$^{-/-}$ mice would be more susceptible than their male counterparts. However, we did find that gender and *Gclm* genotype modulate the lung's pathological response to MWCNT exposure, although not in the manner hypothesized.

Our results indicate that GSH levels significantly alter the lung's innate immune response to an acute MWCNT exposure in a gender-dependent manner. Twenty-four h after exposing the mice via OPA, we found a significant increase in neutrophils recovered from the lungs of *Gclm*$^{+/+}$ mice of both genders. Gender differences emerged when we examined the *Gclm*$^{+/-}$ and *Gclm*$^{-/-}$ mice. While male *Gclm*$^{+/-}$ and *Gclm*$^{-/-}$ mice demonstrated a MWCNT-induced neutrophilia comparable to their *Gclm*$^{+/+}$ counterparts, female *Gclm*$^{+/-}$ and *Gclm*$^{-/-}$ mice had significantly less neutrophilia than their *Gclm*$^{+/+}$ counterparts. Intriguingly, MWCNT exposure was associated with increased levels of pro-inflammatory cytokines, regardless of *Gclm* genotype or gender—indicating that the differences in neutrophilia are likely to be independent of altered pro-inflammatory cytokine signaling.

These differences in neutrophilia between the genders may relate to steroid hormone regulation of the inflammatory response and gene expression. One possibility is that the male mice may have developed greater neutrophilia because of their higher levels of androgens, which can enhance the lung's inflammatory response. In support of this, lipopolysaccharide was reported to induce significantly less neutrophil influx into the lungs of castrated male mice, compared to intact mice (Card *et al.*, 2006). Another possibility is that the female *Gclm*$^{+/-}$ and *Gclm*$^{-/-}$ mice may have been protected against inflammation because of their higher levels of estrogens, which can regulate macrophage-monocyte systems, inhibit the binding of transcription factor NF-κB to regulatory regions of pro-inflammatory genes (Harkonen and Vaananen, 2006), and upregulate expression *in vitro* of glutathione-S-transferase Pi (*GSTp*) and *Gclc* (Montano *et al.*, 2004). While we did not observe a significant increase in *Gclc* mRNA or protein expression, the female *Gclm*$^{+/-}$ and *Gclm*$^{-/-}$ mice may have had an estrogen-dependent

upregulation of other mechanisms which protected them against MWCNT-induced neutrophilia. Indeed, a previous study found that acute ozone exposure induced significantly greater lung injury (as indicated by BALF total protein levels) in *Gclm*$^{+/+}$ mice compared to *Gclm*$^{-/-}$ mice, which had significantly higher levels of protective enzymes in their lungs (e.g., metallothionein, α-tocopherol transporter protein, sodium-dependent vitamin C transporter) (Johansson *et al.*, 2010).

It is also possible that the reduced neutrophilia among female *Gclm*$^{+/-}$ and *Gclm*$^{-/-}$ mice may be due to impairment of a GSH-dependent neutrophil response, with potential repercussions on longer-term pathology. Previously, chemical depletion of GSH in a mouse cecum-puncture model of sepsis was associated with a decrease in neutrophil influx to the infection site, and a concomitant increase in bacterial infection (Villa *et al.*, 2002). The lack of a robust neutrophil response among female GSH-deficient mice may similarly impair clearance of MWCNTs from the lung, particularly because of the absence of neutrophil-dependent myeloperoxidase activity. Mice deficient in myeloperoxidase—an enzyme critical to the neutrophil's respiratory burst—were observed to retain CNT significantly longer in their lungs, and to develop significantly more fibrosis (Shvedova *et al.*, 2012a). The absence of neutrophils and myeloperoxidase activity may therefore impose similar pathology on GSH-deficient female mice. Moreover, the efficacy of those neutrophils which do influx may be further compromised in GSH-deficient mice, as chemical depletion of GSH in human neutrophils *ex vivo* reduced the efficacy of neutrophil phagocytosis (Oliver *et al.*, 1976). If this is the case in humans, women workers who are GSH-deficient because of pre-existing health conditions, nutritional status, or common genetic polymorphisms may be at greater risk of an impaired neutrophil response to CNTs, and may therefore be at greater risk for CNTs persisting in the lung and inducing fibrosis.

We also observed that, regardless of MWCNT exposure or *Gclm* genotype, female mice had significantly higher expression of the genes *Gmcsf*, *Kc*, and *Mcp1*. These cytokines are produced by numerous cell types (e.g., macrophages, endothelial cells) possessing steroid hormone receptors (Shi *et al.*, 2006; Gupta and Singh, 2008). Indeed, progesterone pretreatment is reported to increase mRNA expression of *Kc* in female BALB/cCrSlc mice (Toyoda *et al.*, 2012). Similarly, progesterone treatment of mouse peritoneal macrophages *ex vivo* enhanced the expression of MCP-1 and other cytokines following hydrogen peroxide exposure (Huang *et al.*, 2008). Differences in *Kc/CXCL1* mRNA expression have also

been reported among humans, where a study of whole blood from healthy volunteers found that women had a small but significant 1.3- to 1.5-fold increase in levels of *Kc/CXCL1* mRNA compared to men (Karlovich *et al.*, 2009). The functional effects of higher mRNA levels may be limited in this aim, however, as we did not observe significant differences between the genders for cytokine protein levels.

Surprisingly, we did not find evidence for MWCNT-induced oxidative or nitrative stress. Twenty-four h after MWCNT exposure, we found that total GSH levels were significantly associated with *Gclm* genotype in lung tissue, but not in ELF. However, total GSH levels in either lung tissue or ELF did not differ with MWCNT exposure for either gender or any *Gclm* genotype. We did not observe any formation of 3-nitrotyrosine residues on proteins in lung tissue homogenate.

There are at least four possible explanations for these observations. First, we may have missed subtle changes in the cell's redox status by measuring total GSH, rather than evaluating the ratio of oxidized to reduced glutathione (Weldy *et al.*, 2012). However, we did not detect subtle changes in redox status when we measured mRNA levels or protein expression of the redox-sensitive proteins GCLC, GCLM, and HMOX1 (McConnachie *et al.*, 2013). Second, CNT-induced GSH depletion may not be detected until more time has elapsed after exposure. Shvedova *et al.* reported that CNT exposure *in vivo* did not deplete total GSH levels in lung tissue until 7 days post-exposure (Shvedova *et al.*, 2008). Third, our MWCNT sample in this aim may generate relatively few radicals through acellular Fenton reactions, because these MWCNTs contains low (< 1%) levels of metals such as iron and nickel (Madl *et al.*, 2014). Muhlfeld *et al.* reported that MWCNT with 1.76% iron generated significantly more acellular radicals than MWCNT with 0.34%, as measured by electron paramagnetic resonance (Muhlfeld *et al.*, 2012). Indeed, Shvedova's study used CNTs contaminated with significantly higher levels of iron (17.7%) than our MWCNTs (0.4%) (Shvedova *et al.*, 2008). And fourth, GSH depletion may only be associated with prolonged exposures, such the GSH depletion observed in mice after a 7-d-long inhalation exposure (Ravichandran *et al.*, 2011) or after five weekly exposures (Luyts *et al.*, 2014).

There are several limitations inherent in this aim. First, there are many MWCNTs available on the market with physicochemical characteristics different from the sample we examined. Because the pathological effects of MWCNTs have been shown to vary with physicochemical characteristics (e.g., length, width, surface modification, metal contamination) (Muller *et al.*, 2005; Johnston *et al.*, 2010;

Muhlfeld *et al.*, 2012; Hamilton *et al.*, 2013), our results may not extrapolate perfectly to other MWCNTs. Second, our results are derived from an artificial exposure method—a single OPA of a liquid MWCNT bolus—rather than chronic inhalation of MWCNT, which may better model human occupational exposure. Nonetheless, Shvedova *et al.* demonstrated in mice that a single aspiration of CNTs recapitulated the pathological response of CNT inhalation, although the response to the aspirated CNTs was less robust than to the inhaled CNTs (Shvedova *et al.*, 2008). Our results indicate that further studies involving sub-chronic or chronic inhalation of MWCNTs would be warranted in *Gclm* mice of both genders, and would hopefully provide useful information on the effects of GSH and gender on MWCNT clearance and lung fibrosis.

In conclusion, this aim shows that female mice are more vulnerable to acute MWCNT-induced pathology. Female mice which were moderately and severely GSH-deficient had a significantly impaired neutrophil response to MWCNTs, compared to the robust neutrophilia of their male counterparts. Furthermore, all female mice developed mild eosinophilia following MWCNT exposure. These results indicate that women workers exposed to CNT may be at greater risk of CNT-induced eosinophilia—a characteristic of occupational asthma. Furthermore, women workers who are GSH-deficient may be at risk of impaired neutrophil-based clearance of CNT from the lung, which may put them at greater risk of developing lung fibrosis. Given that GSH levels can be influenced by pre-existing health conditions, nutrition status, and genetic polymorphisms present in 20 – 30% of humans (Nakamura *et al.*, 2002; Siedlinski *et al.*, 2008), a significant proportion of the CNT workforce may therefore be more sensitive to CNT-induced lung pathology. Future risk assessments to set occupational exposure limits should account for these sensitive subpopulations, to ensure optimal protection of the growing CNT workforce against CNT-induced lung inflammation, fibrosis, and oxidative stress.

4.5. Figures

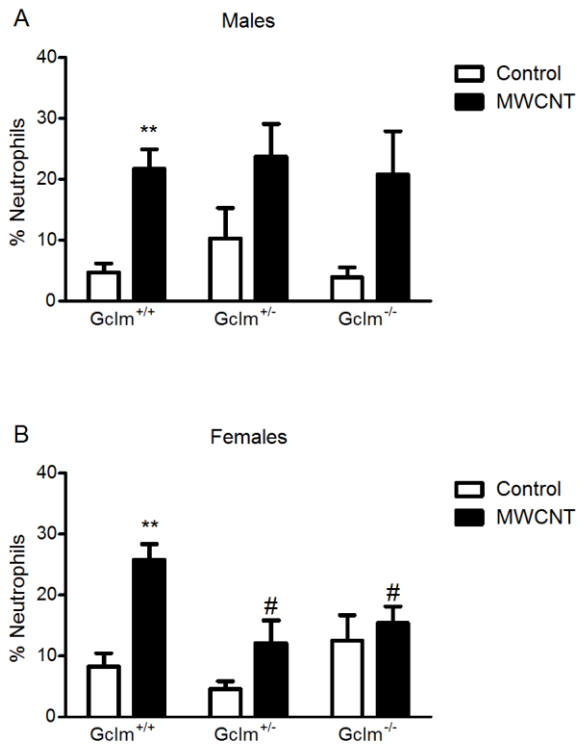

Figure 4.1. Lung neutrophilia.

Percentage of neutrophils in cells recovered through bronchoalveolar lavage of (A) male and (B) female *Gclm* mice, 24 h after aspiration of dispersion medium vehicle (Control) or 25 µg MWCNT. Results are means and SEM (n = 5 – 6 mice/group). ** $p < 0.01$ compared to same-genotype control, # $p < 0.05$ compared to MWCNT-exposed *Gclm*$^{+/+}$. Abbreviation: MWCNT, multi-walled carbon nanotube.

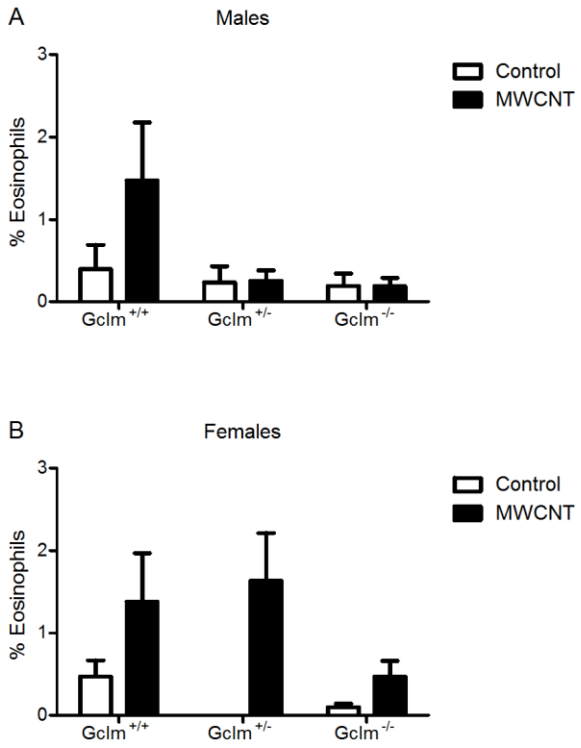

Figure 4.2. Lung eosinophilia.

Percentage of eosinophils in cells recovered through bronchoalveolar lavage of (A) male and (B) female *Gclm* mice, 24 h after aspiration of dispersion medium vehicle (Control) or 25 µg MWCNT. Results are means and SEM (n = 5 – 6 mice/group). Abbreviation: MWCNT, multi-walled carbon nanotube.

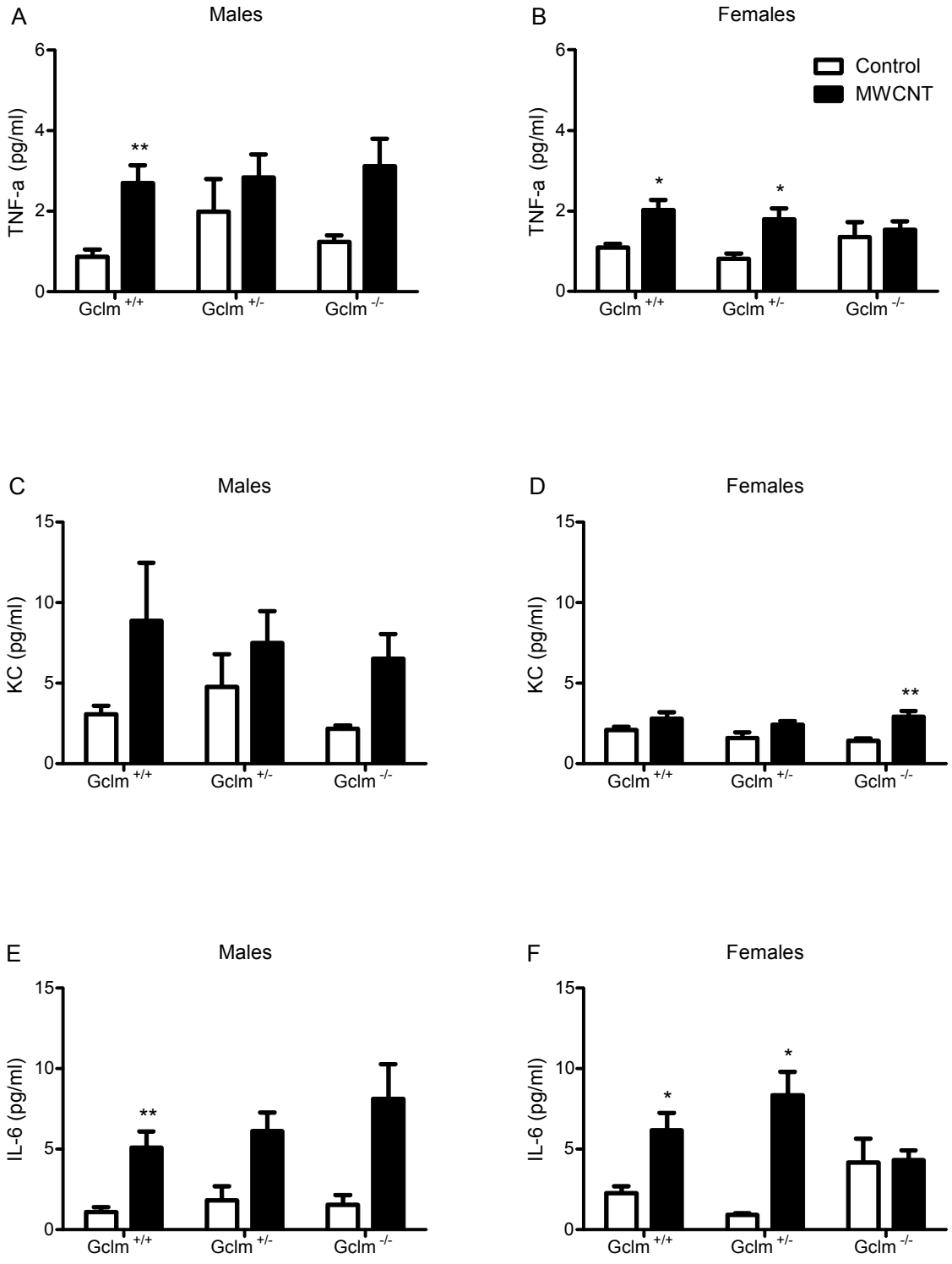

Figure 4.3. Pro-inflammatory cytokines in lungs.

Levels of inflammation-associated cytokines in bronchoalveolar lavage fluid recovered 24 h after aspiration of dispersion medium vehicle (Control) or 25 μg MWCNT by male and female *Gclm* mice. Cytokines include TNF-α (A, male; B, female), KC (C, male; D, female), and IL-6 (E, male; F, female). Results are means and SEM (n = 5 – 6 mice/group). * $p < 0.05$, ** $p < 0.01$ compared to same-genotype control. Abbreviation: MWCNT, multi-walled carbon nanotube.

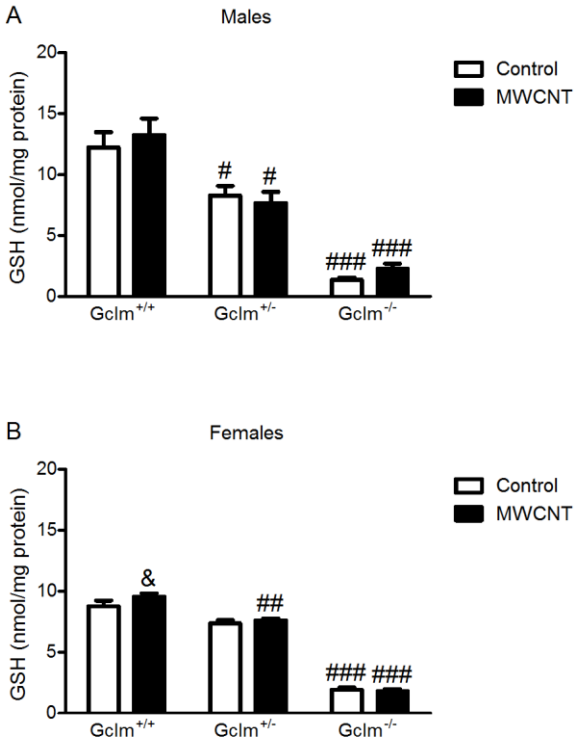

Figure 4.4. Glutathione levels in lungs.

Lung total glutathione content measured 24 h after aspiration of dispersion medium vehicle (Control) or 25 µg MWCNT by (A) male and (B) female *Gclm* mice. Results are means and SEM (n = 5 – 6 mice/group). # $p < 0.05$, ## $p < 0.01$, ### $p < 0.001$ compared to same-treatment *Gclm*$^{+/+}$, & $p < 0.05$ compared to same-treatment, same-genotype males. Abbreviations: GSH, glutathione; MWCNT, multi-walled carbon nanotube.

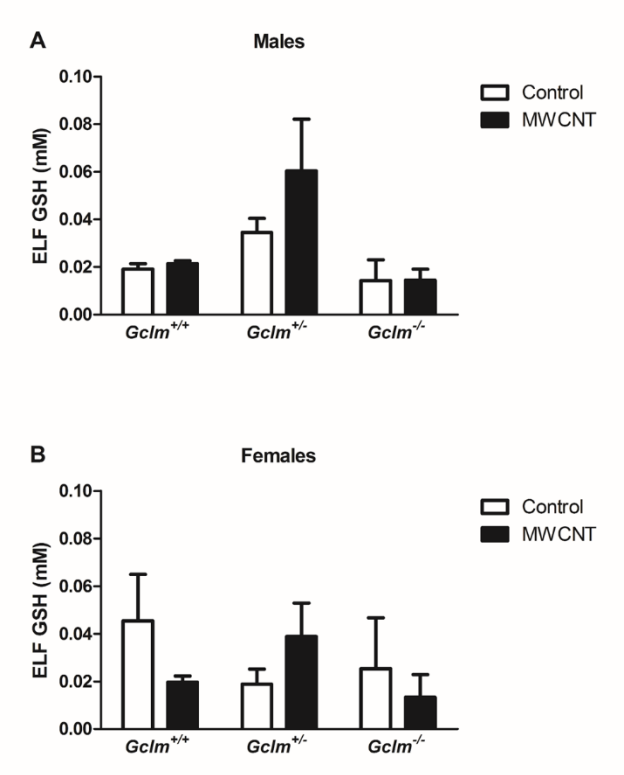

Figure 4.5. Glutathione levels in epithelial lining fluid.

Total glutathione content of lung ELF recovered through bronchoalveolar lavage of (A) male and (B) female *Gclm* mice, 24 h after aspiration of dispersion medium vehicle (Control) or 25 µg MWCNT. Results are means and SEM (n = 5 – 6 mice/group), corrected for lavage dilution using the urea serum:BALF ratio. Abbreviations: BALF, bronchoalveolar lavage fluid; ELF, epithelial lining fluid; GSH, glutathione; MWCNT, multi-walled carbon nanotube.

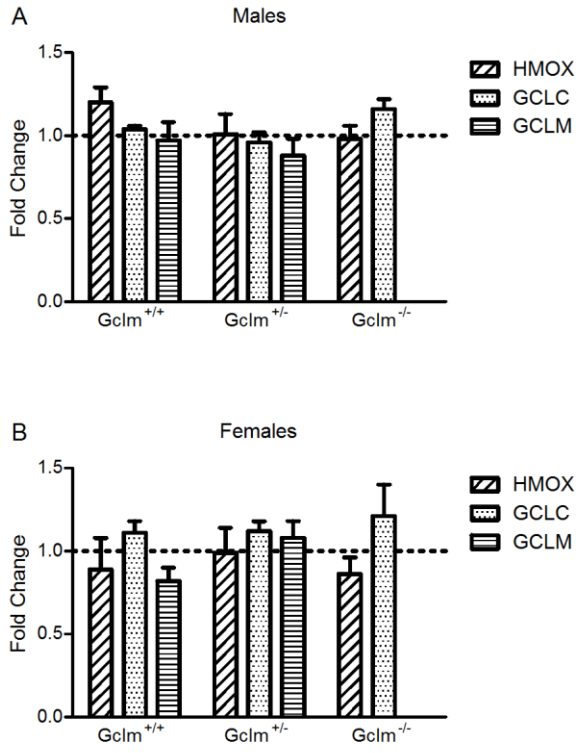

Figure 4.6. Expression of redox-sensitive proteins.

Densitometry analyses of Western blots for expression of redox-sensitive proteins GCLC, GCLM, and HMOX1 in lung homogenates from (A) male and (B) female *Gclm* mice, 24 h after aspiration of dispersion medium vehicle (Control) or 25 μg MWCNT. The results are means and SEM (n = 5 – 6 mice/group), adjusted to the loading control, β-actin, and calculated as the fold-change relative to the mean of each genotype's control.

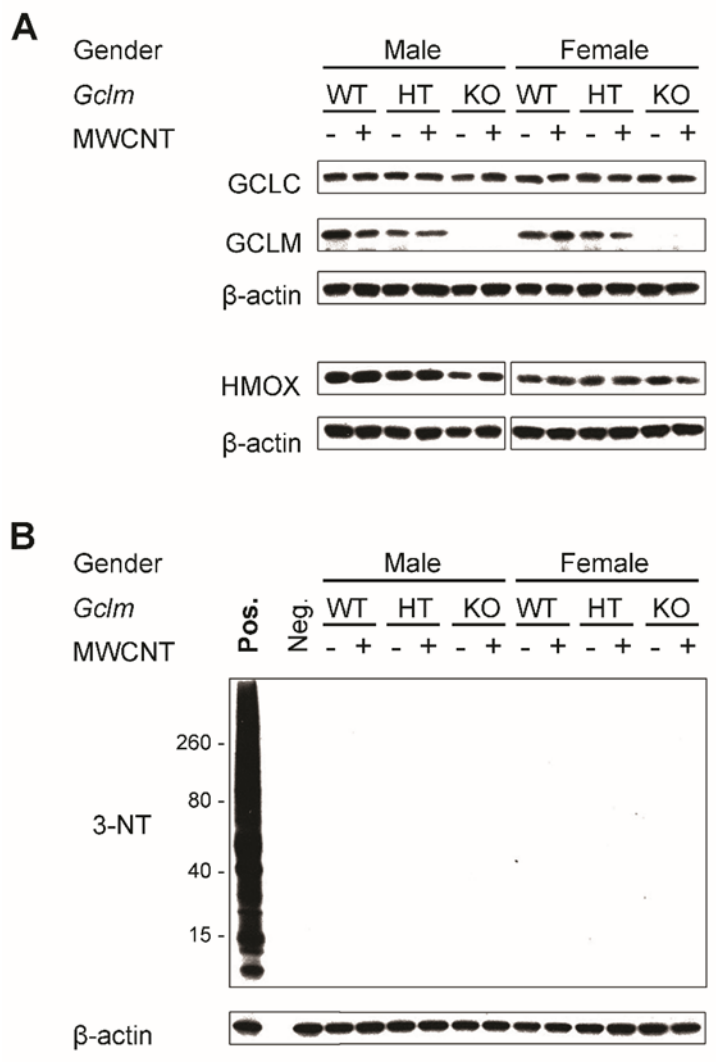

Figure 4.7. Representative Western blots for redox-sensitive proteins and nitrated residues. Representative blots for GCLC, GCLM, HMOX1, and 3-nitrotyrosine. The 3-nitrotyrosine film was exposed for 1 h to increase signal sensitivity. Abbreviations: 3-NT, 3-nitrotyrosine; MWCNT, multi-walled carbon nanotube; Neg., negative control (untreated lung homogenate); Pos., positive control (peroxynitrite-treated lung homogenate).

4.6. Tables

Table 4.1

Lung mRNA Expression Levels of Inflammation-, Oxidative Stress-, and Fibrosis-Associated Genes 24 h After Aspiration of MWCNTs by Male *Gclm* Mice.

Gene	*Gclm*$^{+/+}$ Control	*Gclm*$^{+/+}$ MWCNT	*Gclm*$^{+/-}$ Control	*Gclm*$^{+/-}$ MWCNT	*Gclm*$^{-/-}$ Control	*Gclm*$^{-/-}$ MWCNT
Cftr	6.38 ± 0.50	6.63 ± 0.70	6.45 ± 0.56	6.86 ± 0.51	7.10 ± 0.62	6.15 ± 0.87
Gclc	178.57 ± 7.46	203.20 ± 13.88	178.45 ± 5.95	167.25 ± 9.14	199.34 ± 23.48	167.45 ± 15.97
Gclm	45.13 ± 3.07	36.89 ± 4.52	19.80 ± 1.00$^{###}$	20.48 ± 1.15$^{\#}$	0.02 ± 0.01$^{###}$	0.01 ± 0.01$^{###}$
Gmcsf	0.23 ± 0.05	0.39 ± 0.01*	0.20 ± 0.03	0.35 ± 0.07	0.25 ± 0.07	0.27 ± 0.09
Hmox1	55.78 ± 2.54	60.33 ± 1.85	60.20 ± 3.10	57.46 ± 2.88	68.03 ± 4.73	62.83 ± 5.77
Il1β	5.52 ± 0.41	6.71 ± 1.60	6.47 ± 0.93	6.24 ± 1.74	4.99 ± 1.21	3.54 ± 0.83
Kc	0.33 ± 0.06	0.73 ± 0.36	0.28 ± 0.05	0.28 ± 0.07	0.16 ± 0.03	0.29 ± 0.12
Mcp1	0.27 ± 0.05	0.44 ± 0.16	0.23 ± 0.02	0.22 ± 0.03	0.22 ± 0.02	0.29 ± 0.04
Tfgβ1	38.93 ± 1.24	40.52 ± 2.08	32.03 ± 2.07$^{\#}$	34.41 ± 3.29	27.71 ± 2.99$^{\#\#}$	27.88 ± 4.37
Tnfα	1.03 ± 0.05	1.18 ± 0.10	1.01 ± 0.07	1.07 ± 0.17	0.92 ± 0.09	1.16 ± 0.14

The results are reported as means ± SEM (x 10^{-3}), normalized to *Gapdh* expression. Abbreviations: MWCNT, multi-walled carbon nanotube.

* $p < 0.05$ compared to same-genotype control. # $p < 0.05$, ## $p < 0.01$, ### $p < 0.001$ compared to same-treatment *Gclm*$^{+/+}$.

Table 4.2

Lung mRNA Expression Levels of Inflammation-, Oxidative Stress-, and Fibrosis-Associated Genes 24 h After Aspiration of MWCNTs by Female *Gclm* Mice.

Gene	*Gclm*$^{+/+}$ Control	*Gclm*$^{+/+}$ MWCNT	*Gclm*$^{+/-}$ Control	*Gclm*$^{+/-}$ MWCNT	*Gclm*$^{-/-}$ Control	*Gclm*$^{-/-}$ MWCNT
Cftr	9.68 ± 0.89$^{\&}$	11.05 ± 0.70$^{\&\&}$	12.38 ± 1.10	8.51 ± 0.96	8.81 ± 1.04	7.99 ± 1.17
Gclc	200.61 ± 7.65	218.84 ± 14.18	221.06 ± 25.17	186.26 ± 27.84	215.30 ± 19.87	204.81 ± 9.04
Gclm	23.58 ± 2.56$^{\&\&\&}$	37.57 ± 8.37	15.14 ± 1.07$^{\#,\ \&\&}$	13.23 ± 0.57$^{\#,\ \&\&\&}$	n.d.	n.d.
Gmcsf	1.34 ± 0.16$^{\&\&\&}$	1.62 ± 0.18$^{\&\&}$	1.30 ± 0.08$^{\&\&\&}$	1.43 ± 0.11$^{\&\&\&}$	1.48 ± 0.09$^{\&\&\&}$	1.33 ± 0.13$^{\&\&\&}$
Hmox1	55.34 ± 9.04	49.67 ± 5.19	54.54 ± 2.91	41.65 ± 1.75	41.21 ± 3.29	37.20 ± 1.88
Il1β	14.81 ± 4.75	7.14 ± 1.20	7.51 ± 0.69	5.55 ± 0.55	6.51 ± 1.02	8.77 ± 2.77
Kc	4.97 ± 2.95	1.41 ± 0.17	1.51 ± 0.17$^{\&\&\&}$	1.25 ± 0.26$^{\&}$	0.98 ± 0.18$^{\&\&}$	1.27 ± 0.54
Mcp1	3.99 ± 0.84	2.03 ± 0.47	2.10 ± 0.24$^{\&\&\&}$	1.93 ± 0.21$^{\&\&\&}$	1.52 ± 0.30$^{\&\&}$	2.55 ± 1.37
Tfgβ1	41.87 ± 4.32	45.78 ± 3.85	45.39 ± 3.24$^{\&}$	41.42 ± 4.05	57.59 ± 5.26$^{\&\&}$	58.52 ± 5.04$^{\&\&}$
Tnfα	3.33 ± 1.51	1.20 ± 0.11	1.63 ± 0.28	1.34 ± 0.21	1.26 ± 0.25	1.35 ± 0.27

The results are reported as means ± SEM (x 10^{-3}), normalized to *Gapdh* expression. Abbreviations: MWCNT, multi-walled carbon nanotube; n.d., not detected.

# $p < 0.05$ compared to same-treatment *Gclm*$^{+/+}$. & $p < 0.05$, && $p < 0.01$, &&& $p < 0.001$ compared to same-treatment, same-genotype males.

Table 4.3

Parameters for Lung Toxicity and Alveolar/Capillary Barrier Integrity 24 h After Aspiration of MWCNTS by *Gclm* Mice.

Group		MWCNT (µg/mouse)	LDH (ng/ml BALF)	Protein (µg/ml BALF)
Males				
	Gclm$^{+/+}$	0	137.3 ± 6.4	241.5 ± 31.5
		25	179.3 ± 8.4	287.1 ± 38.0
	Gclm$^{+/-}$	0	147.3 ± 5.9	220.0 ± 13.6
		25	177.3 ± 18.6	288.7 ± 96.7
	Gclm$^{-/-}$	0	311.5 ± 115.5	234.8 ± 42.9
		25	179.2 ± 28.9	240.4 ± 30.5
Females				
	Gclm$^{+/+}$	0	149.3 ± 13.9	425.2 ± 145.8
		25	155.0 ± 15.8	246.2 ± 35.5
	Gclm$^{+/-}$	0	183.8 ± 47.2	630.0 ± 274.9
		25	167.7 ± 15.1	296.7 ± 38.5
	Gclm$^{-/-}$	0	175.3 ± 28.7	237.8 ± 18.8
		25	158.7 ± 15.4	249.4 ± 37.7

The results are reported as means ± SEM. Abbreviations: BALF, bronchoalveolar lavage fluid; LDH, lactate dehydrogenase; MWCNT, multi-walled carbon nanotube.

Chapter 5 : Conclusions

With the dramatic and ongoing increase in global production of CNTs, more people are at risk for being exposed to manufactured MWCNTs (Dahm *et al.*, 2012; De Volder *et al.*, 2013). While the general population may also be exposed to MWCNTs created through the combustion of diesel or other fuels (Lam *et al.*, 2006; Wu *et al.*, 2010; Kolosnjaj-Tabi *et al.*, 2015), the principal population at risk for exposure is workers manufacturing and handling MWCNTs (Lam *et al.*, 2006).

Inhalation of MWCNTs may lead to lung inflammation, oxidative stress, fibrosis, and even an increased risk of lung cancer (Shvedova *et al.*, 2008; Ma-Hock *et al.*, 2009; Pauluhn, 2010b; Grosse *et al.*, 2014; Liao *et al.*, 2014; Lee *et al.*, 2015b). To protect the health of workers, risk assessments have proposed varying airborne concentrations of respirable elemental carbon that range from 1 $\mu g/m^3$ (NIOSH, 2013) to 21 $\mu g/m^3$ (Dahm *et al.*, 2012) to as a high as 50 $\mu g/m^3$ (Pauluhn, 2010a). However, these risk assessments relied on data from a narrow selection of studies, which in turn had little variation in MWCNT properties and rodent models. Thus, these studies that formed the basis for risk assessments to protect workers may not capture the potential variability possible in a genetically heterogeneous worker population handling MWCNTs with diverse physicochemical properties.

To address these deficits, I developed three specific aims. In the first aim, we examined which physicochemical properties among nine MWCNTs were most associated with acute lung pathology in A/J mice. In the second aim, we determined if there was a strain-differential response to MWCNT-induced acute lung pathology across ten isogenic mouse strains which represented a genetically heterogeneous population. And in the third aim, we investigated how workers with genetic- or health-induced deficiencies in the major antioxidant glutathione may be rendered more vulnerable to MWCNT-induced pathology in a gender-dependent manner, by examining how *Gclm* status modulated susceptibility to acute lung pathology in male and female mice.

The results from the first aim showed that specific physicochemical properties are indeed associated with acute lung pathology *in vivo*. Consistent with hypothesis 1.1, we found that the stock, unpurified MWCNTs within each aspect ratio series were the most inflammogenic and, in the case of MWCNTs with the greatest length (#14 series), capable of causing cellular toxicity in the lung. In contrast to hypothesis 1.2, we found the shortest MWCNTs with the widest diameter (#13 series) were the most

inflammogenic overall, followed by the short, narrow MWCNTs (#12 series), and then the long, narrow MWCNTs (#14 series).

For all MWCNTs, inflammogenicity as reflected in lung neutrophilia strongly correlated with internalization of MWCNTs by alveolar macrophages, suggesting that increased phagocytosis lead to increased levels of pro-inflammatory cytokines (e.g., TNF-α) and to increased neutrophil influx. Therefore, physical dimension may play a strong role in inflammogenicity by affecting macrophage uptake. Shorter lengths may have enabled increased uptake (Johnston *et al.*, 2010; Bhattacharya *et al.*, 2013), while thicker, stiffer MWCNTs may have led to increased permeabilization of the phagolysosome with concomitant inflammasome activation (Hamilton *et al.*, 2013).

These results for the first aim suggest that workers may be at greater risk for acute lung pathology when handling unpurified MWCNTs and/or MWCNTs with short lengths and wide diameters. Unpurified MWCNT exposure may occur when workers are opening the synthesis reactor, while exposure to short, wide MWCNTs may occur during post-synthesis grinding or purification following acid treatments—processes which can both generate shorter MWCNTs (De Volder *et al.*, 2013; Lee *et al.*, 2015a). Hence, our results from the first aim indicate that stringent engineering controls and personal protective equipment should be especially used during these and related procedures in order to reduce worker exposure to unpurified and short/wide MWCNTs. Future studies could examine the associations between physicochemical properties and pathological processes in the longer term, such as fibrosis and cancer.

The results from our second aim demonstrated that genetic heterogeneity is associated with a greater range in lung neutrophilia following acute MWCNT exposure, and that overreliance on the isogenic C57BL/6 strain may limit both risk assessments and mechanistic understanding of MWCNT-induced pathology (Montagutelli, 2000; King-Herbert and Thayer, 2006). While our observations of a strain-differential response supported hypothesis 2.1, these results did not support hypothesis 2.2. Contrary to this second hypothesis, we found that rather than being the strain most susceptible to MWCNT-induced pathology, the A/J mice actually were the strain closest to the overall mean responses for lung neutrophilia in the control and exposed groups. In contrast, the C57BL/6 mice were among the strains more resistant to lung neutrophilia.

These results from the second aim suggest that the use of only one isogenic strain of rodents—whether mice or rats—may underestimate the range of responses possible in a genetically heterogeneous worker population, and potentially lead to risk assessments suggesting levels which may not protect the most vulnerable workers (Rivera and Tessarollo, 2008). Furthermore, our results suggest that future studies to identify loci associated with this strain-differential response should compare the highly-susceptible 129S1/SvImJ strain to the highly-resistant WSB/EiJ strain (Bauer *et al.*, 2004; Walkin *et al.*, 2013).

The results from our third aim showed that female mice with genetically-induced moderate and severe deficiencies in GSH had a reduced neutrophilic response to acute MWCNT exposure. These results did not support either hypothesis 3.1, in that the *Gclm* heterozygous mice were not the most vulnerable, nor did they support hypothesis 3.2, in that the female *Gclm* heterozygous and null mice experienced greater neutrophilia than their male counterparts. However, given that reduced GSH levels have been associated with impaired phagocytosis (Oliver *et al.*, 1976), and that an impaired neutrophilic response was associated with reduced MWCNT clearance and increased fibrosis (Shvedova *et al.*, 2012a), these results indicate that female mice may be more vulnerable to longer-term pathological conditions.

Therefore, glutathione deficiencies among workers—which can derive from either common genetic polymorphisms (Nakamura *et al.*, 2002; Siedlinski *et al.*, 2008) or health conditions (Biswas and Rahman, 2009; Ghezzi, 2011)—may reduce the neutrophilic response to acute MWCNT exposure in women, and thus may impair neutrophil-based clearance of MWCNTs from the lung while increasing women's risk for fibrosis. Future risk assessments need to account for this potentially vulnerable subpopulation of workers, while clinicians should be aware that women workers with conditions or genetic polymorphisms affecting GSH levels may be at greater risk for MWCNT-induced lung pathology. These results suggest that future studies could examine the effects of GSH depletion on clearance and fibrosis, and that studies examining mechanisms unrelated to glutathione should include both genders.

Altogether, the results from these three aims suggest that future risk assessments and industrial hygiene practices should account for physicochemical properties of MWCNTs; a range of genetic susceptibilities in workers greater than that represented by only one isogenic rodent strain; and increased

susceptibility of women workers with conditions or genetic polymorphisms that decrease their GSH reserves.

References

Bauer, A.K., Malkinson, A.M., Kleeberger, S.R., 2004. Susceptibility to neoplastic and non-neoplastic pulmonary diseases in mice: genetic similarities. Am J Physiol Lung Cell Mol Physiol **287**, L685-703.

Bell, M.L., Ebisu, K., Peng, R.D., Samet, J.M., Dominici, F., 2009. Hospital admissions and chemical composition of fine particle air pollution. Am J Respir Crit Care Med **179**, 1115-1120.

Bhattacharya, K., Andon, F.T., El-Sayed, R., Fadeel, B., 2013. Mechanisms of carbon nanotube-induced toxicity: focus on pulmonary inflammation. Adv Drug Deliv Rev **65**, 2087-2097.

Biswas, S.K., Rahman, I., 2009. Environmental toxicity, redox signaling and lung inflammation: the role of glutathione. Mol Aspects Med **30**, 60-76.

Bonner, J.C., Silva, R.M., Taylor, A.J., Brown, J.M., Hilderbrand, S.C., Castranova, V., Porter, D., Elder, A., Oberdorster, G., Harkema, J.R., Bramble, L.A., Kavanagh, T.J., Botta, D., Nel, A., Pinkerton, K.E., 2013. Interlaboratory evaluation of rodent pulmonary responses to engineered nanomaterials: the NIEHS Nano GO Consortium. Environ Health Perspect **121**, 676-682.

Botta, D., Shi, S., White, C.C., Dabrowski, M.J., Keener, C.L., Srinouanprachanh, S.L., Farin, F.M., Ware, C.B., Ladiges, W.C., Pierce, R.H., Fausto, N., Kavanagh, T.J., 2006. Acetaminophen-induced liver injury is attenuated in male glutamate-cysteine ligase transgenic mice. J Biol Chem **281**, 28865-28875.

Bradford, M.M., 1976. A rapid and sensitive method for the quantitation of microgram quantities of protein utilizing the principle of protein-dye binding. Anal Biochem **72**, 248-254.

Bussy, C., Pinault, M., Cambedouzou, J., Landry, M.J., Jegou, P., Mayne-L'hermite, M., Launois, P., Boczkowski, J., Lanone, S., 2012. Critical role of surface chemical modifications induced by length shortening on multi-walled carbon nanotubes-induced toxicity. Part Fibre Toxicol **9**, 46.

Cao, Y., Jacobsen, N.R., Danielsen, P.H., Lenz, A.G., Stoeger, T., Loft, S., Wallin, H., Roursgaard, M., Mikkelsen, L., Moller, P., 2014. Vascular effects of multiwalled carbon nanotubes in dyslipidemic ApoE-/- mice and cultured endothelial cells. Toxicol Sci **138**, 104-116.

Card, J.W., Carey, M.A., Bradbury, J.A., DeGraff, L.M., Morgan, D.L., Moorman, M.P., Flake, G.P., Zeldin, D.C., 2006. Gender differences in murine airway responsiveness and lipopolysaccharide-induced inflammation. J Immunol **177**, 621-630.

CDC, 2013. Asthma Surveillance Data. Centers for Disease Control and Prevention, Atlanta, GA, pp.

Chen, R., Zhang, L., Ge, C., Tseng, M.T., Bai, R., Qu, Y., Beer, C., Autrup, H., Chen, C., 2015. Subchronic toxicity and cardiovascular responses in spontaneously hypertensive rats after exposure to multiwalled carbon nanotubes by intratracheal instillation. Chem Res Toxicol **28**, 440-450.

Coultas, D.B., Zumwalt, R.E., Black, W.C., Sobonya, R.E., 1994. The epidemiology of interstitial lung diseases. Am J Respir Crit Care Med **150**, 967-972.

Cuevas, A.K., Niu, J., Zhong, M., Liberda, E.N., Ghio, A., Qu, Q., Chen, L.C., 2015. Metal rich particulate matter impairs acetylcholine-mediated vasorelaxation of microvessels in mice. Part Fibre Toxicol **12**, 14.

Dahm, M.M., Evans, D.E., Schubauer-Berigan, M.K., Birch, M.E., Fernback, J.E., 2012. Occupational exposure assessment in carbon nanotube and nanofiber primary and secondary manufacturers. Ann Occup Hyg **56**, 542-556.

Dalton, T.P., Dieter, M.Z., Yang, Y., Shertzer, H.G., Nebert, D.W., 2000. Knockout of the mouse glutamate cysteine ligase catalytic subunit (Gclc) gene: embryonic lethal when homozygous, and proposed model for moderate glutathione deficiency when heterozygous. Biochem Biophys Res Commun **279**, 324-329.

De Volder, M.F., Tawfick, S.H., Baughman, R.H., Hart, A.J., 2013. Carbon nanotubes: present and future commercial applications. Science **339**, 535-539.

DeForge, L.E., Remick, D.G., 1991. Kinetics of TNF, IL-6, and IL-8 gene expression in LPS-stimulated human whole blood. Biochem Biophys Res Commun **174**, 18-24.

Delogu, L.G., Vidili, G., Venturelli, E., Menard-Moyon, C., Zoroddu, M.A., Pilo, G., Nicolussi, P., Ligios, C., Bedognetti, D., Sgarrella, F., Manetti, R., Bianco, A., 2012. Functionalized multiwalled carbon nanotubes as ultrasound contrast agents. Proc Natl Acad Sci U S A **109**, 16612-16617.

Fenoglio, I., Aldieri, E., Gazzano, E., Cesano, F., Colonna, M., Scarano, D., Mazzucco, G., Attanasio, A., Yakoub, Y., Lison, D., Fubini, B., 2012. Thickness of multiwalled carbon nanotubes affects their lung toxicity. Chem Res Toxicol **25**, 74-82.
Fenoglio, I., Greco, G., Tomatis, M., Muller, J., Raymundo-Pinero, E., Beguin, F., Fonseca, A., Nagy, J.B., Lison, D., Fubini, B., 2008. Structural defects play a major role in the acute lung toxicity of multiwall carbon nanotubes: physicochemical aspects. Chem Res Toxicol **21**, 1690-1697.
Festing, M.F., 1995. Use of a multistrain assay could improve the NTP carcinogenesis bioassay. Environ Health Perspect **103**, 44-52.
Franklin, C.C., Backos, D.S., Mohar, I., White, C.C., Forman, H.J., Kavanagh, T.J., 2009. Structure, function, and post-translational regulation of the catalytic and modifier subunits of glutamate cysteine ligase. Mol Aspects Med **30**, 86-98.
Gao, N., Zhang, Q., Mu, Q., Bai, Y., Li, L., Zhou, H., Butch, E.R., Powell, T.B., Snyder, S.E., Jiang, G., Yan, B., 2011. Steering carbon nanotubes to scavenger receptor recognition by nanotube surface chemistry modification partially alleviates NFkappaB activation and reduces its immunotoxicity. ACS Nano **5**, 4581-4591.
Ghezzi, P., 2011. Role of glutathione in immunity and inflammation in the lung. Int J Gen Med **4**, 105-113.
Gordon, T., Bosland, M., 2009. Strain-dependent differences in susceptibility to lung cancer in inbred mice exposed to mainstream cigarette smoke. Cancer Lett **275**, 213-220.
Gould, N.S., Min, E., Gauthier, S., Chu, H.W., Martin, R., Day, B.J., 2010. Aging adversely affects the cigarette smoke-induced glutathione adaptive response in the lung. Am J Respir Crit Care Med **182**, 1114-1122.
Gould, N.S., Min, E., Martin, R.J., Day, B.J., 2012. CFTR is the primary known apical glutathione transporter involved in cigarette smoke-induced adaptive responses in the lung. Free Radic Biol Med **52**, 1201-1206.
Gribbin, J., Hubbard, R.B., Le Jeune, I., Smith, C.J., West, J., Tata, L.J., 2006. Incidence and mortality of idiopathic pulmonary fibrosis and sarcoidosis in the UK. Thorax **61**, 980-985.
Grosse, Y., Loomis, D., Guyton, K.Z., Lauby-Secretan, B., El Ghissassi, F., Bouvard, V., Benbrahim-Tallaa, L., Guha, N., Scoccianti, C., Mattock, H., Straif, K., International Agency for Research on Cancer Monograph Working, G., 2014. Carcinogenicity of fluoro-edenite, silicon carbide fibres and whiskers, and carbon nanotubes. Lancet Oncol **15**, 1427-1428.
Gupta, V., Singh, S.M., 2008. Gender dimorphism of macrophage response to GMCSF and IL-4 for differentiation into dendritic cells. Am J Reprod Immunol **60**, 43-54.
Hamilton, R.F., Jr., Buford, M., Xiang, C., Wu, N., Holian, A., 2012. NLRP3 inflammasome activation in murine alveolar macrophages and related lung pathology is associated with MWCNT nickel contamination. Inhal Toxicol **24**, 995-1008.
Hamilton, R.F., Wu, Z., Mitra, S., Shaw, P.K., Holian, A., 2013. Effect of MWCNT size, carboxylation, and purification on in vitro and in vivo toxicity, inflammation and lung pathology. Particle and Fibre Toxicology **10**, 57.
Han, J.H., Lee, E.J., Lee, J.H., So, K.P., Lee, Y.H., Bae, G.N., Lee, S.B., Ji, J.H., Cho, M.H., Yu, I.J., 2008. Monitoring multiwalled carbon nanotube exposure in carbon nanotube research facility. Inhal Toxicol **20**, 741-749.
Harkonen, P.L., Vaananen, H.K., 2006. Monocyte-macrophage system as a target for estrogen and selective estrogen receptor modulators. Ann N Y Acad Sci **1089**, 218-227.
Heurtault, B., Saulnier, P., Pech, B., Proust, J.-E., Benoit, J.-P., 2003. Physico-chemical stability of colloidal lipid particles. Biomaterials **24**, 4283-4300.
Hewett, P., Ganser, G.H., 2007. A comparison of several methods for analyzing censored data. Ann Occup Hyg **51**, 611-632.
Huang, H., He, J., Yuan, Y., Aoyagi, E., Takenaka, H., Itagaki, T., Sannomiya, K., Tamaki, K., Harada, N., Shono, M., Shimizu, I., Takayama, T., 2008. Opposing effects of estradiol and progesterone on the oxidative stress-induced production of chemokine and proinflammatory cytokines in murine peritoneal macrophages. J Med Invest **55**, 133-141.
Iijima, S., 1991. Helical microtubules of graphitic carbon. Nature **354**, 56-58.
Inoue, K., Koike, E., Yanagisawa, R., Hirano, S., Nishikawa, M., Takano, H., 2009. Effects of multi-walled carbon nanotubes on a murine allergic airway inflammation model. Toxicol Appl Pharmacol **237**, 306-316.

Inoue, K., Yanagisawa, R., Koike, E., Nishikawa, M., Takano, H., 2010. Repeated pulmonary exposure to single-walled carbon nanotubes exacerbates allergic inflammation of the airway: Possible role of oxidative stress. Free Radic Biol Med **48**, 924-934.
Jain, K.K., 2012. Advances in use of functionalized carbon nanotubes for drug design and discovery. Expert Opin Drug Discov **7**, 1029-1037.
Johansson, E., Wesselkamper, S.C., Shertzer, H.G., Leikauf, G.D., Dalton, T.P., Chen, Y., 2010. Glutathione deficient C57BL/6J mice are not sensitized to ozone-induced lung injury. Biochem Biophys Res Commun **396**, 407-412.
Johnston, H.J., Hutchison, G.R., Christensen, F.M., Peters, S., Hankin, S., Aschberger, K., Stone, V., 2010. A critical review of the biological mechanisms underlying the in vivo and in vitro toxicity of carbon nanotubes: The contribution of physico-chemical characteristics. Nanotoxicology **4**, 207-246.
Jun, S., Fattman, C.L., Kim, B.J., Jones, H., Dory, L., 2011. Allele-specific effects of ecSOD on asbestos-induced fibroproliferative lung disease in mice. Free Radic Biol Med **50**, 1288-1296.
Karlovich, C., Duchateau-Nguyen, G., Johnson, A., McLoughlin, P., Navarro, M., Fleurbaey, C., Steiner, L., Tessier, M., Nguyen, T., Wilhelm-Seiler, M., Caulfield, J.P., 2009. A longitudinal study of gene expression in healthy individuals. BMC Med Genomics **2**, 33.
Kim, J.E., Kang, S.H., Moon, Y., Chae, J.J., Lee, A.Y., Lee, J.H., Yu, K.N., Jeong, D.H., Choi, M., Cho, M.H., 2014. Physicochemical determinants of multiwalled carbon nanotubes on cellular toxicity: influence of a synthetic method and post-treatment. Chem Res Toxicol **27**, 290-303.
King-Herbert, A., Thayer, K., 2006. NTP workshop: animal models for the NTP rodent cancer bioassay: stocks and strains--should we switch? Toxicol Pathol **34**, 802-805.
Kolosnjaj-Tabi, J., Just, J., Hartman, K.B., Laoudi, Y., Boudjemaa, S., Alloyeau, D., Szwarc, H., Wilson, L.J., Moussa, F., 2015. Anthropogenic Carbon Nanotubes Found in the Airways of Parisian Children. EBioMedicine.
Krejsa, C.M., Franklin, C.C., White, C.C., Ledbetter, J.A., Schieven, G.L., Kavanagh, T.J., 2010. Rapid activation of glutamate cysteine ligase following oxidative stress. J Biol Chem **285**, 16116-16124.
Kuempel, E.D., Geraci, C.L., Schulte, P.A., 2012. Risk assessment and risk management of nanomaterials in the workplace: translating research to practice. Ann Occup Hyg **56**, 491-505.
Lam, C.W., James, J.T., McCluskey, R., Arepalli, S., Hunter, R.L., 2006. A review of carbon nanotube toxicity and assessment of potential occupational and environmental health risks. Crit Rev Toxicol **36**, 189-217.
Laverny, G., Casset, A., Purohit, A., Schaeffer, E., Spiegelhalter, C., de Blay, F., Pons, F., 2013. Immunomodulatory properties of multi-walled carbon nanotubes in peripheral blood mononuclear cells from healthy subjects and allergic patients. Toxicol Lett **217**, 91-101.
Lee, J.H., Ahn, K.H., Kim, S.M., Kim, E., Lee, G.H., Han, J.H., Yu, I.J., 2015a. Three-Day Continuous Exposure Monitoring of CNT Manufacturing Workplaces. Biomed Res Int **2015**, 237140.
Lee, J.H., Lee, S.B., Bae, G.N., Jeon, K.S., Yoon, J.U., Ji, J.H., Sung, J.H., Lee, B.G., Yang, J.S., Kim, H.Y., Kang, C.S., Yu, I.J., 2010. Exposure assessment of carbon nanotube manufacturing workplaces. Inhal Toxicol **22**, 369-381.
Lee, J.S., Choi, Y.C., Shin, J.H., Lee, J.H., Lee, Y., Park, S.Y., Baek, J.E., Park, J.D., Ahn, K., Yu, I.J., 2015b. Health surveillance study of workers who manufacture multi-walled carbon nanotubes. Nanotoxicology **9**, 802-811.
Lee, V., McMahan, R.S., Hu, X., Gao, X., Faustman, E.M., Griffith, W.C., Kavanagh, T.J., Eaton, D.L., McGuire, J.K., Parks, W.C., 2015c. Amphiphilic polymer-coated CdSe/ZnS quantum dots induce pro-inflammatory cytokine expression in mouse lung epithelial cells and macrophages. Nanotoxicology **9**, 336-343.
Lesur, I., Textoris, J., Loriod, B., Courbon, C., Garcia, S., Leone, M., Nguyen, C., 2010. Gene expression profiles characterize inflammation stages in the acute lung injury in mice. PLoS One **5**, e11485.
Liao, H.Y., Chung, Y.T., Lai, C.H., Wang, S.L., Chiang, H.C., Li, L.A., Tsou, T.C., Li, W.F., Lee, H.L., Wu, W.T., Lin, M.H., Hsu, J.H., Ho, J.J., Chen, C.J., Shih, T.S., Lin, C.C., Liou, S.H., 2014. Six-month follow-up study of health markers of nanomaterials among workers handling engineered nanomaterials. Nanotoxicology **8 Suppl 1**, 100-110.
Liu, K., Sun, Y., Lin, X., Zhou, R., Wang, J., Fan, S., Jiang, K., 2010. Scratch-resistant, highly conductive, and high-strength carbon nanotube-based composite yarns. ACS Nano **4**, 5827-5834.

Luyts, K., Smulders, S., Napierska, D., Van Kerckhoven, S., Poels, K., Scheers, H., Hemmeryckx, B., Nemery, B., Hoylaerts, M.F., Hoet, P.H., 2014. Pulmonary and hemostatic toxicity of multi-walled carbon nanotubes and zinc oxide nanoparticles after pulmonary exposure in Bmal1 knockout mice. Part Fibre Toxicol **11**, 61.

Ma-Hock, L., Treumann, S., Strauss, V., Brill, S., Luizi, F., Mertler, M., Wiench, K., Gamer, A.O., van Ravenzwaay, B., Landsiedel, R., 2009. Inhalation toxicity of multiwall carbon nanotubes in rats exposed for 3 months. Toxicol Sci **112**, 468-481.

Madl, A.K., Plummer, L.E., Carosino, C., Pinkerton, K.E., 2014. Nanoparticles, lung injury, and the role of oxidant stress. Annu Rev Physiol **76**, 447-465.

Maynard, A.D., Baron, P.A., Foley, M., Shvedova, A.A., Kisin, E.R., Castranova, V., 2004. Exposure to carbon nanotube material: aerosol release during the handling of unrefined single-walled carbon nanotube material. J Toxicol Environ Health A **67**, 87-107.

McConnachie, L.A., Botta, D., White, C.C., Weldy, C.S., Wilkerson, H.W., Yu, J., Dills, R., Yu, X., Griffith, W.C., Faustman, E.M., Farin, F.M., Gill, S.E., Parks, W.C., Hu, X., Gao, X., Eaton, D.L., Kavanagh, T.J., 2013. The glutathione synthesis gene Gclm modulates amphiphilic polymer-coated CdSe/ZnS quantum dot-induced lung inflammation in mice. PLoS One **8**, e64165.

McConnachie, L.A., Mohar, I., Hudson, F.N., Ware, C.B., Ladiges, W.C., Fernandez, C., Chatterton-Kirchmeier, S., White, C.C., Pierce, R.H., Kavanagh, T.J., 2007. Glutamate cysteine ligase modifier subunit deficiency and gender as determinants of acetaminophen-induced hepatotoxicity in mice. Toxicol Sci **99**, 628-636.

Mitchell, L.A., Gao, J., Wal, R.V., Gigliotti, A., Burchiel, S.W., McDonald, J.D., 2007. Pulmonary and systemic immune response to inhaled multiwalled carbon nanotubes. Toxicol Sci **100**, 203-214.

Mitchell, L.A., Lauer, F.T., Burchiel, S.W., McDonald, J.D., 2009. Mechanisms for how inhaled multiwalled carbon nanotubes suppress systemic immune function in mice. Nat Nanotechnol **4**, 451-456.

Miyata, Y., Mizuno, K., Kataura, H., 2011. Purity and Defect Characterization of Single-Wall Carbon Nanotubes Using Raman Spectroscopy. Journal of Nanomaterials **2011**, 7.

Moller, P., Christophersen, D.V., Jensen, D.M., Kermanizadeh, A., Roursgaard, M., Jacobsen, N.R., Hemmingsen, J.G., Danielsen, P.H., Cao, Y., Jantzen, K., Klingberg, H., Hersoug, L.G., Loft, S., 2014. Role of oxidative stress in carbon nanotube-generated health effects. Arch Toxicol **88**, 1939-1964.

Montagutelli, X., 2000. Effect of the genetic background on the phenotype of mouse mutations. J Am Soc Nephrol **11 Suppl 16**, S101-105.

Montano, M.M., Deng, H., Liu, M., Sun, X., Singal, R., 2004. Transcriptional regulation by the estrogen receptor of antioxidative stress enzymes and its functional implications. Oncogene **23**, 2442-2453.

Muhlfeld, C., Poland, C.A., Duffin, R., Brandenberger, C., Murphy, F.A., Rothen-Rutishauser, B., Gehr, P., Donaldson, K., 2012. Differential effects of long and short carbon nanotubes on the gas-exchange region of the mouse lung. Nanotoxicology **6**, 867-879.

Muller, J., Delos, M., Panin, N., Rabolli, V., Huaux, F., Lison, D., 2009. Absence of carcinogenic response to multiwall carbon nanotubes in a 2-year bioassay in the peritoneal cavity of the rat. Toxicol Sci **110**, 442-448.

Muller, J., Huaux, F., Fonseca, A., Nagy, J.B., Moreau, N., Delos, M., Raymundo-Pinero, E., Beguin, F., Kirsch-Volders, M., Fenoglio, I., Fubini, B., Lison, D., 2008. Structural defects play a major role in the acute lung toxicity of multiwall carbon nanotubes: toxicological aspects. Chem Res Toxicol **21**, 1698-1705.

Muller, J., Huaux, F., Moreau, N., Misson, P., Heilier, J.F., Delos, M., Arras, M., Fonseca, A., Nagy, J.B., Lison, D., 2005. Respiratory toxicity of multi-wall carbon nanotubes. Toxicol Appl Pharmacol **207**, 221-231.

Murphy, F.A., Poland, C.A., Duffin, R., Al-Jamal, K.T., Ali-Boucetta, H., Nunes, A., Byrne, F., Prina-Mello, A., Volkov, Y., Li, S., Mather, S.J., Bianco, A., Prato, M., Macnee, W., Wallace, W.A., Kostarelos, K., Donaldson, K., 2011. Length-dependent retention of carbon nanotubes in the pleural space of mice initiates sustained inflammation and progressive fibrosis on the parietal pleura. Am J Pathol **178**, 2587-2600.

Nagai, H., Okazaki, Y., Chew, S.H., Misawa, N., Yamashita, Y., Akatsuka, S., Ishihara, T., Yamashita, K., Yoshikawa, Y., Yasui, H., Jiang, L., Ohara, H., Takahashi, T., Ichihara, G., Kostarelos, K., Miyata, Y., Shinohara, H., Toyokuni, S., 2011. Diameter and rigidity of multiwalled carbon nanotubes are

critical factors in mesothelial injury and carcinogenesis. Proc Natl Acad Sci U S A **108**, E1330-1338.
Nakamura, S., Kugiyama, K., Sugiyama, S., Miyamoto, S., Koide, S., Fukushima, H., Honda, O., Yoshimura, M., Ogawa, H., 2002. Polymorphism in the 5'-flanking region of human glutamate-cysteine ligase modifier subunit gene is associated with myocardial infarction. Circulation **105**, 2968-2973.
NCI, 2012. Characterization data for multi-walled carbon nanotubes.
NIH, 2015. Comparison of Stationary Breast Tomosynthesis and 2-D Digital Mammography in Patients With Known Breast Lesions. ClinicalTrials.gov, pp.
NIOSH, 2013. Current Intelligence Bulletin 65 Occupational Exposure to Carbon Nanotubes and Nanofibers.
NRC, 2011a. Guide for the Care and Use of Laboratory Animals. National Academies Press, Washington, D.C.
NRC, 2011b. Working with Nanoparticles, Prudent Practices in the Laboratory: Handling and Management of Chemical Hazards: Updated Version. National Academies Press, pp. 141-146.
Nymark, P., Jensen, K.A., Suhonen, S., Kembouche, Y., Vippola, M., Kleinjans, J., Catalan, J., Norppa, H., van Delft, J., Briede, J.J., 2014. Free radical scavenging and formation by multi-walled carbon nanotubes in cell free conditions and in human bronchial epithelial cells. Part Fibre Toxicol **11**, 4.
Ogden, T.L., 2010. Handling results below the level of detection. Ann Occup Hyg **54**, 255-256.
Oliver, J.M., Albertini, D.F., Berlin, R.D., 1976. Effects of glutathione-oxidizing agents on microtubule assembly and microtubule-dependent surface properties of human neutrophils. J Cell Biol **71**, 921-932.
Pacurari, M., Qian, Y., Porter, D.W., Wolfarth, M., Wan, Y., Luo, D., Ding, M., Castranova, V., Guo, N.L., 2011. Multi-walled carbon nanotube-induced gene expression in the mouse lung: association with lung pathology. Toxicol Appl Pharmacol **255**, 18-31.
Pauluhn, J., 2010a. Multi-walled carbon nanotubes (Baytubes): approach for derivation of occupational exposure limit. Regul Toxicol Pharmacol **57**, 78-89.
Pauluhn, J., 2010b. Subchronic 13-week inhalation exposure of rats to multiwalled carbon nanotubes: toxic effects are determined by density of agglomerate structures, not fibrillar structures. Toxicol Sci **113**, 226-242.
Poland, C.A., Duffin, R., Kinloch, I., Maynard, A., Wallace, W.A., Seaton, A., Stone, V., Brown, S., Macnee, W., Donaldson, K., 2008. Carbon nanotubes introduced into the abdominal cavity of mice show asbestos-like pathogenicity in a pilot study. Nat Nanotechnol **3**, 423-428.
Porter, D.W., Hubbs, A.F., Mercer, R.R., Wu, N., Wolfarth, M.G., Sriram, K., Leonard, S., Battelli, L., Schwegler-Berry, D., Friend, S., Andrew, M., Chen, B.T., Tsuruoka, S., Endo, M., Castranova, V., 2010. Mouse pulmonary dose- and time course-responses induced by exposure to multi-walled carbon nanotubes. Toxicology **269**, 136-147.
Pothmann, D., Simar, S., Schuler, D., Dony, E., Gaering, S., Le Net, J.L., Okazaki, Y., Chabagno, J.M., Bessibes, C., Beausoleil, J., Nesslany, F., Regnier, J.F., 2015. Lung inflammation and lack of genotoxicity in the comet and micronucleus assays of industrial multiwalled carbon nanotubes Graphistrength((c)) C100 after a 90-day nose-only inhalation exposure of rats. Part Fibre Toxicol **12**, 21.
Poulsen, S.S., Saber, A.T., Mortensen, A., Szarek, J., Wu, D., Williams, A., Andersen, O., Jacobsen, N.R., Yauk, C.L., Wallin, H., Halappanavar, S., Vogel, U., 2015a. Changes in cholesterol homeostasis and acute phase response link pulmonary exposure to multi-walled carbon nanotubes to risk of cardiovascular disease. Toxicol Appl Pharmacol **283**, 210-222.
Poulsen, S.S., Saber, A.T., Williams, A., Andersen, O., Kobler, C., Atluri, R., Pozzebon, M.E., Mucelli, S.P., Simion, M., Rickerby, D., Mortensen, A., Jackson, P., Kyjovska, Z.O., Molhave, K., Jacobsen, N.R., Jensen, K.A., Yauk, C.L., Wallin, H., Halappanavar, S., Vogel, U., 2015b. MWCNTs of different physicochemical properties cause similar inflammatory responses, but differences in transcriptional and histological markers of fibrosis in mouse lungs. Toxicol Appl Pharmacol **284**, 16-32.
Ravichandran, P., Baluchamy, S., Gopikrishnan, R., Biradar, S., Ramesh, V., Goornavar, V., Thomas, R., Wilson, B.L., Jeffers, R., Hall, J.C., Ramesh, G.T., 2011. Pulmonary biocompatibility assessment of inhaled single-wall and multiwall carbon nanotubes in BALB/c mice. J Biol Chem **286**, 29725-29733.

Rivera, J., Tessarollo, L., 2008. Genetic background and the dilemma of translating mouse studies to humans. Immunity **28**, 1-4.
Rondini, E.A., Walters, D.M., Bauer, A.K., 2010. Vanadium pentoxide induces pulmonary inflammation and tumor promotion in a strain-dependent manner. Part Fibre Toxicol **7**, 9.
Ronzani, C., Casset, A., Pons, F., 2014. Exposure to multi-walled carbon nanotubes results in aggravation of airway inflammation and remodeling and in increased production of epithelium-derived innate cytokines in a mouse model of asthma. Archives of toxicology **88**, 489-499.
Rusyn, I., Gatti, D.M., Wiltshire, T., Kleeberger, S.R., Threadgill, D.W., 2010. Toxicogenetics: population-based testing of drug and chemical safety in mouse models. Pharmacogenomics **11**, 1127-1136.
Ryman-Rasmussen, J.P., Tewksbury, E.W., Moss, O.R., Cesta, M.F., Wong, B.A., Bonner, J.C., 2009. Inhaled Multiwalled Carbon Nanotubes Potentiate Airway Fibrosis in Murine Allergic Asthma. American Journal of Respiratory Cell and Molecular Biology **40**, 349-358.
Saber, A.T., Jacobsen, N.R., Bornholdt, J., Kjaer, S.L., Dybdahl, M., Risom, L., Loft, S., Vogel, U., Wallin, H., 2006. Cytokine expression in mice exposed to diesel exhaust particles by inhalation. Role of tumor necrosis factor. Part Fibre Toxicol **3**, 4.
Sargent, L.M., Porter, D.W., Staska, L.M., Hubbs, A.F., Lowry, D.T., Battelli, L., Siegrist, K.J., Kashon, M.L., Mercer, R.R., Bauer, A.K., Chen, B.T., Salisbury, J.L., Frazer, D., McKinney, W., Andrew, M., Tsuruoka, S., Endo, M., Fluharty, K.L., Castranova, V., Reynolds, S.H., 2014. Promotion of lung adenocarcinoma following inhalation exposure to multi-walled carbon nanotubes. Part Fibre Toxicol **11**, 3.
Scoville, D.K., White, C.C., Botta, D., McConnachie, L.A., Zadworny, M.E., Schmuck, S.C., Hu, X., Gao, X., Yu, J., Dills, R.L., Sheppard, L., Delaney, M.A., Griffith, W.C., Beyer, R.P., Zangar, R.C., Pounds, J.G., Faustman, E.M., Kavanagh, T.J., 2015. Susceptibility to quantum dot induced lung inflammation differs widely among the Collaborative Cross founder mouse strains. Toxicol Appl Pharmacol.
Shi, Y., Liu, C.H., Roberts, A.I., Das, J., Xu, G., Ren, G., Zhang, Y., Zhang, L., Yuan, Z.R., Tan, H.S., Das, G., Devadas, S., 2006. Granulocyte-macrophage colony-stimulating factor (GM-CSF) and T-cell responses: what we do and don't know. Cell Res **16**, 126-133.
Shulaker, M.M., Hills, G., Patil, N., Wei, H., Chen, H.Y., Wong, H.S., Mitra, S., 2013. Carbon nanotube computer. Nature **501**, 526-530.
Shvedova, A.A., Kapralov, A.A., Feng, W.H., Kisin, E.R., Murray, A.R., Mercer, R.R., St Croix, C.M., Lang, M.A., Watkins, S.C., Konduru, N.V., Allen, B.L., Conroy, J., Kotchey, G.P., Mohamed, B.M., Meade, A.D., Volkov, Y., Star, A., Fadeel, B., Kagan, V.E., 2012a. Impaired clearance and enhanced pulmonary inflammatory/fibrotic response to carbon nanotubes in myeloperoxidase-deficient mice. PLoS One **7**, e30923.
Shvedova, A.A., Kisin, E., Murray, A.R., Johnson, V.J., Gorelik, O., Arepalli, S., Hubbs, A.F., Mercer, R.R., Keohavong, P., Sussman, N., Jin, J., Yin, J., Stone, S., Chen, B.T., Deye, G., Maynard, A., Castranova, V., Baron, P.A., Kagan, V.E., 2008. Inhalation vs. aspiration of single-walled carbon nanotubes in C57BL/6 mice: inflammation, fibrosis, oxidative stress, and mutagenesis. Am J Physiol Lung Cell Mol Physiol **295**, L552-565.
Shvedova, A.A., Kisin, E.R., Murray, A.R., Gorelik, O., Arepalli, S., Castranova, V., Young, S.H., Gao, F., Tyurina, Y.Y., Oury, T.D., Kagan, V.E., 2007. Vitamin E deficiency enhances pulmonary inflammatory response and oxidative stress induced by single-walled carbon nanotubes in C57BL/6 mice. Toxicol Appl Pharmacol **221**, 339-348.
Shvedova, A.A., Pietroiusti, A., Fadeel, B., Kagan, V.E., 2012b. Mechanisms of carbon nanotube-induced toxicity: focus on oxidative stress. Toxicol Appl Pharmacol **261**, 121-133.
Siedlinski, M., Postma, D.S., van Diemen, C.C., Blokstra, A., Smit, H.A., Boezen, H.M., 2008. Lung function loss, smoking, vitamin C intake, and polymorphisms of the glutamate-cysteine ligase genes. Am J Respir Crit Care Med **178**, 13-19.
Siegrist, K.J., Reynolds, S.H., Kashon, M.L., Lowry, D.T., Dong, C., Hubbs, A.F., Young, S.H., Salisbury, J.L., Porter, D.W., Benkovic, S.A., McCawley, M., Keane, M.J., Mastovich, J.T., Bunker, K.L., Cena, L.G., Sparrow, M.C., Sturgeon, J.L., Dinu, C.Z., Sargent, L.M., 2014. Genotoxicity of multi-walled carbon nanotubes at occupationally relevant doses. Part Fibre Toxicol **11**, 6.
Silva, R.M., Doudrick, K., Franzi, L.M., TeeSy, C., Anderson, D.S., Wu, Z., Mitra, S., Vu, V., Dutrow, G., Evans, J.E., Westerhoff, P., Van Winkle, L.S., Raabe, O.G., Pinkerton, K.E., 2014. Instillation

versus inhalation of multiwalled carbon nanotubes: exposure-related health effects, clearance, and the role of particle characteristics. ACS Nano **8**, 8911-8931.
Stocker, R., Perrella, M.A., 2006. Heme oxygenase-1: a novel drug target for atherosclerotic diseases? Circulation **114**, 2178-2189.
Sun, B., Wang, X., Ji, Z., Wang, M., Liao, Y.P., Chang, C.H., Li, R., Zhang, H., Nel, A.E., Xia, T., 2015. NADPH Oxidase-Dependent NLRP3 Inflammasome Activation and its Important Role in Lung Fibrosis by Multiwalled Carbon Nanotubes. Small **11**, 2087-2097.
Tabet, L., Bussy, C., Setyan, A., Simon-Deckers, A., Rossi, M.J., Boczkowski, J., Lanone, S., 2011. Coating carbon nanotubes with a polystyrene-based polymer protects against pulmonary toxicity. Part Fibre Toxicol **8**, 3.
Takakusa, H., Mohar, I., Kavanagh, T.J., Kelly, E.J., Kaspera, R., Nelson, S.D., 2012. Protein tyrosine nitration of mitochondrial carbamoyl phosphate synthetase 1 and its functional consequences. Biochem Biophys Res Commun **420**, 54-60.
Thompson, S.A., White, C.C., Krejsa, C.M., Diaz, D., Woods, J.S., Eaton, D.L., Kavanagh, T.J., 1999. Induction of glutamate-cysteine ligase (gamma-glutamylcysteine synthetase) in the brains of adult female mice subchronically exposed to methylmercury. Toxicol Lett **110**, 1-9.
Tkach, A.V., Shurin, G.V., Shurin, M.R., Kisin, E.R., Murray, A.R., Young, S.H., Star, A., Fadeel, B., Kagan, V.E., Shvedova, A.A., 2011. Direct effects of carbon nanotubes on dendritic cells induce immune suppression upon pulmonary exposure. ACS Nano **5**, 5755-5762.
Townsend, D.M., Tew, K.D., Tapiero, H., 2003. The importance of glutathione in human disease. Biomed Pharmacother **57**, 145-155.
Toyoda, Y., Endo, S., Tsuneyama, K., Miyashita, T., Yano, A., Fukami, T., Nakajima, M., Yokoi, T., 2012. Mechanism of exacerbative effect of progesterone on drug-induced liver injury. Toxicol Sci **126**, 16-27.
Ursini, C.L., Cavallo, D., Fresegna, A.M., Ciervo, A., Maiello, R., Buresti, G., Casciardi, S., Tombolini, F., Bellucci, S., Iavicoli, S., 2012. Comparative cyto-genotoxicity assessment of functionalized and pristine multiwalled carbon nanotubes on human lung epithelial cells. Toxicol In Vitro **26**, 831-840.
Vancza, E.M., Galdanes, K., Gunnison, A., Hatch, G., Gordon, T., 2009. Age, strain, and gender as factors for increased sensitivity of the mouse lung to inhaled ozone. Toxicol Sci **107**, 535-543.
Villa, P., Saccani, A., Sica, A., Ghezzi, P., 2002. Glutathione protects mice from lethal sepsis by limiting inflammation and potentiating host defense. J Infect Dis **185**, 1115-1120.
Vogel, C., Marcotte, E.M., 2012. Insights into the regulation of protein abundance from proteomic and transcriptomic analyses. Nat Rev Genet **13**, 227-232.
Walkin, L., Herrick, S.E., Summers, A., Brenchley, P.E., Hoff, C.M., Korstanje, R., Margetts, P.J., 2013. The role of mouse strain differences in the susceptibility to fibrosis: a systematic review. Fibrogenesis Tissue Repair **6**, 18.
Wang, X., Katwa, P., Podila, R., Chen, P., Ke, P.C., Rao, A.M., Walters, D.M., Wingard, C.J., Brown, J.M., 2011. Multi-walled carbon nanotube instillation impairs pulmonary function in C57BL/6 mice. Part Fibre Toxicol **8**, 24.
Wang, X., Zang, J.J., Wang, H., Nie, H., Wang, T.C., Deng, X.Y., Gu, Y.Q., Liu, Z.H., Jia, G., 2010. Pulmonary toxicity in mice exposed to low and medium doses of water-soluble multi-walled carbon nanotubes. J Nanosci Nanotechnol **10**, 8516-8526.
Weldy, C.S., Luttrell, I.P., White, C.C., Morgan-Stevenson, V., Bammler, T.K., Beyer, R.P., Afsharinejad, Z., Kim, F., Chitaley, K., Kavanagh, T.J., 2012. Glutathione (GSH) and the GSH synthesis gene Gclm modulate vascular reactivity in mice. Free Radic Biol Med **53**, 1264-1278.
Weldy, C.S., White, C.C., Wilkerson, H.W., Larson, T.V., Stewart, J.A., Gill, S.E., Parks, W.C., Kavanagh, T.J., 2011. Heterozygosity in the glutathione synthesis gene Gclm increases sensitivity to diesel exhaust particulate induced lung inflammation in mice. Inhal Toxicol **23**, 724-735.
Wesselkamper, S.C., Chen, L.C., Gordon, T., 2001a. Development of pulmonary tolerance in mice exposed to zinc oxide fumes. Toxicol Sci **60**, 144-151.
Wesselkamper, S.C., Chen, L.C., Kleeberger, S.R., Gordon, T., 2001b. Genetic variability in the development of pulmonary tolerance to inhaled pollutants in inbred mice. Am J Physiol Lung Cell Mol Physiol **281**, L1200-1209.
Wild, A.C., Mulcahy, R.T., 2000. Regulation of gamma-glutamylcysteine synthetase subunit gene expression: insights into transcriptional control of antioxidant defenses. Free Radic Res **32**, 281-301.

Wu, M., Gordon, R.E., Herbert, R., Padilla, M., Moline, J., Mendelson, D., Litle, V., Travis, W.D., Gil, J., 2010. Case report: Lung disease in World Trade Center responders exposed to dust and smoke: carbon nanotubes found in the lungs of World Trade Center patients and dust samples. Environ Health Perspect **118**, 499-504.

Xia, T., Hamilton, R.F., Bonner, J.C., Crandall, E.D., Elder, A., Fazlollahi, F., Girtsman, T.A., Kim, K., Mitra, S., Ntim, S.A., Orr, G., Tagmount, M., Taylor, A.J., Telesca, D., Tolic, A., Vulpe, C.D., Walker, A.J., Wang, X., Witzmann, F.A., Wu, N., Xie, Y., Zink, J.I., Nel, A., Holian, A., 2013. Interlaboratory evaluation of in vitro cytotoxicity and inflammatory responses to engineered nanomaterials: the NIEHS Nano GO Consortium. Environ Health Perspect **121**, 683-690.

Yamashita, K., Yoshioka, Y., Higashisaka, K., Morishita, Y., Yoshida, T., Fujimura, M., Kayamuro, H., Nabeshi, H., Yamashita, T., Nagano, K., Abe, Y., Kamada, H., Kawai, Y., Mayumi, T., Yoshikawa, T., Itoh, N., Tsunoda, S., Tsutsumi, Y., 2010. Carbon nanotubes elicit DNA damage and inflammatory response relative to their size and shape. Inflammation **33**, 276-280.

Yu, K.N., Kim, J.E., Seo, H.W., Chae, C., Cho, M.H., 2013. Differential toxic responses between pristine and functionalized multiwall nanotubes involve induction of autophagy accumulation in murine lung. J Toxicol Environ Health A **76**, 1282-1292.

Appendix: Acronyms and Abbreviations

#

129 – 129S1/SvImJ
3-NT – 3-nitrotyrosine
4-HHE – 4-hydroxyhexenal

A

AJ – A/J
AKR – AKR/J
ANOVA – analysis of variance

B

BAL – bronchoalveolar lavage
BALF – bronchoalveolar lavage fluid

C

C57 – C57BL/6J
CEEH FGPC – University of Washington's Center for Ecogenetics and Environmental Health Functional Genomics and Proteomics Core
CNT – carbon nanotube
COX-2 – cyclooxygenase-2
CSH – CSH/HeJ

D

DBA – DBA/2J
DCFDA – 2',7'-dichlorofluorescin diacetate
DM – dispersion medium
DPPC – 1,2-dipalmitoyl-sn-glycero-3-phosphocholine

E

EDS – energy dispersive x-ray spectroscopy
ELF – epithelial lining fluid
ESR – electron spin resonance
EU – endotoxin unit

F

FVB – FVB/NJ

G

GCL – glutamate cysteine ligase
GCLC – glutamate cysteine ligase catalytic subunit
GCLM – glutamate cysteine ligase modifier subunit
GSH – glutathione
GSSG – oxidized glutathione

H

HMOX – heme oxygenase
HRP – horseradish peroxidase

I

IARC – International Agency for Research on Cancer
ICP-MS – inductively coupled plasma mass spectrometry
I_D – intensity of the signature peak corresponding to defective bonding in Raman spectroscopy
I_G – intensity of the signature peak corresponding to intact graphene bonding in Raman spectroscopy
IL – interleukin
IT – intratracheal instillation

J

K

KC/CXCL1/GRO – chemokine (X-X-C motif) ligand 1

L

LDH – lactate dehydrogenase
LOD – limit of detection

M

MCP-1 – monocyte chemotactic protein 1
MWCNT – multi-walled carbon nanotube

N

NADPH – Nicotinamide adenine dinucleotide phosphate, reduced
NCNHIRC – NIEHS Centers for Nanotechnology Health Implications Research Consortium
NF-κB – nuclear factor kappa-light-chain-enhancer of activated B cells
NIEHS – National Institute of Environmental Health Sciences
NIH – National Institutes of Health
NIOSH – National Institute for Occupational Safety and Health
NOD – NOD/ShiLtJ
NZO – NZO/HiLtJ

O

OD – outer diameter
OPA – oropharyngeal aspiration

P

PBS – phosphate buffered saline
PCR – polymerase chain reaction
PDGF – platelet-derived growth factor
PNNL – Pacific Northwest National Laboratory
PTGES2 – prostaglandin E synthase 2

Q

qRT-PCR – quantitative real-time polymerase chain reaction
QTL – quantitative trait loci

R

S

SDS-PAGE – sodium dodecyl sulfate polyacrylamide gel electrophoresis
SEM – scanning electron microscopy
SEM – standard error of the mean
SWCNT – single-walled carbon nanotube

T

TGF-β – transforming growth factor-β
TNF-α – tumor necrosis factor-α

U

V

W

WSB – WSB/EiJ

X

Y

Z